CRANFIELD INSTITUTE OF TECHNOLOGY

J. R. BARBOSA

A STREAMLINE CURVATURE COMPUTATIONAL PROGRAMME FOR AXIAL COMPRESSOR PERFORMANCE PREDICTION

VOL. I - THE PROGRAMME

SCHOOL OF MECHANICAL ENGINEERING

Ph.D. Thesis

IMAGING SERVICES NORTH
Boston Spa, Wetherby
West Yorkshire, LS23 7BQ
www.bl.uk

VOLUME 2 IS UNAVAILABLE. PLEASE CONTACT THE UNIVERSITY FOR FURTHER INFORMATION

CRANFIELD INSTITUTE OF TECHNOLOGY

SCHOOL OF MECHANICAL ENGINEERING

PhD Thesis

Academic Year 1986/1987

J. R. BARBOSA

A STREAMLINE CURVATURE COMPUTATIONAL PROGRAMME FOR AXIAL COMPRESSOR PERFORMANCE PREDICTION

Volume I - The Programme

Supervisor: Prof. K. W. Ramsden

September 1987

SUMMARY

Accurate prediction of overall performance is vital if the extremely high design and development costs of modern high speed compressors are to be minimised. This fact, which is not novel, has led to the development of many computer programmes for such prediction. However, the most useful of these are proprietary. Some of those that are accessible in the open literature are of limited application to high performance axial compressors. This is mainly because they cannot reliably handle the transonic flows which characterise modern designs; nor are they generally easy to use from an interactive stand point.

Accordingly, this report describes the origination of a streamline curvature programme for compressor performance prediction which attempts to bridge the gap in the existing literature base.

The correlations used allow the package to be applied to more recent compressors at the highest level of the technology.

In general, the programme is both interactive and fully modular. The former makes it easy for the user to access the programme quickly and effectively whilst the latter facilitates the use, for example, of alternative

loss and deviation models to those prescribed within the programme.

A further important feature of this new programme is its flexibility. For example, it can be used in three modes: firstly, as an analysis programme for performance prediction of compressors of known geometry; secondly, as a design/development tool to assess the likely performance changes occasioned by the introduction of geometrical variations in both blading and annulus shape; thirdly, as a straight design programme for new compressors provided a project analysis has been carried out beforehand.

In the first two modes of operation, the programme requires details of standard blading, annulus geometry, design mass flow and pressure ratio. In the third, the user is free to prescribe his own blade shapes.

The combined features described were introduced to make the package an ideal teaching tool. In this respect it should be emphasised that the complete novice to axial compressor design and performance assessment would experience difficulties using the package. However, the user who has some background, perhaps through lectures or in an appropriate industrial environment would quickly become adept.

Against this background, whilst the programme is very interactive, it cannot claim, in its own right, to be an

Expert System. The latter capability, however, can with some development easily be built in at a later stage.

In order to minimise the time required accessing the programme, the report includes a comprehensive "user-guide".

The validity of the prediction method is tested against an actual transonic compressor of known performance. The output is various and includes graphical presentation of all significant design/performance parameters throughout the compressor, including the compressor overall characteristic.

ACKNOWLEDGEMENT

The author wishes to convey his thanks to his supervisor for assistance with this work, as well as for the encouragement to pursue the objectives. He is sure that without the supervisor constant assistance and encouragement it was impossible to conclude this work.

He would also like to express sincere gratitude to the necessarily anonymous provider of the actual compressor data, against which the prediction programme was compared. His patient and considerable advice on the subject of the loss model used has proved invaluable to the success of the prediction method.

His gratitude is extended to Alberto Shiniti Takeda and his wife Mary Honda Takeda for the invaluable help in the preparation of the figures and text.

Finally thanks are due to my family for their patience during the busy period of this study, especially for my wife that typed the text.

NOTATION

A	coefficient matrix (Matrix Method)
A	coefficient (Radial Equilibrium Equation)
B	matrix (Matrix Method)
B	coefficient (Radial Equilibrium Equation)
b	exponent (deviation)
c	blade chord; speed of sound
c_a	axial chord
C_D	Drag coefficient (secondary losses)
C_L	lift coefficient (secondary losses)
c_p	specific heat at constant pressure
c_v	specific heat at constant volume
D	distance
D	auxiliary constant
D	Diffusion Factor
$d\vec{A}$	element of area
D/Dt	material derivative
d/dt	ordinary derivative
D_{eq}	Equivalent Diffusion Factor
dm	elemental distance in the streamline direction
dr	elemental distance in the radial direction
ds	elemental distance in the blade edge
D_T	throat width
DV	velocity increment
dx, dr, dz	elemental distances in the Cartesian system
$d\delta/di$	coefficient (deviation rule)
E	specific internal energy
$\vec{e}_r, \vec{e}_\theta, \vec{e}_z$	base vector in the cylindrical co-ordinate system
$\vec{F}$	blade force
F	function
f_5	function (Equivalent Diffusion Factor)
f_{Re}	Reynolds number correction (losses)
H	static enthalpy, form factor
h	distance (throat)
I	rothalpy
i	incidence
i*	minimum loss incidence
i**	unique incidence
$(io)_{10}$	coefficient (incidence)
j	streamline counting
K	constant
k_1, k_2, k_3, k_4	constants (Equivalent Diffusion Factor)

k_B	blockage factor
K_i	coefficient (incidence)
K_δ	coefficient (deviation)
M	Mach number
m	distance along the streamline
m_C	coefficient (Carter's rule)
$\dot{m}$	mass flow
$\dot{m}_A$, $\dot{m}_B$, $\dot{m}_C$	intermediate mass flow calculation
n	coefficient (deviation)
n	exponent (Swan's off-design correlation)
P	static pressure
R	air constant
R	radius
r	radius
r	position vector
r_b	blade edge radii
R_c	radius of curvature
Re	Reynolds number
S	entropy
s	distance along blade edges
s	blade spacing
s/c	space-chord ratio
T	static temperature
t	blade thickness
t_e	blade maximum thickness
U	wheel speed
V	air velocity
v	specific volume
V_A, V_B, V_C	intermediate meridional velocities
W	relative air velocity
x_T	distance (throat)
Y	(= V^2_m - radial equilibrium equation)
y	function
y	distance (Cartesian co-ordinate)
Y_{Rc}	distance (throat)
z	axial distance

GREEK LETTERS

α	air angle
β	blade angle
γ	blade sweep
δ	deviation
$(\delta_o)_{10}$	coefficient (deviation)
Δ	increment
δ_c	off-design correction for deviation
$\frac{\partial}{\partial s}$	partial derivative
ε	streamline slope
γ	blade sweep
η	efficiency
λ	blade dihedral (skew)
ρ	density
μ	kinematics viscosity
$\vec{\nabla}$	gradient
Φ	auxiliary angle (blade geometry)
θ	blade camber
θ/c	boundary-layer wake momentum thickness
Ψ	stream function
σ	c/s
τ	Prandtl-Meyer expansion angle
ξ	auxiliary angle (shock loss)
ζ	stagger
ω	rotational speed
$\overline{\omega}_p$	profile loss
$\overline{\omega}_{sh}$	shock loss
$\overline{\omega}_s$	secondary loss
$\overline{\omega}_T$	total loss
$\overline{\omega}_{cor}$	correction (losses)

SUBSCRIPT

1	blade inlet
1	inlet relative angle
2	blade outlet
c	critical
H	hub
is	isentropic
m	meridional
max	maximum
o	reference
o	inlet absolute angle
r	radial component
R	relative
t	total
T	tip
z	axial

SUPERSCRIPT

*	minimum loss condition
*	boundary layer
**	unique incidence
$\overline{Y}$	(overbar) - average
n	order of iteration
-1	inverse of a matrix

CONTENTS

FIGURES

TABLES

1. - INTRODUCTION

1.1. BACKGROUND

The axial flow compressor designer is constantly under pressure to find ways of reducing the time and, therefore, costs of design and development. This has always been the case.

As a result, former design methods effectively cut corners by making extensive use of accumulated experience to establish design rules through correlation techniques. Much of this data represented the particular company's experience. This method achieved a great deal in enhancing the designer's confidence in making performance predictions at an early phase in a new project. Similarly, improved design confidence meant performance targets were more quickly and reliably achieved.

Relatively recently, performance prediction methods have relied more and more on development of computational models of compressor flows as an alternative to costly and time consuming experimental studies. These models similarly rely heavily on correlations of in-house experimental data combined with the widely available cascade data published

in the open literature. Clearly, computational techniques are much faster but can only compete with well-tried experimental methods if they can be made at least as reliable. Unfortunately, the complex flow field of axial flow compressors is notoriously difficult to model accurately. Despite this, several attempts have been made to predict both localized flow within the compressor and to reproduce the overall performance characteristic. Almost without exception the models thus produced fail to compare with experimental observations over the entire range of operations. In particular, the models fall short at the design speed at both very low mass flows (surge) and at high flows (choke). The reasons are nearly always associated with the difficulty of representing the real flows with adequate loss/deviation models, particularly for cases both near stall and at high incident Mach numbers, respectively. This fact has led to the development of a wide variety of alternative loss models, some of which are proprietary.

A further severe limitation to computational packages is that invariably it is not easy or even sometimes possible to replace the loss model used with an alternative defined by the user.

Development in recent years of high performance compressors to higher stage pressure ratios has exacerbated

these problems and introduced further difficulties in accurate modelling. For example, typical transonic compressors have very steep constant speed characteristics. Accordingly, the range of operating mass flow from surge to choke is very small. It is then, imperative, that the loss models used can adequately allow the prediction of the large changes in both pressure ratio and efficiency taking place over this narrow variation of mass flow.

Against this background, it is not surprising that a full theoretical three-dimensional treatment of the flow within high performance multistage axial flow compressors is still not possible.

Even so, there are many computational procedures available for performance calculations. A few of these appear in the open literature, but perhaps for obvious reasons, the most reliable are proprietary. Those that are published suffer some or all of the limitations discussed above. It is further true that few is user friendly, most are difficult to access and even more difficult to modify. For example, alternative loss models are not easy to incorporate. The latter is considered a very desirable feature since, as compressors continue to develop, successful computational prediction depends almost entirely on the ability to develop all or part of the software to the new requirements.

As a typical example, the eventual results from end bend treatments of compressor blading currently being researched both in the United Kingdom and Germany will inevitably modify loss correlations in the tip region. Such modification to the loss model used here can easily be incorporated into the programme.

It should also be said that of the models available some are one-dimensional and cannot therefore represent, for example, the non-uniform radial velocity profiles typifying all compressors.

On the other hand, the use of a full three-dimensional representation, were it possible today, would prove extremely costly in running time.

Furthermore, it is unlikely that in the foreseeable future, sufficiently reliable and accurate data will be available to support fully three-dimensional models.

Whatever the modelling technique used, of paramount importance is the need for it to be representative of the environment of modern high performance compressors.

In order to satisfy the current need and to produce an acceptable prediction programme, the method chosen in this work is a pseudo three-dimensional model, which treats the flow locally within the compressor as two-dimensional. The streamline curvature method used is coupled with what are considered to be reliable experimental correlations for

losses and deviations drawn from the open literature, namely, those due to Swan and Monsaratt. Particular attention is paid to the need for the model to be able to handle the most up to date high performance compressors.

1.2. OBJECTIVES

The overall objective of this work was to produce a computational analysis model, which could accurately predict the performance map for modern multistage axial flow compressors.

Accordingly, the programme had to be capable of:

- Performance prediction at design speed for a range of mass flows between surge and choke.
- Performance prediction at off-design speeds and over a full range of mass flows.
- Handling transonic flows.

To achieve these objectives, only the geometry of the annulus and the blading together with the design speed, mass flow and pressure ratio were to be required as input data.

An important primary objective, in addition to the above, was that the programme could be effectively used as a teaching aid for the student whose general turbomachinery

background is limited.

At the same time as setting the above general objectives, it was realized that it would be relatively easy to produce yet another software package to set alongside those already available in the market place. Since this serves little purpose, it was important that the shortcomings of existing packages should, as far as is possible, be avoided as a major prerequisite.

It was also recognized that the programme users were likely to fall into two categories, namely;

(i) The student of turbomachinery whose background and experience is limited but who needs fast access to a software package capable of demonstrating principles, and later on for more advanced applications.

(ii) The compressor designer with perhaps considerable experience, who would use the programme in both the analysis role as well as a tool for "tweaking" existing compressor designs in his quest for improved performance.

Accordingly, in addition to the main objectives set out above, the following subsidiary requirements were introduced into the programme development plan to meet the needs of the two user groups defined above.

1.2.1. USE AS A TEACHING TOOL

The programme should be readily usable as a teaching aid. In building in this capability it was recognised that for first and early confrontations at the terminal, a typical student experiences frustrations due to:

- Non-familiarity with the particular software package or perhaps even with any software system.
- A frequently interrupted accessibility through lecture programme schedules.
- A limited number of computer time units at his disposal through academic economies.

In addition, as the student develops his user skills and turbomachinery knowledge, the programme should have the flexibility for exchange of Subroutines with alternatives prescribed by himself. To this end several subsidiary requirements were laid down, namely that the programme:

- Should have associated with it a comprehensive "User-guide".
- Should be quickly accessible to the student with relatively little background in compressor technology.
- Should be user friendly and substantially interactive.

- Should have a mid-programme restart capability to obviate repeat calculations and thus save time and cost when the programme has to be interrupted for external reasons.
- Should be of fully modular construction so that the more experienced student can use his own developing skills to investigate parametric influences.
- Should be capable of producing answers very quickly to minimise user costs.

1.2.2. USE AS DESIGN/DEVELOPMENT TOOL

In addition to the overall programme objectives set out in the beginning of this section, and to maximise its use in compressor development, the programme should incorporate assessment of variable geometry influences.

In particular, the package should be capable of investigating the effect of geometrical changes to an existing compressor on overall performance. For example, and for transonic compressors in particular, the effect of changes in the type of base profile and perhaps even in annulus geometry could prove very useful for compressor development assessment. Similarly, the effect on off-design

performance of variable IGV's, stators and compressor air bleed would be a useful addition to the capabilities of existing packages.

1.2.3. PROGRAMME RATIONALE

In order to achieve the objectives set out in the previous sections of 1.2, the following main features of the prediction programme have been incorporated:

- Fully modular construction with many subroutines replaceable with alternatives.
- A comprehensive user-guide included with the programme (see volume 2).
- A limited interactive capability but very user friendly.
- A restart capability.
- A full access, through graphical output, to all major performance parameters.
- The ability to carry out a full analysis for a single point in a relatively short time.

In conclusion, there still remains considerable scope for development of the programme to become more interactive than currently, especially for the student with little or no background in turbomachinery.

1.3. REVIEW OF PREDICTION METHODS

The different methods available for the analysis of a compressor are discussed in the following. Reference is made to gas turbine applications since axial compressors are extensively utilised in these cases.

The design of a successful gas turbine relies on a fairly accurate knowledge of the flow properties throughout the engine. The ever increasing costs of development of engine components, as well as the need to make the engine operational in the shortest possible period, imposes a heavy burden on the design and analysis phases.

For many years a great deal of effort has been expended in development of mathematical models, in order to improve their prediction capabilities.

The simplest and the fastest use a laminar one-dimensional approach but are not appropriate to the high performance components they are supposedly modelling. In reality, the flow is far from one-dimensional in most working conditions.

Two-dimensional approaches on the other hand have been very successful combining their simplicity with empirical data. By this means, the need to fully account for viscous effects and three-dimensionality of the flow is obviated.

The modelling of three-dimensional flows, by today's

standards, is very costly. The quasi-three-dimensional approach, which considers the flow as being locally two dimensional, is a compromise between the easiest and the most complex approaches, which can generate reliable information for the designer.

The simulation of engines running at different conditions is a must at the design stage. This is the only may to know, in advance, likely compressor performance, if and when the compressor is eventually built. The better the prediction of performance of each component at both design and off-design, the closer the simulation corresponds to the actual characteristic.

There are two important requirements a particular performance prediction programme must fulfil, namely:

a) To synthesise the overall performance maps, and

b) To synthesise the flow field at different locations throughout the compressor.

The first requirement can be met by a one- dimensional approach.

The second requirement can be met by either two or three-dimensional methods.

The multidimensional approaches have the ability to provide information to effect subsequent design improvement because they make it possible to analyse the flow field throughout the compressor.

Although the literature reveals many techniques for modelling compressors and for solving the relevant equations in order to estimate their behaviour, they are generally very restrictive as far as their applications are concerned. Needless to say, many of those programs are proprietary.

The early work of Wu [1], in the fifties, is still the best starting point for flow modelling. The equations he derived at that time remained for a long period, because of the huge amount of numerical calculation necessary for their solution when applied to a specific problem. With the advent of computers, however, researchers attempted the solution of some of the more simplified forms of these equations. The large and powerful number crunching machines of today, however, enable the utilisation of the complete equations.

The iterative process of finding a mid-channel two-dimensional solution as the starting point for blade-to--blade solutions and, therefore, an approximate three-dimensional solution to the flow equations, as initially suggested by Wu, could only be undertaken later. Nevertheless, the complete viscous solutions still remain largely open for all intents and purposes.

Engineers need quick and cheap answers to problems and therefore, time consuming and expensive techniques cannot

be seen as practical solutions. There is a need, therefore, to produce models, which may be used as engineering tools. Different considerations have resulted in different methods being adopted for dealing with both flow modelling and their numerical solutions.

These methods, in general, can be grouped into three categories, depending on the dimension of the space in which the equations are assembled namely; one, two and three-dimensional.

As the name implies the first of these methods analyses the flow as if it were one-dimensional. The most common of the **one-dimensional** methods are:

- The Stage Stacking method, which uses individual stage characteristics to assemble multistage compressor overall performance maps. This method has been applied for more than forty years and is still in use today [2],[3].
- The Pitch Line or Mean Radius method, which uses the flow properties at blade mid height only to estimate the overall performance [3].

Two-dimensional methods, which analyse the flow field as if it was two-dimensional in the mid-channel or from blade-to-blade. Simultaneous utilisation of mid-channel and blade-to-blade flow is sometimes accepted as a three-

dimensional technique [1].

The most common two-dimensional techniques are:

The Matrix Through Flow Method: this was pioneered by Marsh at NGTE and solves the discrete equations on a fixed mesh applied to the flow passage. The name of the method derives from the fact that a matrix is used with geometrical information in an iterative process. The grid in many cases must be orthogonal and therefore, irregular. The equations of motion, state and energy are combined into a second order partial differential equation, where the dependent variable is the stream function.

It generally takes the form

$$\frac{\partial^2\Psi}{\partial x^2} + \frac{\partial^2\Psi}{\partial y^2} = F\left(x, y, \frac{\partial\Psi}{\partial x}, \frac{\partial\Psi}{\partial y}\right) \qquad (1.1)$$

which is non-linear. The function F in equation (1.1) is a non-linear function of the solution Ψ and its derivatives. No closed algebraic solution is possible. A finite difference or finite element technique is used to approximate the solution Ψ at every mode. After the finite difference approximation is applied and similar terms are collected, equation (1.1) can be written finally in the matrix form

$$A\Psi = B \tag{1.2}$$

where A, the Coefficient Matrix associated with the problem, is, fortunately, a constant and depends only on the grid shape;

Ψ is the solution vector, and

B is the collection of all remaining terms.

Equation (1.2) must be solved iteratively because B depends on Ψ. After a first guess of Ψ, B can be calculated and a new approximation, Ψ_1, obtained iteratively from

$$\Psi_1 = A^{-1} B(\Psi) \tag{1.3}$$

It is known that Ψ_1 is a better approximation than Ψ to the actual solution and that the iterative process is convergent.

The advantage of this method is that A is a function of the grid only, A^{-1} need only be computed once and is independent of the mass flow and compressor speed.

The matrix technique offers rapid convergence, better than second order accuracy and stability at high flows and machine speeds [4]. The velocity field, however, can only be established after the converged solution of (1.1) is

obtained.

The Streamline Curvature Method was pioneered by Hearsey when with British Siddeley and more recently by Ringrose at NGTE. The method solves the discrete equations on a mesh, which changes at each iteration. The name of the method derives from the fact that the mesh is defined by the flow streamlines. The way their curvatures are calculated plays an important role in the stability of the process. At each iteration the streamlines have their positions changed and so does the grid. Details of the method adopted in this work are given in the following chapters.

Although the fundamental equations used in both methods are exactly the same, they are written differently to best suit each method. In the Matrix Method, the stream function is first calculated and subsequently the velocity field. In the streamline curvature method the velocity field is calculated at once.

There are advantages and disadvantages of each of the methods. From a user's point of view there is little to differentiate between them [5].

The preference for the Streamline Curvature method, used in this work, is that it is more suitable to interactive use. In particular, it handles more simply any modifications to geometry whilst the program is running.

Additionally it is better for teaching applications.

It is a fact that only experience in utilising the various methods, together with a specific case to be analysed, can determine, which is the best for the particular application in question.

The Three-dimensional Methods ultimately aim at solving the conservation equations of a real fluid applied to the compressor, as indicated by Wu [1]. The calculations are so vast as to be beyond the scope of the fast running programme to predict compressor maps set as an objective for the present work. However, they can be applied quite well for detailed design of blades and ducts, both for the direct and inverse problems. The Finite Element technique is well suited to application to three-dimensional methods and the emerging Boundary Element Method could be of importance in the future.

The literature reveals many techniques for dealing with three-dimensional boundary layers on blades, shock-boundary layer interactions, etc. None, however, deals with the real and complete compressor. If there is one, it is proprietary and therefore, not available for review here.

The improvements in modern analyses [6] of compressors can be drawn from several published papers.

For each particular application one method is perhaps best suited. There is no single method that can be applied

to all compressors with the same expectation of success.

1.4. APPLICATIONS

The need for a relatively fast and general computer programme, for the design and analysis of axial flow compressors, has been stated before. If such a programme were capable of incorporating in-house knowledge, without complex modifications it would certainly be a very powerful tool.

The design and performance analyses of a simple axial stage is very time consuming, even if only a few calculating stations are placed across the annulus. Hand calculations are very limited, except those very crude estimates corresponding to simple flow models. Design optimisation through hand calculation is therefore discarded.

There are two major applications envisaged for the present work, namely: teaching and engineering analysis.

* From the teaching and learning point of view, it is important to the lecturer not just to explain the importance and difficulties involved in a detailed calculation, but also to make it possible for the student to perform his own design and analysis calculations to the

fullest extent.

Both lack of time and the enormous amount of calculation necessary are to blame when design, analysis and optimisation are generally truncated at the first stages of calculations. It would then be only possible to have a feel for the interaction of the various parameters if design and analyses are to be carried out extensively.

The difficulties encountered, and the amount of work to be undertaken during the optimisation of a high performance compressor for today's application, are of an order of magnitude greater. The shorter the compressor the greater is the influence of streamline curvature. This imposes additional calculations before a final solution is achieved.

* From an engineering point of view, the analysis and optimisation of compressors is possible with the programme for most of which have already been designed preliminarily.

Since users are likely to have their own expertise in assessing deviations and losses, a package, which utilizes a fixed model for those parameters, is not of practical application. It would of course, be preferable if the user's own models could be merged with the package without major modifications. The present work makes this possible because in addition to standard and well-tried correlations concerning incidence, deviation and losses, the user's own

models can simply be added into the package, without any modifications to the main body of the programme.

1.5. SCOPE OF THE PROGRAMME

The present work makes available a computer programme, which can be used both as an engineering package as well as a teaching tool. The analysis of axial flow compressors and annular ducts in both subsonic and transonic regimes is possible.

The programme will handle:

(1) The analysis of compressors with British C-series, NACA 65-series, DCA or user-defined blades.

(2) Detailed calculation of flow properties at the blade edges and in bladeless ducts.

(3) The calculation of the overall compressor performance map.

(4) General blade stacking and skewing.

(5) Standard or user defined loss correlations.

(6) Standard or user-defined deviations.

(7) Non-uniform inlet flow conditions.

(8) Modifications to geometry, mass-flow, speed or loss correlations during a specific programme

run.

The package is designed with a view to it being:

(1) User oriented, in the sense that the user's expertise can be incorporated into the package as far as losses and deviations are concerned.

(2) Machine independent, in the sense that the programme is written in Fortran 77 and is auto-sufficient, except for graphical outputs. It does not require external specialised subroutines particular to a specific operating system.

(3) Modular, in the sense that there is only one routine to perform a specific task.

(4) Capable of restarting without losing previous calculations.

(5) Capable of producing graphical output both on the screen and in hard copy.

(6) Capable of changing the number of streamlines during a programme run.

1.6. THE STREAMLINE CURVATURE METHOD

The streamline curvature method is chosen for the present work since it best suits the requirements for

interactive design modifications. When associated with the restart capability, it is a very powerful tool. For example the effect of any reasonable change to the geometry, mass flow or speed can be registered almost instantaneously.

Essentially, the method consists of writing the equations of continuity, motion, energy and state in a form that incorporates the geometry of the streamlines.

A detailed development of the equations is given in the section entitled Flow Modelling.

After the transformations have been made, the result is a non-linear partial differential equation. This must be solved in the domain defined by the passages inside the compressor with the boundary conditions imposed by the compressor geometry. The initial conditions are set by the ambient conditions of the incoming air, the mass flow and the compressor rotational speed.

The partial differential equation is solved by a finite difference approximation on a mesh constructed in the meridional plane. The nodes are the intersection of the streamlines and the blade edges (Fig. 1.1). Additional nodes are placed along the streamlines in the inlet and outlet ducts.

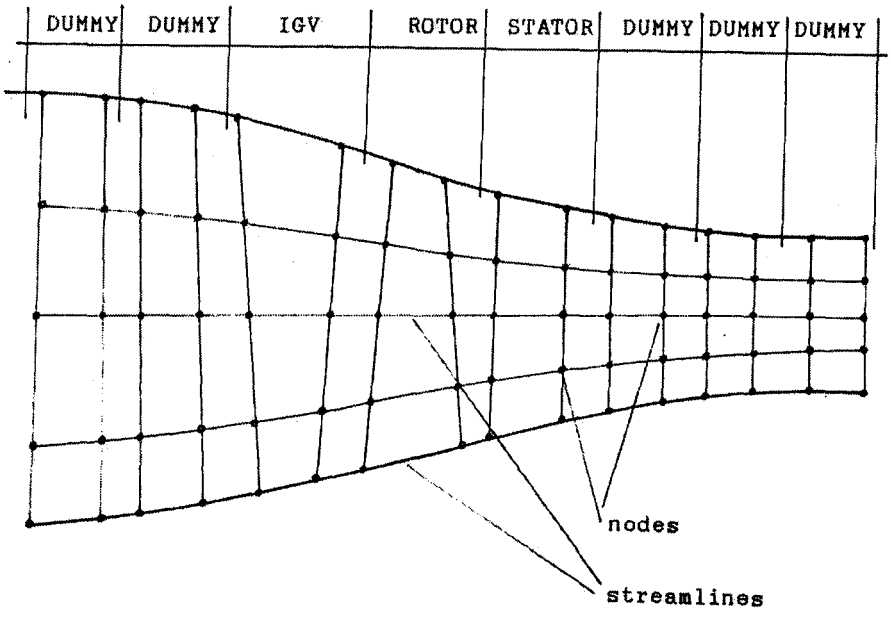

Figure 1-1 - Streamlines and Nodes

The technique for determining the mesh is explained later. The equations are integrated at each node, from the compressor inlet to its outlet.

The positions of the nodes are not known in advance because the streamlines have not at that point been determined. After an initial guess of the streamline positions, the calculation can be carried out. New positions for the nodes are determined and subsequently an assessment of the previous guess can be made. An iterative procedure is defined such that the streamlines are repositioned until, eventually, their position remains constant and the solution is achieved.

This particular method is chosen because, in an interactive application, it is possible to follow the calculation progress and intervene in that process if modifications are needed at any node.

There are no limitations to the compressor geometry provided the latter can be approximated by smooth curves. The adoption of loss correlations enables the continuation of the calculations from the leading to the trailing edges of each blade. As a result, fewer mesh points are needed and less computer time is spent.

The algorithm adopted allows rapid convergence so that, after a few iterations, a fair approximation to the compressor behaviour is calculated. There is no need to wait for the converged solution before considering the incorporation of modification. A thorough description is given in the chapter on Algorithms.

Despite the enormous generality and capability of the computer programme, the converged solution is obtained quickly.

The model can handle transonic flows since the meridional velocity is subsonic in all circumstances.

2. - FLOW MODELLING

2.1. THE STREAMLINE CURVATURE METHOD

The flow in a compressor is three-dimensional, viscous and turbulent. The use of a mathematical model to represent such a complex flow is beyond the scope of this work, as has already been explained. However, an inviscid model, in which the effects of viscosity are incorporated by empirical means, can offer sufficient accuracy. This is the method adopted here. Indeed, the axisymmetric non-viscous model is a close approximation to the actual flow provided blades spacing are small. Discrepancies appear only when large values of space-chord ratio (s/c) are considered.

The flow is divided into a finite number of stream tubes, inside which the flow is axisymmetric. The effects of losses due to the interaction of the blades in the flow are lumped at each blade trailing edge. Therefore, the integration of the conservation equations of momentum, energy, mass flow and the equation of state, give an overall description of the flow inside the compressor. In order to simplify the model further, it is convenient to chose a privileged system of co-ordinates to write the

equations. Fig. 2.1 shows one possible blade configuration at the meridional plane, together with the major nomenclature.

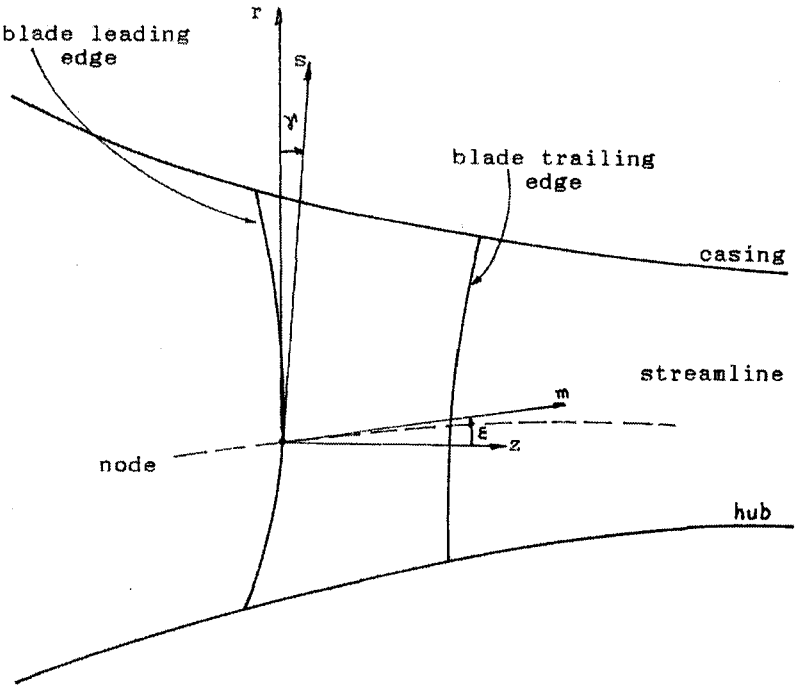

Figure 2.1

Figure 2-1 - Streamline nomenclature

A comprehensive derivation of the main equations is carried out here for the sake of easy reference to the computer programme.

Let $\vec{V}$, $\vec{W}$ and $\vec{U}$ be the absolute, relative and blade velocities of any flow particle, (Fig. 2.2), respectively.

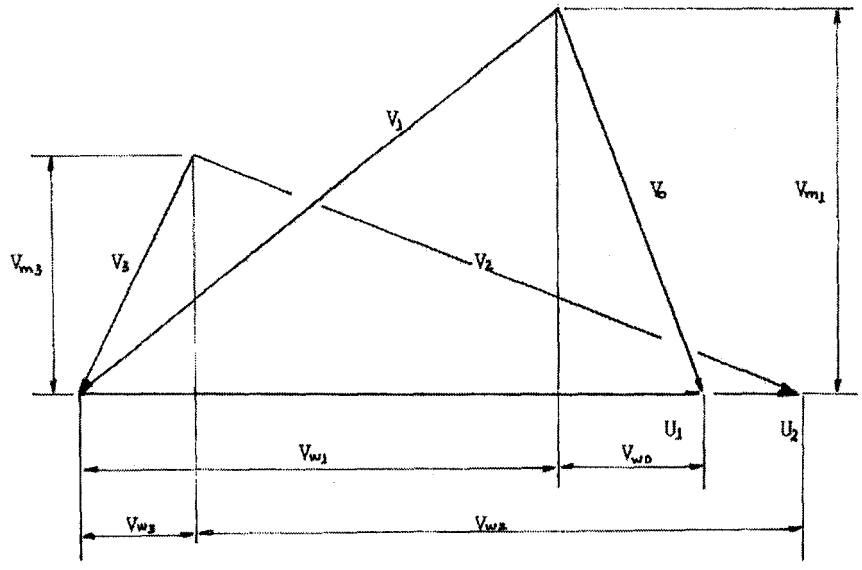

Figure 2-2- Velocity triangles

Then

$$\vec{V} = \vec{W} + \vec{U}, \qquad \vec{U} = \vec{\omega} \times \vec{r} \tag{2.1}$$

$$\vec{V} = V_r \vec{e}_r + V_w \vec{e}_\omega + V_z \vec{e}_z \tag{2.2}$$

$$\vec{W} = W_r \vec{e}_r + W_w \vec{e}_\omega + W_z \vec{e}_z \tag{2.3}$$

$$\vec{U} = \omega r \vec{e}_\omega \tag{2.4}$$

From (2.1), (2.2), (2.3) and (2.4), it follows that

$$V_r = W_r \tag{2.5}$$

$$V_w = W_w + \omega r$$

$$V_z = W_z$$

In what follows, the equations are initially derived in the relative co-ordinate system. This will facilitate the incorporation of calculations inside blade passages in future development work.

Accordingly, the non-viscous momentum equation can be written as

$$-\frac{1}{\rho}\vec{\nabla}P = \frac{D\vec{W}}{Dt} + \vec{\omega} \times \vec{\omega} \times \vec{r} + 2\vec{\omega} \times \vec{W} + \vec{F} \tag{2.6}$$

where

$$\frac{D\vec{W}}{Dt} = V_r \frac{\partial \vec{W}}{\partial r} + \frac{W_\omega}{r} \frac{\partial \vec{W}}{\partial \omega} + V_z \frac{\partial \vec{W}}{\partial z} \tag{2.7}$$

and is the steady-state representation of the variation of the relative velocity of a particle, with relative velocity $\vec{W}$ along one streamline.

Then

$$-\frac{1}{\rho}\vec{\nabla}P = V_r \frac{\partial \vec{W}}{\partial r} + \frac{W_\omega}{r} \frac{\partial \vec{W}}{\partial \omega} + V_z \frac{\partial \vec{W}}{\partial z} + \vec{\omega} \times \vec{\omega} \times \vec{r} + 2\vec{\omega} \times \vec{W} + \vec{F} \tag{2.8}$$

Equation (2.8) represents momentum equation of a steady state non-viscous flow relative to a cylindrical system of co-ordinates rotating with speed about a fixed

axis.

Equation (2.8), expressed in radial, tangential and axial components is

$$-\frac{1}{\rho}\frac{\partial P}{\partial r} = V_r\frac{\partial V_r}{\partial r} + \frac{W_\omega}{r}\frac{\partial V_r}{\partial \omega} + V_z\frac{\partial V_r}{\partial z} - \frac{W_\omega^2}{r} - \omega^2 r - 2\omega W_\omega$$

$$-\frac{1}{r\rho}\frac{\partial P}{\partial \omega} = V_r\frac{\partial W_\omega}{\partial r} + \frac{W_\omega}{r}\frac{\partial W_\omega}{\partial \omega} + V_z\frac{\partial W_\omega}{\partial z} + \frac{V_r W_\omega}{r} + 2\omega V_r \qquad (2.8a)$$

$$-\frac{1}{\rho}\frac{\partial P}{\partial z} = V_r\frac{\partial V_z}{\partial r} + \frac{W_\omega}{r}\frac{\partial V_z}{\partial \omega} + V_z\frac{\partial V_z}{\partial z}$$

The terms in (2.8a), involving $\frac{\partial}{\partial \omega}$, can be dropped if the flow is considered axisymmetric.

Equation (2.8) and its scalar components must be integrated in order to give information about the flow in the blade passages. In order to know the flow properties at the blade edges at the mid-channel surface, it is convenient to rewrite (2.8) as a function of both the blades edges and the streamlines curves m and s.

Defining a meridional velocity V_m by

$$V_m = \left(V_r^2 + V_z^2\right)^{1/2} \qquad (2.9)$$

From Fig. 2.1 it is easily seen that

$$V_r = V_m \sin(\varepsilon)$$

$$V_z = V_m \cos(\varepsilon) \qquad (2.10)$$

If the streamline curve is written in terms of r and m, that is, m=m(r,z), then

$$\frac{\partial}{\partial m} = \frac{\partial r}{\partial m}\frac{\partial}{\partial r} + \frac{\partial r}{\partial m}\frac{\partial}{\partial z}$$

From Fig. 2.1 and equation (2.10) it follows that

$$\frac{\partial r}{\partial m} = \sin(\varepsilon) = \frac{V_r}{V_m}$$

$$\frac{\partial z}{\partial m} = \cos(\varepsilon) = \frac{V_z}{V_m} \qquad (2.11)$$

$$\frac{\partial r}{\partial z} = tg(\varepsilon) = \frac{V_r}{V_z}$$

$$\frac{\partial}{\partial m} = \sin(\varepsilon)\frac{\partial}{\partial r} + \cos(\varepsilon)\frac{\partial}{\partial z} \quad \text{or}$$

$$V_m \frac{\partial}{\partial m} = V_r \frac{\partial}{\partial r} + V_z \frac{\partial}{\partial z} \qquad (2.12)$$

$$\frac{\partial V_r}{\partial m} = \frac{V_r}{V_m}\frac{\partial V_r}{\partial r} + \frac{V_z}{V_m}\frac{\partial V_r}{\partial z} \quad \text{or}$$

$$\frac{\partial V_r}{\partial m} = \frac{1}{V_m}\left(V_r \frac{\partial V_r}{\partial r} + V_z \frac{\partial V_r}{\partial z}\right) \qquad (2.13)$$

Then

$$\frac{\partial V_z}{\partial m} = \frac{V_r}{V_m}\frac{\partial V_z}{\partial r} + \frac{V_z}{V_m}\frac{\partial V_z}{\partial z} \quad \text{or}$$

$$\frac{\partial V_r}{\partial m} = \frac{1}{V_m}\left(V_r\frac{\partial V_z}{\partial r} + V_z\frac{\partial V_z}{\partial z}\right) \tag{2.14}$$

$$\frac{\partial(rV_\omega)}{\partial m} = r\frac{\partial V_\omega}{\partial m} + V_\omega\frac{\partial r}{\partial m} \quad \text{or}$$

$$\frac{\partial(rV_\omega)}{\partial m} = \frac{r}{V_m}\left(V_r\frac{\partial V_\omega}{\partial r} + V_z\frac{\partial V_\omega}{\partial z} + \frac{V_rV_\omega}{r}\right) \tag{2.15}$$

Rewriting equations (2.8a) taking into account the fact that $V_\omega = U + W_\omega$:

$$-\frac{1}{\rho}\frac{\partial P}{\partial r} = V_r\frac{\partial V_r}{\partial r} + V_z\frac{\partial V_r}{\partial z} - \frac{(V_\omega - U)^2}{r} - \omega^2 r - 2\omega(W_\omega - U) =$$

$$= V_r\frac{\partial V_r}{\partial r} + V_z\frac{\partial V_r}{\partial z} - \frac{V_\omega^{\,2}}{r}$$

$$-\frac{1}{r\rho}\frac{\partial P}{\partial \omega} = 0 = V_r\frac{\partial(W_\omega - U)}{\partial r} + V_z\frac{\partial(W_\omega - U)}{\partial z} + \frac{V_\omega^2}{r} + 2\omega V_r =$$

$$= V_r\frac{\partial V_\omega}{\partial r} + V_z\frac{\partial V_\omega}{\partial z} + \frac{V_rW_\omega}{r}$$

$$-\frac{1}{\rho}\frac{\partial P}{\partial z} = V_r\frac{\partial V_z}{\partial r} + V_z\frac{\partial V_z}{\partial z}$$

Finally

$$
\begin{aligned}
-\frac{1}{\rho}\frac{\partial P}{\partial r} &= V_r \frac{\partial V_r}{\partial r} + V_z \frac{\partial V_r}{\partial z} - \frac{V_\omega^2}{r} \\
0 &= V_r \frac{\partial V_\omega}{\partial r} + V_z \frac{\partial V_\omega}{\partial z} + \frac{V_r W_\omega}{r} \\
-\frac{1}{\rho}\frac{\partial P}{\partial z} &= V_r \frac{\partial V_z}{\partial r} + V_z \frac{\partial V_z}{\partial z}
\end{aligned}
\qquad (2.8.b)
$$

Equations (2.13), (2.14) and (2.15) substituted into (2.8b) give the result

$$
-\frac{1}{\rho}\frac{\partial P}{\partial r} = V_m \frac{\partial V_r}{\partial m} - \frac{V_\omega^2}{r} \qquad (2.16)
$$

$$
0 = \frac{V_m}{r}\frac{\partial (r V_\omega)}{\partial m} \qquad (2.17)
$$

$$
-\frac{1}{\rho}\frac{\partial P}{\partial z} = V_m \frac{\partial V_z}{\partial m} \qquad (2.18)
$$

The second terms in equations (2.16) to (2.18) are written in terms of streamline curves. The next step is to rewrite the first components of the equations in terms of the distance along the blade edges, s.

If r = r(s) and z = z(s) on a blade edge, then along that edge,

$$\frac{\partial}{\partial s} = \frac{\partial r}{\partial s}\frac{\partial}{\partial r} + \frac{\partial r}{\partial s}\frac{\partial}{\partial z} \qquad (2.19)$$

Defining γ as the angle between the r-axis and the tangent to the blade edges in the meridional plane, (Fig. 2.3)

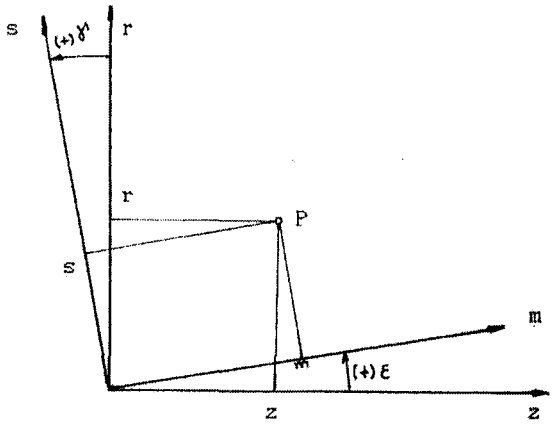

Figure 2-3 - System of Co-ordinates

$$\frac{\partial r}{\partial s} = \cos(\gamma)$$

$$\frac{\partial z}{\partial s} = \sin(\gamma$$

$$\frac{\partial}{\partial s} = \cos(\gamma)\frac{\partial}{\partial r} + \sin(\gamma)\frac{\partial}{\partial z}$$

Then

$$-\frac{1}{\rho}\frac{\partial P}{\partial s} = \cos(\gamma)\left(-\frac{1}{\rho}\frac{\partial P}{\partial r}\right) + \sin(\gamma)\left(-\frac{1}{\rho}\frac{\partial P}{\partial z}\right) \tag{2.20}$$

Substituting (2.16) and (2.18) into (2.20):

$$-\frac{1}{\rho}\frac{\partial P}{\partial s} = \cos(\gamma)V_m\frac{\partial V_r}{\partial m} - \cos(\gamma)\frac{V_\omega^2}{r} + \sin(\gamma)V_m\frac{\partial V_z}{\partial m}$$

Taking into account equations (2.10),

$$-\frac{1}{\rho}\frac{\partial P}{\partial s} = \cos(\gamma)V_m\frac{\partial(\sin(\varepsilon)V_m)}{\partial m} - \cos(\gamma)\frac{V_\omega^2}{r} + \sin(\gamma)V_m\frac{\partial(\cos(\varepsilon)V_m)}{\partial m}$$

Collecting similar terms:

$$-\frac{1}{\rho}\frac{\partial P}{\partial s} = V_m^2\frac{\partial \varepsilon}{\partial m}\cos(\varepsilon+\gamma) + V_m\frac{\partial V_m}{\partial m}\sin(\varepsilon+\gamma) - \cos(\gamma)\frac{V_\omega^2}{r} \tag{2.21}$$

The streamline curvature $\frac{\partial \varepsilon}{\partial m}$, can be rewritten as follows:

$$tg(\varepsilon) = \frac{\partial r}{\partial z}$$

$$\sec^2(\varepsilon)\frac{\partial \varepsilon}{\partial m} = \frac{d^2r}{dz^2}\frac{\partial z}{\partial m} = \frac{d^2r}{dz^2}\cos(\varepsilon)$$

$$\frac{\partial \varepsilon}{\partial m} = \frac{d^2r}{dz^2}\left\{\frac{dz}{\sqrt{dr^2+dz^2}}\right\}^3$$

$$\frac{\partial \varepsilon}{\partial m} = \frac{\dfrac{d^2 r}{dz^2}}{\left\{1 + \left(\dfrac{dr}{dz}\right)^2\right\}^{3/2}} = \frac{1}{R_c} \tag{2.22}$$

Then, equation (2.21) can be rewritten as

$$-\frac{1}{\rho}\frac{\partial P}{\partial s} = \frac{V_m^2}{R_c}\cos(\varepsilon + \gamma) + V_m \frac{\partial V_m}{\partial m}\sin(\varepsilon + \gamma) - \cos(\gamma)\frac{V_\omega^2}{r} \tag{2.23}$$

Equation (2.23) can be used for the calculation of the meridional velocity distribution along a path, s, following the blade edges. It is, however, necessary to evaluate the term $V_m \frac{\partial V_m}{\partial m}$, which represents the rate of change of V_m^2 along the streamline. $V_m \frac{\partial V_m}{\partial m}$ can be calculated through the continuity equation, as follows.

Let $m = m(r,z)$ and $s = s(r,z)$. Then

$$\frac{\partial}{\partial m} = \sin(\varepsilon)\frac{\partial}{\partial r} + \cos(\varepsilon)\frac{\partial}{\partial z}$$

and

$$\frac{\partial}{\partial s} = \cos(\gamma)\frac{\partial}{\partial r} + \sin(\gamma)\frac{\partial}{\partial z}$$

Then

$$\frac{\partial}{\partial r} = \frac{1}{\cos(\varepsilon + \gamma)}\left\{\cos(\varepsilon)\frac{\partial}{\partial s} - \sin(\gamma)\frac{\partial}{\partial m}\right\} \tag{2.24}$$

$$\frac{\partial}{\partial z} = \frac{1}{\cos(\varepsilon + \gamma)} \left\{ - \sin(\varepsilon) \frac{\partial}{\partial s} + \cos(\gamma) \frac{\partial}{\partial m} \right\} \tag{2.25}$$

For an axisymmetric flow, the continuity equation is

$$\frac{\partial}{\partial r} (r\rho V_r) + \frac{\partial}{\partial z} (r\rho V_z) = 0 \tag{2.26}$$

From (2.24), (2.25) and (2.26) it follows that

$$\frac{1}{\cos(\varepsilon + \gamma)} \left\{ \cos(\varepsilon) \frac{\partial}{\partial s} (r\rho V_r) - \sin(\gamma) \frac{\partial}{\partial m} (r\rho V_r) \right\} +$$
$$+ \frac{1}{\cos(\varepsilon + \gamma)} \left\{ - \sin(\varepsilon) \frac{\partial}{\partial s} (r\rho V_z) + \cos(\gamma) \frac{\partial}{\partial m} (r\rho V_z) \right\} = 0$$

From equation (2.10):

$$\cos(\varepsilon) \frac{\partial}{\partial s} (r\rho V_m \sin(\varepsilon)) - \sin(\gamma) \frac{\partial}{\partial m} (r\rho V_m \sin(\varepsilon)) +$$
$$- \sin(\varepsilon) \frac{\partial}{\partial s} (r\rho V_m \cos(\varepsilon)) + \cos(\gamma) \frac{\partial}{\partial m} (r\rho V_m \cos(\varepsilon)) = 0$$

$$\cos(\varepsilon) \left\{ r\rho V_m \sin(\varepsilon) \frac{\partial \varepsilon}{\partial s} + \sin(\varepsilon) \frac{\partial (r\rho V_m)}{\partial s} \right\} +$$
$$- \sin(\gamma) \left\{ r\rho V_m \cos(\varepsilon) \frac{\partial \varepsilon}{\partial m} + \sin(\varepsilon) \frac{\partial (r\rho V_m)}{\partial m} \right\} +$$
$$- \sin(\varepsilon) \left\{ - r\rho V_m \sin(\varepsilon) \frac{\partial \varepsilon}{\partial s} + \cos(\varepsilon) \frac{\partial}{\partial m} (r\rho V_m) \right\} +$$
$$+ \cos(\gamma) \left\{ - r\rho V_m \sin(\varepsilon) \frac{\partial \varepsilon}{\partial s} + \cos(\varepsilon) \frac{\partial}{\partial m} (r\rho V_m) \right\} = 0$$

$$r\rho V_m \frac{\partial \varepsilon}{\partial s} - (\sin(\gamma)\cos(\varepsilon) + \cos(\gamma)\sin(\varepsilon)) r\rho V_m \frac{\partial \varepsilon}{\partial m} +$$

$$+ (\cos(\gamma)\cos(\varepsilon) - \sin(\gamma)\sin(\varepsilon)) \frac{\partial (r\rho V_m)}{\partial m} = 0$$

$$\sec(\varepsilon + \gamma) \frac{\partial \varepsilon}{\partial s} - tg(\varepsilon + \gamma) \frac{\partial \varepsilon}{\partial m} + \frac{1}{V_m} \frac{\partial V_m}{\partial m} + \frac{\partial (\ln(r\rho))}{\partial m} = 0$$

Then

$$V_m \frac{\partial V_m}{\partial m} = V_m^2 \left\{ - \sec(\varepsilon + \gamma) \frac{\partial \varepsilon}{\partial s} + tg(\varepsilon + \gamma) \frac{\partial \varepsilon}{\partial m} - \frac{\partial (\ln(r\rho))}{\partial m} \right\}$$

or

$$V_m \frac{\partial V_m}{\partial m} = V_m^2 \left\{ - \sec(\varepsilon + \gamma) \frac{\partial \varepsilon}{\partial s} + tg(\varepsilon + \gamma) \frac{1}{R_c} - \frac{\partial (\ln(r\rho))}{\partial m} \right\} \qquad (2.27)$$

From the second law of thermodynamics,

$$dH = TdS + vdP = TdS + d(Pv) - Pdv$$

$$dH = dE + d(Pv) = c_v\, dT + d(Pv)$$

Then, $TdS - Pdv = c_v\, dT$

$$c_v\, dT/T = dS - (P/T)dv = dS - R\, dv/v$$

and, finally,

$$\rho = \rho_0 \left(\frac{T}{T_0} \right)^{\frac{1}{\gamma - 1}} e^{\left(-\frac{S - S_0}{R} \right)}$$

If $H = c_p T$

then

$$\rho = \left(\frac{H}{H_0}\right)^{\frac{1}{\gamma-1}} \left(\frac{c_{p0}}{c_p}\right)^{\frac{1}{\gamma-1}} e^{\left(-\frac{S-S_0}{R}\right)}$$

Let

$$A = \left(\frac{c_{p0}}{H_0 c_p}\right)^{\frac{1}{\gamma-1}}$$

Then

$$\rho = A H^{\frac{1}{\gamma-1}} e^{\left(-\frac{S-S_0}{R}\right)}$$

and

$$\frac{1}{\rho}\frac{\partial \rho}{\partial m} = \frac{1}{c^2}\frac{\partial H}{\partial m} - \frac{1}{R}\frac{\partial S}{\partial m}, \qquad c^2 = \gamma R T \tag{2.28}$$

Equation (2.27) becomes

$$V_m \frac{\partial V_m}{\partial m} = V_m^2 \left\{ \begin{array}{l} -\sec(\varepsilon + \gamma)\dfrac{\partial \varepsilon}{\partial s} + \dfrac{\mathrm{tg}(\varepsilon + \gamma)}{R_c} + \\ -\dfrac{1}{c^2}\dfrac{\partial H}{\partial m} + \dfrac{1}{R}\dfrac{\partial S}{\partial m} - \dfrac{1}{r}\sin(\varepsilon) \end{array} \right\} \tag{2.29}$$

Expressing H in terms of T and velocities, using the energy equation:

$$H = c_p T = c_p T_t - V^2/2 \tag{2.30}$$

$$V^2 = W^2 - U^2 + 2UV_\omega \tag{2.31}$$

From equations (2.30) and (2.31)

$$H = (c_p T_t - UV_\omega) + U^2/2 - W^2/2 \tag{2.32}$$

Defining the Rothalpy $I = (c_p T_t - UV_\omega)$, which is a constant along a streamline, in a stationary row $I = H_t$, so that the total enthalpy is constant along a streamline.

Calculating the derivative of H in the m direction gives, after considering $W^2 = V_m^2 + W_\omega^2$

$$\frac{\partial H}{\partial m} = \frac{\partial I}{\partial m} - V_m \frac{\partial V_m}{\partial m} - V_\omega \frac{\partial V_\omega}{\partial m} + V_\omega \frac{\partial U}{\partial m} + U \frac{\partial V_\omega}{\partial m} \tag{2.33}$$

From (2.17) $V_m \frac{\partial (rV_\omega)}{\partial m} = 0$, so that equation (2.33) becomes

$$\frac{\partial H}{\partial m} = \frac{\partial I}{\partial m} - V_m \frac{\partial V_m}{\partial m} + V_\omega^2 \frac{\sin(\varepsilon)}{r} \tag{2.34}$$

Along any streamline $\frac{\partial I}{\partial m} = 0$. Then

$$\frac{\partial H}{\partial m} = -V_m \frac{\partial V_m}{\partial m} + V_\omega^2 \frac{\sin(\varepsilon)}{r} \tag{2.35}$$

Substituting (2.35) into (2.29):

$$V_m \frac{\partial V_m}{\partial m}\left(1 - M_m^2\right) = V_m^2\left\{\begin{array}{l} -\sec(\varepsilon + \gamma)\frac{\partial \varepsilon}{\partial s} + \frac{tg(\varepsilon + \gamma)}{R_c} + \\ + \frac{1}{R}\frac{\partial S}{\partial m} - \left(1 + M_m^2\right)\frac{1}{r}\sin(\varepsilon) \end{array}\right\} \qquad (2.36)$$

where $M_m = V_m/c$, $M_\omega = V_\omega/c$

Then

$$V_m \frac{\partial V_m}{\partial m} = \frac{V_m^2}{\left(1 - M_m^2\right)}\left\{\begin{array}{l} -\sec(\varepsilon + \gamma)\frac{\partial \varepsilon}{\partial s} + \frac{tg(\varepsilon + \gamma)}{R_c} + \\ + \frac{1}{R}\frac{\partial S}{\partial m} - \left(1 + M_m^2\right)\frac{1}{r}\sin(\varepsilon) \end{array}\right\} \qquad (2.37)$$

Equation (2.37) will give the meridional velocity along any streamline.

In order to calculate the axial velocity distribution both in front of and behind the blades, equation (2.23) can be used, modified to express the pressure term as a function of temperature and entropy.

From the first equation after 2.27, with $v = 1/\rho$

$$dP/\rho = dH - TdS$$

and, from equation 2.32:

$$\frac{\partial H}{\partial s} = \frac{\partial I}{\partial s} - \frac{1}{2}\frac{\partial W^2}{\partial s} + \frac{1}{2}\frac{\partial U^2}{\partial s}$$

Then

$$\frac{1}{\rho}\frac{\partial P}{\partial s} = \frac{\partial I}{\partial s} - \frac{V_m}{\cos^2(\alpha)}\frac{\partial V_m}{\partial s} - \frac{V_m^2}{\cos^2(\alpha)}\,tg(\alpha)\frac{\partial \alpha}{\partial s} + \cos(\gamma)\frac{U^2}{r} - T\frac{\partial S}{\partial s} \qquad (2.39)$$

where α is the relative air angle.

Substituting (2.39) in the first number of (2.23) and collecting similar terms,

$$V_m \frac{\partial V_m}{\partial s} = \cos^2(\alpha)\left\{\left[\frac{\partial I}{\partial s} - T\frac{\partial S}{\partial s}\right] + V_m^2\left[\begin{array}{l}\dfrac{\cos(\varepsilon+\gamma)}{R_c} - \dfrac{tg(\alpha)}{\cos^2(\alpha)}\dfrac{\partial \alpha}{\partial s} + \\ + \dfrac{2U}{V_m}tg(\alpha)\dfrac{\cos(\gamma)}{r} - tg^2(\alpha)\dfrac{\cos(\gamma)}{r} + \\ + \dfrac{\sin(\varepsilon+\gamma)}{V_m}\dfrac{\partial V_m}{\partial m}\end{array}\right]\right\} \qquad (2.40)$$

where

$$V_m \frac{\partial V_m}{\partial m} = \frac{V_m^2}{\left(1 - M_m^2\right)}\left\{\begin{array}{l}-\sec(\varepsilon+\gamma)\dfrac{\partial \varepsilon}{\partial s} + \dfrac{tg(\varepsilon+\gamma)}{R_c} + \\ + \dfrac{1}{R}\dfrac{\partial S}{\partial m} - \left(1 + M_m^2\right)\dfrac{1}{r}\sin(\varepsilon)\end{array}\right\} \qquad (2.41)$$

$V_m \frac{\partial V_m}{\partial m}$ alternatively may be calculated from the previous iteration so that the $M_\omega \neq 1$ requirement is set aside.

Equations (2.40) and (2.41) form a system of non-linear partial differential equations. If it is known in advance that the flow properties, represented by that system, are well behaved, that is, that they vary smoothly at the blade edges, then the system can be solved. If the

flow properties vary smoothly, it is assumed that the coefficients of V_m can be replaced by an average constant value so that equation (2.40) can be rewritten as

$$\frac{dV_m^2}{ds} = A + BV_m^2 \tag{2.42}$$

where

$$A = 2\cos^2(\alpha)\left[\frac{\partial I}{\partial s} - T\frac{\partial S}{\partial s}\right] \tag{2.43}$$

$$B = \cos^2(\alpha)\left[\begin{array}{l}\dfrac{\cos(\varepsilon+\gamma)}{R_c} - \dfrac{tg(\alpha)}{\cos^2(\alpha)}\dfrac{\partial\alpha}{\partial s} + \dfrac{2U}{V_m}tg(\alpha)\dfrac{\cos(\gamma)}{r} + \\ - tg^2(\alpha)\dfrac{\cos(\gamma)}{r} + \dfrac{\sin(\varepsilon+\gamma)}{V_m}\dfrac{\partial V_m}{\partial m}\end{array}\right] \tag{2.44}$$

2.2. FLOW BLOCKAGE

The literature reports that the application of conventional boundary-layer theory to estimate the displacement and momentum thickness is generally inadequate since inside an axial compressor the flow is constantly: changing direction, skewed, energised and de-energised as it progresses through the rows.

Some semi-empirical rules have, through research, been established which can accurately approximate these losses

[7], [8], [9].

Experience has shown [9], [10], that the meridional velocity close to the wall can be taken as an appropriate parameter to assess the effect of the boundary layer in restricting the flow through the compressor.

In order to derive an expression to evaluate boundary layer properties, calculation stations are placed in the bladeless spaces close to the blade edges so that no geometrical obstruction due to the blades is present in the flow. At these stations, blockage can be caused only by the end wall boundary layers. If it is assumed that the flow exists only inside a core, defined by a decrease in the compressor annulus height equivalent to the boundary-layer displacement thickness (shown in Fig. 2.4), a blockage factor can be defined.

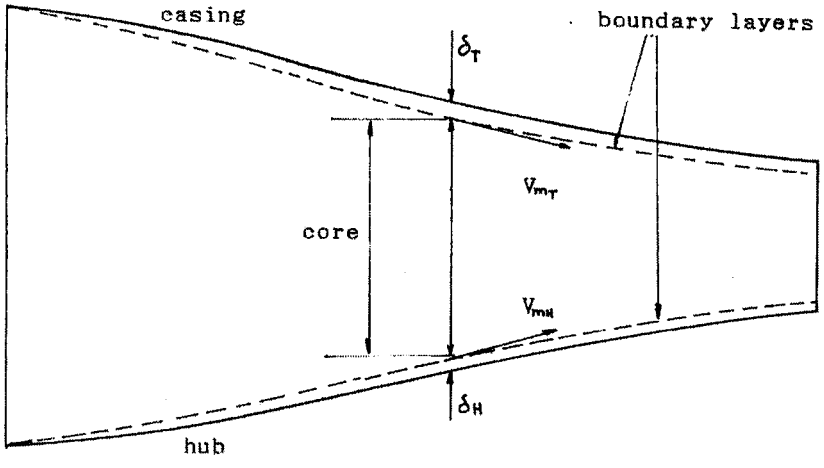

Figure 2-4 - Blockage

Furthermore, if it is assumed that the end-wall boundary-layer can be treated as two dimensional and turbulent and that the meridional flow velocity is the dominant characteristic, then from [10] and [11], it can be shown that:

$$\theta(z)=\theta(z_0)+k_{bl}\left\{\frac{\int_{z_0}^{z} V_m^4(z)dz}{V_m^{3.2}}\right\}^{0.8} \tag{2.45}$$

where

θ is the boundary-layer momentum thickness

z_0 is a reference axial location

V_m is the meridional velocity

z is the calculating location

k_{bl} is a constant, whose magnitude is a function of the system of units only.

If the boundary-layer displacement thickness is known at the reference station, then $\theta(z_0)$ can be calculated by

$$\theta(z_0)=\frac{\delta^*}{H} \tag{2.46}$$

H is initially assumed equal to 1.4.

The shape factor can then be evaluated from

$$H(z) = 1.5 + 30\ d\theta/dz \tag{2.47}$$

and the displacement thickness from

$$\delta^*(z) = \theta(z)H(z) \tag{2.48}$$

Applying equations (2.45) to (2.48) to the hub and to the casing walls, with $V_m(z)$ the local meridional velocity, it is possible to calculate $\delta_H^*(z)$ and $\delta_T^*(z)$, the boundary-layer displacement thickness, respectively, at both hub and casing throughout the compressor. It is then assumed that the meridional velocity at the walls is known in advance.

Defining the blockage factor by

$$k_B = \text{(free-stream area)/(metal area)} \tag{2.49}$$

then

$$k_B = \frac{(R_T - \delta_T^*)^2 + (R_H + \delta_H^*)^2}{R_T^2 - R_H^2} \tag{2.50}$$

where R_T and R_H are the casing and hub radii.

Because the value of k_B is known, only after the meridional velocity is known throughout the compressor, the process of calculating the boundary-layer blockage is iterative.

Defining a hub and a casing blockage due to boundary-layer by

$$k_{BH} = \frac{\left(R_H + \delta_H^*\right)^2 - R_H^2}{R_T^2 - R_H^2} \tag{2.51}$$

$$k_{BT} = \frac{R_T^2 - \left(R_T - \delta_T^*\right)^2}{R_T^2 - R_H^2} \tag{2.52}$$

then

$$k_B = 1 - (k_{BH} + k_{BT}) \tag{2.53}$$

Experience indicates that this approach is valid if the following limitations are imposed:

- for accelerating flows, $H(z) < 2.2$
- for decelerating flows, $H(z) < 1.1$
- $k_B \leq 0.7$ and $k_{BH} \leq 0.25$, $k_{BT} \leq 0.2$

2.3. CONTINUITY

The continuity equation is used in both its divergence and integral forms.

The divergence form,

$$\frac{\partial}{\partial r}(r\rho V_r) + \frac{\partial}{\partial z}(r\rho V_z) = 0 \tag{2.54}$$

is used to evaluate the rate of change of $V_m \frac{\partial V_m}{\partial m}$ which represents the flow acceleration and is dependent on the air mass flow being pumped by the compressor.

The integral form,

$$\dot{m} = \int_A \rho \vec{V} \cdot d\vec{A} \tag{2.55}$$

is used for the calculation of mass flow in streamtubes and the compressor annulus at each blade edge. The integral form is also used for the determination of the constant of integration in the radial equilibrium equation.

The integrand is made discrete over the nodes at the blade edges and a trapezoidal rule is applied for the evaluation of the integral.

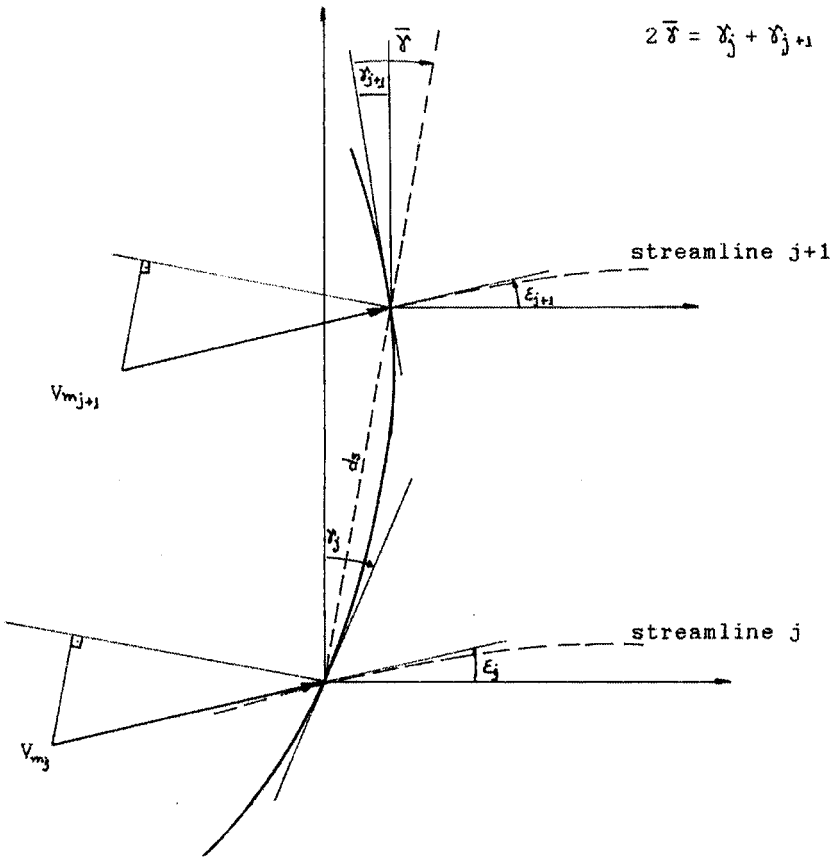

Figure 2-5 - Flow geometry at 2 consecutive nodes

At each streamtube the mass flow (based on Fig. 2.5) is

$$\dot{m}_j = \int_A \bar{\rho}\bar{V}_m dA = \tag{2.56}$$

$$= \frac{\pi}{2}\left[\rho_{j+1}V_{m_{j+1}}\cos(\varepsilon_{j+1} + \gamma_{j+1}) + \rho_j V_{m_j}\cos(\varepsilon_j + \gamma_j)\right]\left[\frac{r_{j+1}^2 - r_j^2}{\cos\left(\frac{\gamma_{j+1} + \gamma_j}{2}\right)}\right]$$

For a large number of streamlines and small values of γ, equation (2.56) can be simplified to

$$\dot{m}_j = \pi\left(r_{j+1}\rho_{j+1}V_{m_{j+1}} \cos(\varepsilon_{j+1}) + r_j\rho_j V_{m_j} \cos(\varepsilon_j)\right)\left(r_{j+1} - r_j\right) \qquad (2.57)$$

To keep the error small in adopting this simple technique, a reasonable number of streamlines must be used, varying in accordance with the loss distribution near the walls: the higher the rate of change in the losses, the closer the streamlines must be chosen.

2.4. CHOKING

At a given rotational speed, the compressor is considered choked when any one row is choked.

The choking is detected when either the annulus or the throat is choked. The annulus or the throat is considered choked when an increase in axial velocity gives rise to a decrease in mass flow. This implies the possibility of choke whilst some of the streamtubes remain un-choked to satisfy radial equilibrium.

The calculations are interrupted when annulus choke is detected. No attempt is made to calculate throat choke.

The actual choking point is difficult to calculate but, if small increments in mass flow are used, it is possible to get very close to it.

2.5. STALL AND SURGE

There are no practical correlations that define precisely the point where blade sections stall or indeed where the compressor surges. Nevertheless, analysis of many blade sections working near and at stall, reveals that the equivalent diffusion factor, D_{eq}, is close to a limiting value of 2.20. Accordingly, the value of 2.20 for D_{eq} is taken as an indication that the blade section is at the point of stall [4], [10], [12].

3. - COMPRESSOR MODELLING

Compressor modelling, in this context, refers to the determination of geometrical data to be input to the computer programme sufficient to define an hypothetical geometry which is very close to the actual geometry through the various interpolations and derivations performed during numerical calculations.

The curvature of the streamlines has a strong influence on the calculations. Therefore, care must be taken when selecting the nodes and their related geometrical parameters for input purposes.

As in an actual compressor, the calculated properties of the flow field are strongly dependent on the duct shape at compressor inlet and outlet. Therefore, in order to compare test results with the programme output, it is necessary to feed the programme with data of the intake and exhaust ducts used in the actual compressor tests.

For the purpose of extracting the data from an actual compressor, or from its drawings, the blades are considered to occupy the whole annulus, tip clearance being ignored.

In order to standardize the calculations and, therefore, simplify the program algorithms, the ducts at the front and at the back of the compressor are filled with

dummy blades. The dummy blades are ideal loss free blades and do not present any obstructions to the flow. They are defined by the program after the node locations have been defined. The dummy blades are set to follow the flow and to serve as an anchor for the nodes.

Annular ducts can be analysed in the same way as the intake and exhaust ducts.

The adoption of the dummy blade concept makes the calculations homogeneous from the intake to the exhaust.

3.1. BLADE GEOMETRY

Three of the most commonly used types of blade section are incorporated in the programme: double circular arc (DCA), NACA 65 series (65S) and the British C series C4). However, the user can define his own blade section if these profiles are not appropriate.

3.1.1. DCA BLADES

DCA blades are simple profiles defined by two circular arcs intersecting at the leading and trailing edges. The geometric approximation adopted in this work is that due to Oldham [13], shown in Fig. 3.1.

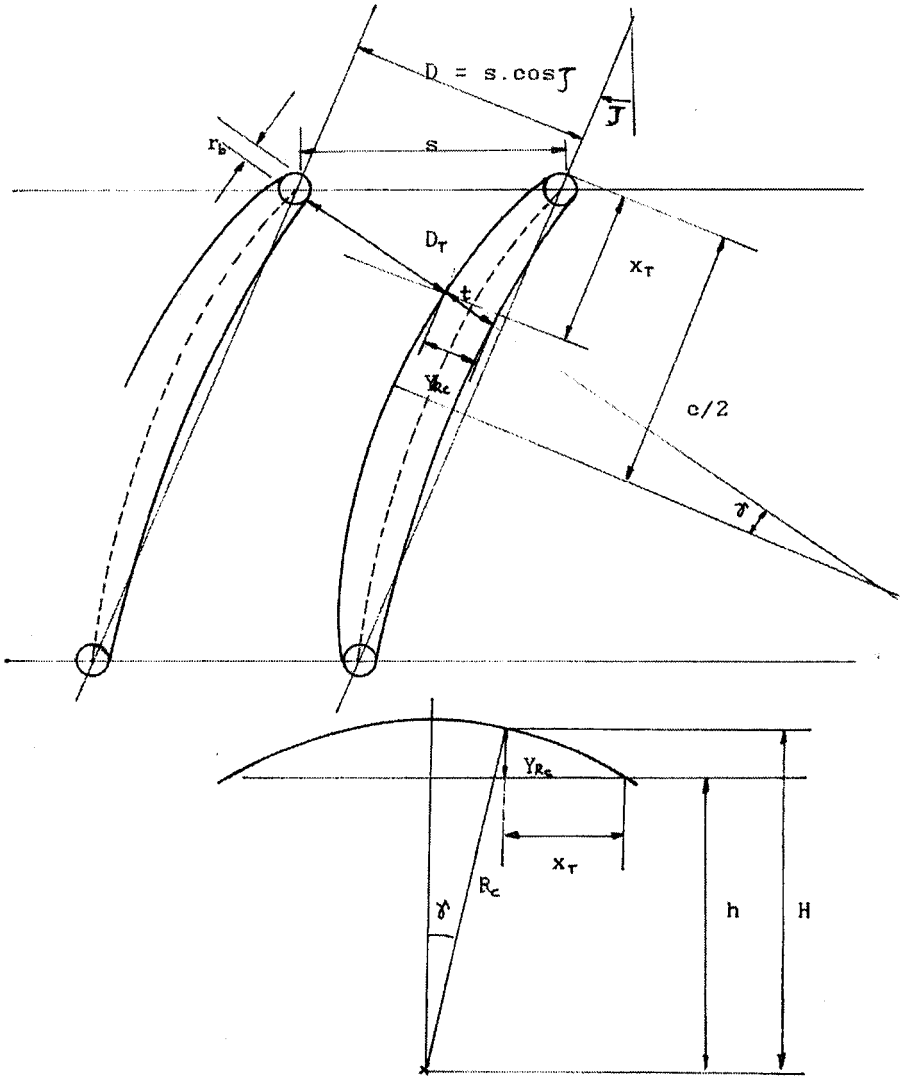

Figure 3-1 - DCA blade throat geometry

The relevant geometric parameters are:

R_{C1} camber line radius

R_{C2} suction surface radius

R_{C3} pressure surface radius

β_1 leading edge angle, measured from the axial

direction

β_2 trailing edge angle, measured from the axial direction

r_b edges radii

c chord

θ camber angle,

t_e maximum thickness

For a given blade chord, maximum thickness, edge radii and camber, the circular arcs R_{C1}, R_{C2}, R_{C3} can be geometrically calculated by

$$R_{C1} = \frac{c}{2\sin\left(\frac{\theta}{2}\right)}$$

$$R_{C2} = \frac{R_{C1}(2R_{C1} + t_e)(1 - \cos(\phi)) + \left(\frac{t_e}{2}\right)^2 - r_b^2}{R_{C1}(1 - \cos(\phi)) + \frac{t_e}{2} - r_b}$$

$$R_{C3} = \frac{R_{C1}(2R_{C1} - t_e)(1 - \cos(\phi)) + \left(\frac{t_e}{2}\right)^2 - r_b^2}{R_{C1}(1 - \cos(\phi)) - \frac{t_e}{2} + r_b}$$

$$\phi = \sin^{-1}\left\{\frac{c - 2r_b}{c}\sin\left(\frac{\theta}{2}\right)\right\}$$

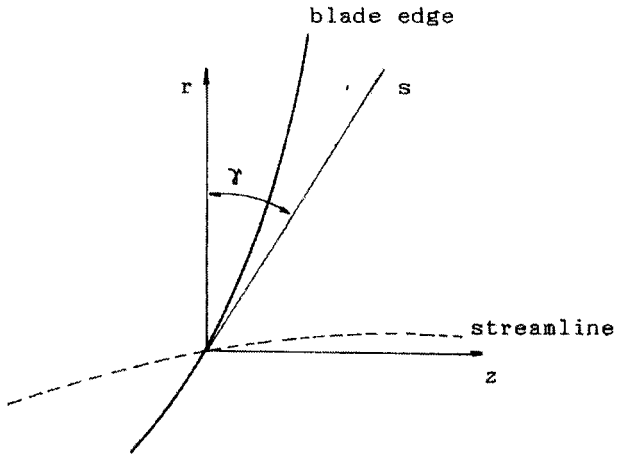

Figure 3-2 - Blade sweep

The angle formed by the tangent to the suction surface and the chord line can be calculated based on Fig. 3.2. The blade throat is calculated, assuming it is located at the leading edge, as follows:

a) For DCA blades

$$D_T = D - r_b - t - \frac{Y_{R_{C3}}}{\cos(\gamma)}$$

b) For other blades on circular camber

$$D_T = D - r_b - t - \frac{Y_{R_{C3}}}{\cos(\gamma)}$$

where

t blade thickness at the throat

$$h = \sqrt{R_c^2 - \left(\frac{c}{2}\right)^2}$$

$$H = \sqrt{R_c^2 - \left(\frac{c}{2} - x_T\right)^2}$$

$$\cos(\gamma) = \frac{\sqrt{R_{c2}^2 - \left(\frac{c}{2} - x_T\right)^2}}{R_C}$$

$$Y_{R_c} = H - h$$

Then, for any of the three arcs:

$$Y_{R_{Ci}} = \sqrt{R_{Ci}^2 - \left(\frac{c}{2} - x_T\right)^2} - \sqrt{R_{Ci}^2 - \left(\frac{c}{2}\right)^2}$$

3.1.2. NACA 65 AND BRITISH C SERIES OF AIRFOILS

The NACA 65 and British C series of airfoils are described by the half thickness distribution, according to Table 3-1 below.

Table 3-1 - 65- and C- series of aerofoils

% chord	Half thickness (t/c) (NACA 65 series)	Camber line chord Cl=1.0 (NACA 65 series)	Half thickness for C profile
0	0.0	0.0	0.0
0.5	0.772	0.250	
0.75	0.932	0.350	
1.25	1.169	0.535	1.375
2.5	1.574	0.930	1.94
5,0	2.177	1.580	2.675
7.5	2.647	2.120	3.225
10	3.040	2.585	3.6
15	3.666	3.365	4.175
20	4.143	3.980	4.55
25	4.503	4.475	
30	4.760	4.860	4.95
35	4.924	5.150	
40	4.996	5.355	4.81
45	4.963	5.475	
50	4.812	5.515	4.37
55	4.530	5.475	
60	4.146	5.355	3.75
65	3.682	5.150	
70	3.156	4.860	2.93
75	2.584	4.475	
80	1.987	3.980	2.05
85	1.385	3.365	
90	0.810	2.585	1.12
95	0.306	1.580	0.65
100	0.0	0.0	0.0
L.E.radius	0.687		0.8

The throat width can be calculated in a similar way to that used for double circular arc blades.

3.1.3. BLADE SWEEP AND SKEW

Blades are said to have sweep when the flow direction is not perpendicular to the leading edge [14] . Fig. 3.2

shows the sweep angle.

Blades are said to have skew when the blade surface is not radial. Fig. 3.3 shows the blade skew angle.

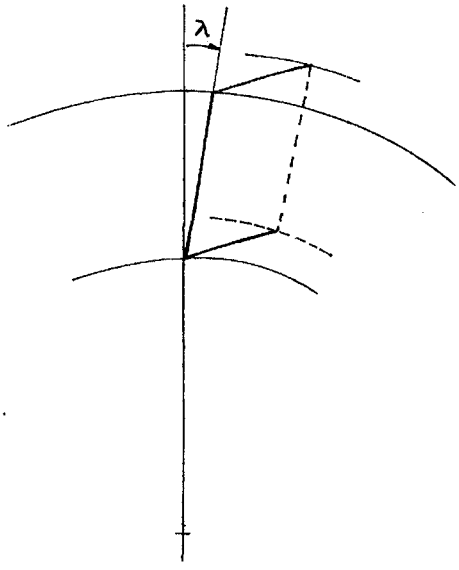

λ = skew angle

Figure 3-3 - Blade skew

Let ε be the streamline slope, γ the sweep and λ the skew. Then, for angles measured on a cylindrical surface, the actual blade angle in the streamline direction is given by

$$\beta_{1s} = \mathrm{tg}^{-1}\left\{\frac{\cos(\varepsilon_1 + \gamma_1)}{\cos(\gamma_1)}\mathrm{tg}(\beta_{1c}) - \sin(\varepsilon_1)\mathrm{tg}(\lambda_1)\right\}$$

$$\beta_{2s} = \mathrm{tg}^{-1}\left\{\frac{\cos(\varepsilon_2 + \gamma_2)}{\cos(\gamma_2)}\mathrm{tg}(\beta_{2c}) - \sin(\varepsilon_2)\mathrm{tg}(\lambda_2)\right\}$$

4. - INCIDENCE

For low speed flows, the NASA minimum loss incidence model [15] is adopted since it is considered to give sufficiently accurate results. The incidence at which minimum loss occurs can be calculated by

$$i^* = K_i(i_0)_{10} + n\theta + (i_D - i_{2D}) \qquad (4.1)$$

where

$K_i(i_0)_{10}$ represents the effect of the blade shape,

$n\theta$ represents the effect of the amount of the turning of the air by the blade

$(i_C - i_{2D})$ represents the correction of the two-dimensional results due to the actual three-dimensional process in a real compressor.

Values of the parameters K_i, $(i_0)_{10}$, n, θ and $(i_C - i_{2D})$ are taken from NASA SP 36 [15].

However, for modern compressors, the flow velocity exceeds the limits of validity of (4.1). For sonic and supersonic flows, cascade experiments have confirmed that there is only one incidence at which minimum losses are achieved: **the unique incidence**. For these high-speed flows, the minimum loss is attained when the flow is parallel to

the blade suction surface. Therefore, equation (4.1) cannot be expected to give accurate results because the term $(i_C - i_{2D})$, which takes account of the effect of Mach number, does not reflect the geometry of the blade. The values of $(i_C - i_{2D})$ given by [15], can represent the true Mach number effect only for a particular radial distribution of maximum thickness-chord ratio.

Equation (4.1) can be applied, with accuracy, only when the flow Mach number is less than 0.5. Thus, for Mach numbers between 0.5 and 1.0, the minimum loss incidence is somewhere between i^* and i^{**} , the unique incidence. As M increases from lower to higher values, the assumption of a sinusoidal variation of $(i_C - i_{2D})$ against Mach number is confirmed by experiments. This can be represented by the equation

$$i_{ml} = i^* + \frac{1}{2}\left(i^{**} - i^*\right)\left\{1 + \sin\left(\frac{\pi}{2}\frac{M_1 - M_0}{1 - M_0}\right)\right\} \qquad (4.2)$$

where M_0 = 0.5 and is the point at which some discrepancy, from the low speed results, occurs.

An alternative method of predicting the minimum loss incidence for sonic and supersonic flows is credited to Levine [16] and [17]. The more advanced user may wish to incorporate this when considering calculations inside blade passages.

Minimum loss conditions are generally used for the design of compressors. The actual incidence, however, depends on the compressor speed and mass flow and is dependent on radial distribution of flow at the blade leading edge. This radial distribution is modelled here by the streamline curvature model and can therefore be obtained from the integration of the equations of motion, continuity, energy and state, as formulated previously.

5. - DEVIATION

5.1. DESIGN

For low speed flows the NASA minimum loss deviation model [15] and Carter's rule [18] are accepted as giving equivalent and sufficiently accurate results. Therefore, both can be applied without major restrictions. The model proposed in NASA SP 36 is in fact, an improvement to Carter's simple rule.

Minimum loss deviation can now be calculated by

$$\delta^* = K_\delta(\delta_0)_{10} + m\sigma^{-b}\theta + (i_c - i_{2D})\left(\frac{d\delta}{di}\right)_{2D} + (\delta_c - \delta_{2D}) \qquad (5.1)$$

SP-36

or

$$\delta^* = m_c\sigma^{-\frac{1}{2}}\theta \qquad (5.2)$$

CARTER

where

$K_\delta(\delta_0)_{10}$ represents the influence of the blade shape and the blade thickness for values other than 10% of chord.

$m\sigma^{-b}\theta$ and $m_c\sigma^{-\frac{1}{2}}\theta$ represent both the influence of the amount of flow turning and the blade

setting

$(i_c - i_{2D})\left(\frac{d\delta}{di}\right)_{2D}$ and $(\delta_c - \delta_{2D})$ represent the correction of two-dimensional results to the actual three-dimensional process in a compressor.

The definitions and the values of the above parameters are as those given in [15].

In equation (5.2), the term m_c can be calculated by (5.3), which is curve fit to the original curve proposed by Carter.

$$m_c = 2.6111\text{x}10^{-5}\zeta^2 + 8.8333\text{x}10^{-4}\zeta + 0.216 \qquad (5.3)$$

where ζ is the stagger.

For modern compressors, however, the flow velocity is usually very high and the deviations observed in actual tests are higher than those predicted by either method. It has been observed [7], that when the inlet Mach number is above the critical, the amount of turning that has to be added to the low speed deviation can be evaluated by

$$\delta_{M1} = k_{M1}(M_1 - M_{1C}) \qquad (5.4)$$

where

k_{M1} is around 8,

M_1 is the inlet relative Mach number

M_{1C} is the critical Mach number defined as the

inlet Mach number that leads to sonic speed at the blade throat, due to flow acceleration in the blade passage.

Equation (5.4) is the equivalent of $(\delta_c - \delta_{2D})$.

The critical Mach number M_{1C} obviously varies with both blade section type and camber. A procedure has been devised [7] to estimate the value of M_{1C}, for DCA and equivalent circular are cambered blades. This can be represented by the following equations.

$$\frac{\Delta P_t}{\frac{1}{2}\rho V_{IC}^2} = \frac{1-\left(\frac{2}{\gamma+1}+\frac{\gamma-1}{\gamma+1}M_{IC}^2\right)^{\frac{\gamma}{\gamma-1}}}{\left(1+\frac{\gamma-1}{2}M_{IC}^2\right)^{\frac{\gamma}{\gamma-1}}-1} \qquad (5.5)$$

$$\frac{V_{max}}{V_1} = 1 + E\left(\frac{\Delta V_\omega}{\sigma V_1}\right) + F \qquad (5.6)$$

$$\frac{\Delta P_t}{\frac{1}{2}\rho V_{IC}^2} \cong \frac{V_{max}^2}{V_1^2} - 1 \qquad (5.7)$$

where]

V_{max} is the maximum velocity in the blade passage.

ΔV_ω is the change in whirl velocity across the blade and

E and F are values dependent on blade maximum thickness-chord ratio. For DCA, 65- and C-

series of compressor blades, it has been found [7] that:

$E = 0.4 + t/c$

$F = 0.03 + 0.7t/c$

These values give accurate results when compared with actual average measurements.

Therefore, V_{max} can be calculated iteratively from (5.5) to (5.7) and hence M_{1C}. It is reported that the values so obtained are within an accuracy of 8% of the maximum velocity, which is sufficient for the present flow model because the deviation correction can always be adjusted through the factor k_{M1}.

5.2. OFF-DESIGN

For off-design calculations, that is, when the flow is not entering the blade at the minimum loss incidence, there are only a few procedures reported that give accuracy. Among them, the one proposed by Swan [19] claims to predict the off-design deviation closest to actual measurements. This is based on statistical evaluations from several compressor rows, working under different conditions.

Defining an Equivalent Diffusion Factor as:

$$D^*_{eq} = \frac{V_1^*}{V_2^*}\{k_1 + k_4 f_5\} \tag{5.8}$$

then the increment in deviation at off-design conditions can be calculated, according to Swan, by

$$\delta_C = \{6.40 - 9.45(M_1 - 0.6)\}(D_{eq} - D^*_{eq}) \tag{5.9}$$

where

$$D_{eq} = \frac{V_1}{V_2}\left\{k_1 + k_2(i - i^*)^{k_3} + k_4 f_5\right\} \tag{5.10}$$

k_1 = 1.12

k_2 = 0.0070 (C – seires and DCA)

k_2 = 0.0117 (65 series)

k_3 = 1.43

k_4 = 0.61

$$f_5 = \frac{s}{c}\cos^2(\alpha_1)\left\{tg(\alpha_1) - \frac{r_2 V_{m2}}{r_1 V_{m1}} tg(\alpha_2) - \frac{U_1}{V_{m1}}\left[1 - \left(\frac{r_2}{r_1}\right)^2\right]\right\} \tag{5.11}$$

Therefore, the deviation at the off-design condition is

$$\delta = \delta^* + \delta_C \tag{5.12}$$

6. - LOSSES

The flow through blade passages is unlikely to behave as laminar, viscous and two-dimensional. Therefore, any attempt to define a mathematical model taking into account these severe restrictions could produce a meaningless performance prediction.

In order to avoid the difficulty of implementing and the costs of operating fully three-dimensional models, researchers have for some time attempted to couple semi empirical equations to the basic two-dimensional versions with success.

The literature reports many successful compressor designs based on such models. Several methods were adopted to solve the corresponding set of equations, as reported by [2], [6], [7], [19], [20].

The success of each model is linked to the way the losses are incorporated in it.

There are many factors influencing losses in a compressor. A good assessment depends on the knowledge of the mechanisms through which they act. Due to the tremendous complexity of these mechanisms through which the losses are generated, and to their interactions, it is unlikely that they act independently. Nevertheless,

different types of losses are considered as independently generated. Correction factors are then applied to overcome these approximations.

Since the early stages of compressor design, an extensive evaluation of those blade profiles best suited to axial compressors has been carried out at many research centres. Most of the results are published and available to the public but key information is retained as proprietary. Company based in-house expertise is the key to good design because it allows the incorporation of correction factors which bring the model closer to reality. Therefore, any attempts to accurately predict the behaviour of a particular compressor will be unsuccessful if that expertise is not available.

Fortunately, some researchers have incorporated their expertise into correlations of parameters which describe the flow in blade passages. Such correlations are an attempt to synthesise the results of many tests into simpler formulae or sets of curves. They are generally, averages of tests results or their statistical curve fits. Hence, they are not expected to represent each individual compressor; that is they cannot give good results every time they are applied. In other words, a general model for all compressors is unrealistic: the model can do well for some compressors and not quite so well for others.

The author does not claim here that his loss model is original. Only the interpretation of the various components to total loss and the method for combining these is original.

6.1. PROFILE LOSS

The loss model adopted in this work is an extension to the NASA SP 36 model, assuming that the total pressure loss is a result only of profile and shock losses. Frictional and secondary losses contribute to profile losses and act through independent mechanisms, i.e., the individual losses are the sum of frictional, secondary and those due to shocks. Although not occurring in the actual compressor, experience shows the results to be a good approximation to reality.

The loss model and the deviation rule are the key to a successful performance prediction model since the flow pattern is highly dependent upon them.

There are two common procedures to correlate losses for a particular type of blade.

- One is to correlate the losses with incidence, usually not making allowance for the influence of the relative position of the section, i.e.,

whether the losses are evaluated at root or at tip.

- The other is to correlate the losses with diffusion factor. These correlations are statistical approximations obtained from several blades tested at different conditions and on different compressors. They generally indicate the relative position of the sections.

The latter will be adopted in this work because it is able to represent the variation in loss near the walls in a more realistic way.

Swan [19] has produced a set of such curves, for DCA blades, for both rotor and stator. A possible criticism of his work is that he shows the loss parameters increasing from hub to tip. A more realistic case would show the loss parameter increasing near the walls only.

Monsarrat [20] has produced a set of similar curves, distributing the loss parameter with higher values near the walls, similar to what actually occurs in real compressors. He gives sets of curves for both rotors and stators, which are the result of the analysis of several transonic compressors during the design of a single stage transonic compressor. His work did not cover the problem of off-design cases.

Despite these criticisms of Swan's design correlations, both his and Monsarrat's are optional correlations that the user can adopt.

Davis and Millar [4] are reported to have applied Monsarrat's correlations with success, combined with Swan's approach for off-design.

In using the performance prediction method of this present work, the user is free to adopt either Swans' or Monsarrat's, or his own correlation.

6.1.1. SWAN'S MODEL

- design

For a particular blade section:

a) Define an Equivalent Diffusion Factor, D_{eq}, as Lieblein [12], by

$$D_{eq} = \frac{V_1}{V_2}\left\{k_1 + k_2\left(i - i^*\right)^{k_3} + k_4 f_5\right\} \qquad (6.1)$$

k_1 = 1.12

k_2 = 0.0070 (C series and DCA)

k_2 = 0.0117 (65 series)

k_3 = 1.43

k_4 = 0.61

$$f_5 = \frac{s}{c}\cos^2(\alpha_1)\left\{tg(\alpha_1) - \frac{r_2 V_{m2}}{r_1 V_{m1}} tg(\alpha_3)\right\} \qquad (5.11)$$

b) Compute the Minimum Loss Equivalent Diffusion Factor, D^*_{eq}, for the minimum loss incidence condition.

c) Compute the minimum loss wake-momentum thickness parameter $(\theta/c)^*$ through the appropriate set of curves of Fig. 6.1.

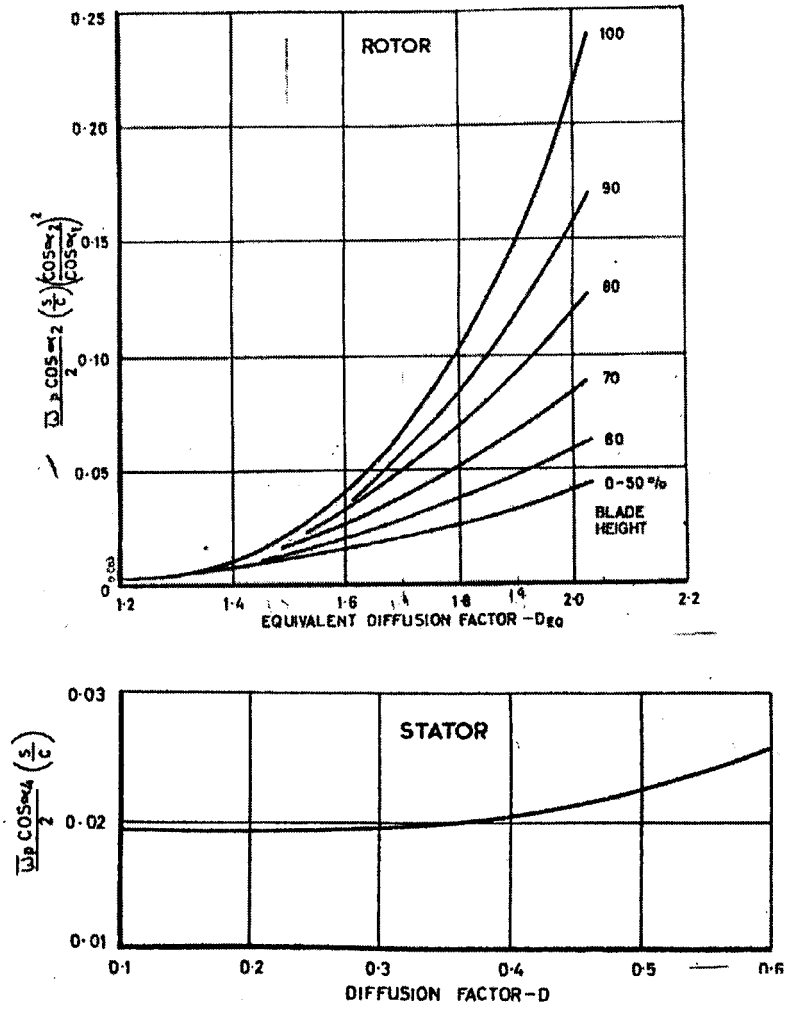

Figure 6-1 - Swan's Loss Correlations - Design

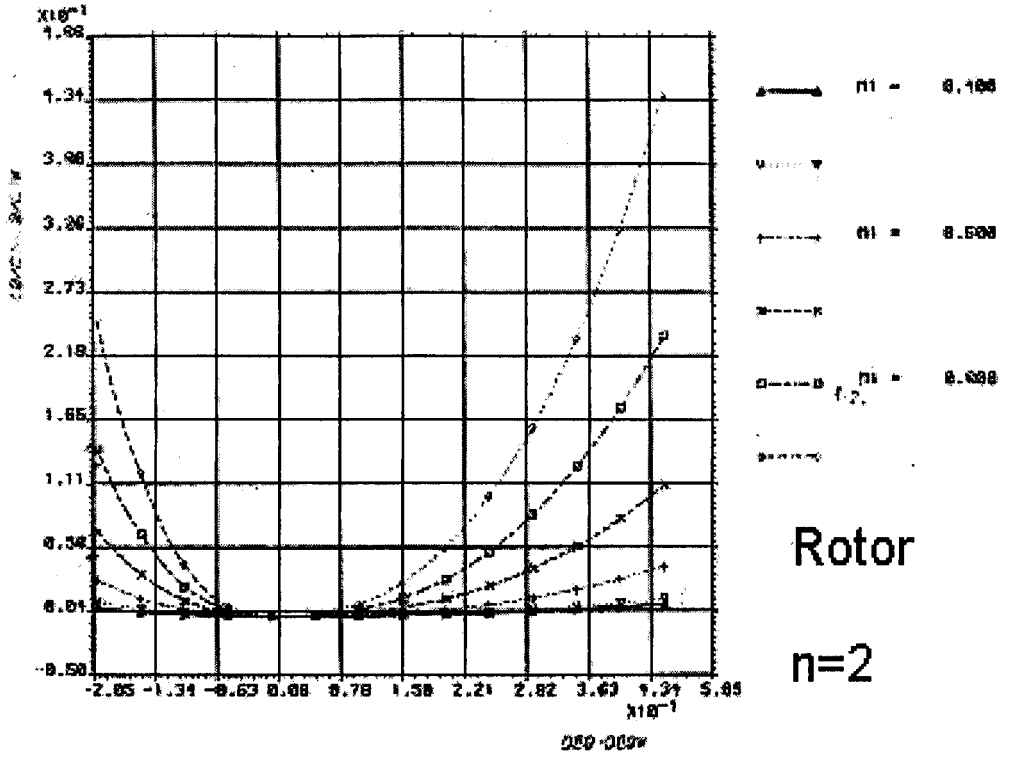

Figure 6-2 - Off-design losses - Swan Correlation for n=2.5

d) Compute the minimum loss parameter, $\overline{\omega}_p^*$, from (Fig.6.2):

$$\left(\frac{\theta}{c}\right)^* = \overline{\omega}_p^* \frac{\cos(\alpha_3^*)}{2\sigma}\left(\frac{\cos^2(\alpha_3^*)}{\cos^2(\alpha_1^*)}\right) \qquad (6.2)$$

- off-design

e) Compute the actual wake momentum thickness, (θ/c), from

$$(\theta/c) = (\theta/c)^* + F(M\ ,\ D_{eq} - D^*_{eq}\ ,\ n) \qquad (6.3)$$

where

$$F = (f_1M_1 + f_1M^2{}_1 + f_3M^3{}_1)(D_{eq} - D^*_{eq})$$

$$\left.\begin{aligned} f_1 &= 2.800 \\ f_2 &= -8.710 \\ f_3 &= 9.860 \end{aligned}\right\} \text{for } D_{eq} < D^*_{eq}$$

$$\left.\begin{aligned} f_1 &= 0.827 \\ f_2 &= -2.692 \\ f_3 &= 2.675 \end{aligned}\right\} \text{for } D_{eq} \geq D^*_{eq}$$

$$n = 2$$

It is worth mentioning that the exponent n has a strong influence on the final value of (θ/c) and, therefore, on the losses. The lower the value of n the greater is the influence of incidence on losses. The constant value of 2 for **n** cannot accommodate all types of geometry.

f) Compute the off-design loss parameter $\overline{\omega}_P$ from

$$\left(\frac{\theta}{c}\right)^* = \overline{\omega}_P \frac{\cos(\alpha_3)}{2\sigma}\left(\frac{\cos^2(\alpha_3)}{\cos^2(\alpha_1)}\right) \qquad (6.4)$$

g) if the inlet flow is supersonic, calculate the shock loss parameter, $\overline{\omega}_{SH}$ by the standard NASA model.

h) Compute the total loss parameter $\overline{\omega}_T$ from

$$\overline{\omega}_T = \overline{\omega}_P + \overline{\omega}_{SH} \qquad (6.5)$$

As far as stall was concerned, if D_{eq} was of the order of 2.0 to 2.2, flow separation was present in many blades analysed. Therefore, a value of D_{eq} = 2.2 is adopted as an indication of blade section stalling in this work.

The limit of operation with negative incidence is set as the condition where the total pressure loss coefficient exceeds twice the minimum loss coefficient for the blade element. Experiments reveal that either separation occurs on the pressure surface or channel choking takes place at high mass flows.

6.1.2. MONSARRAT'S MODEL

Monsarrat's model is, in fact, an adaptation of Swan's model, but the correlation curves, for the design profile losses, are different. Monsarrat derived his correlations for the design of a particular compressor stage, analysing test results from several high speed compressors. His method is as follows

For a particular blade section:

(a) Define the Minimum Loss Diffusion Factor with allowance for radial variation, in a similar way to Lieblein [12], by

$$D^* = 1 - \frac{V_2^*}{V_1^*} + \frac{r_1}{r_1 + r_2}\frac{s}{c}\left[tg(\alpha_1^*) - \frac{r_2 V_{m2}^*}{r_1 V_{m1}^*} tg(\alpha_3^*) \right] \qquad (6.6)$$

(b) Compute the minimum loss parameter $\overline{\omega}_P^*$ from

$$\left(\frac{\theta}{c}\right)^* = \overline{\omega}_P^* \frac{s}{c} \frac{\cos(\alpha_3)}{2} \qquad (6.7)$$

Monsarrat's model is defined only for the design (minimum loss) condition (Fig. 6.3).

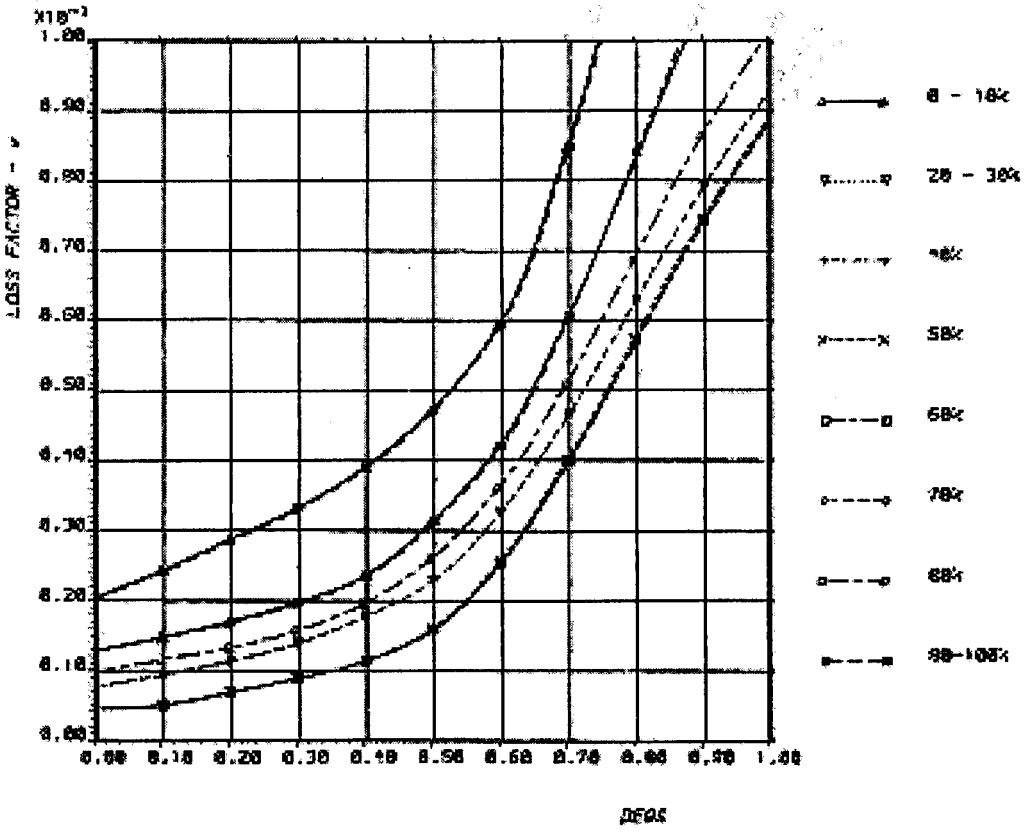

a- spanwise loss distribution - rotor

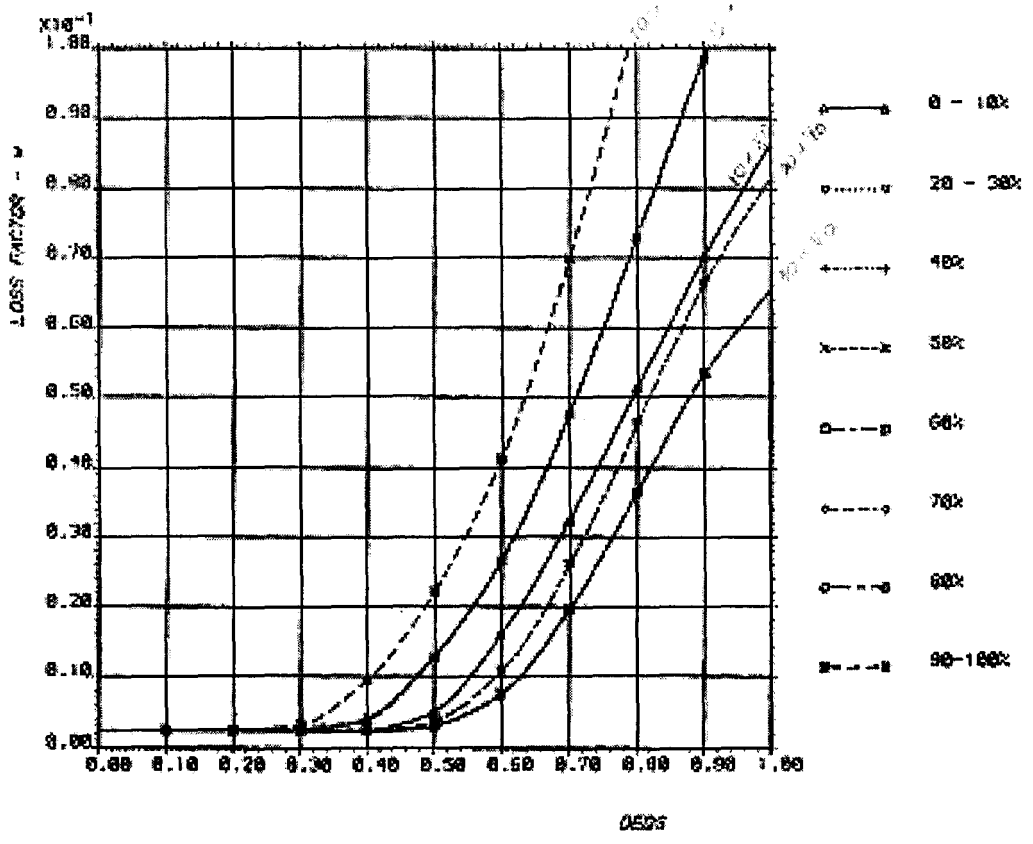

b- spanwise loss distribution - stator

Figure 6-3 - Monsarrat Loss correlations

6.1.3. MOFFATT AND JENSEN'S MODEL

For a particular blade section:

(a) Define the Minimum Loss Diffusion Factor by

$$D^* = 1 + \frac{V^*_{max}}{V^*_1} - \frac{V^*_2}{V^*_1} \qquad (6.8)$$

in the same way as Lieblein [12].

(b) Compute the minimum loss parameter $\overline{\omega}_P^*$ by the equation derived from NASA SP 36

$$\omega_P^* = \frac{2}{\frac{s}{c}\cos(\alpha_2^*)}\left(0.003 + 0.02375D^* - 0.05(D^*)^2 + 0.125(D^*)^3\right) \tag{6.9}$$

(c) If the section operates above the critical Mach number, add to the minimum loss parameter a correction given by

$$\overline{\omega}_{cor}^* = \overline{\omega}_P^*[2(M_1 - M_{1C})] \tag{6.10}$$

(d) If the relative inlet Mach number is in excess of 0.7, correct the following positive stalling, negative stalling and, by

$$\alpha_{1_{-s}}^* = \alpha_{1_{-s}} \tag{6.11}$$

$$\alpha_{1_{+s}}^* = \alpha_{1_{+s}} + 15(M_1 - 0.7) \tag{6.12}$$

$$\alpha_{1_{ml}}^* = \alpha_1^* + 10(M_1 - 0.7) \tag{6.13}$$

(e) If the blade section is operating away from the design condition, compute the loss parameter by

$$\overline{\omega}_p = \overline{\omega}_p^*\left(1 + 0.1667S - 0.8333S^2\right) \tag{6.14}$$

where

$$S = \frac{\alpha_1 - \alpha_1^*}{\alpha_{1_{-s}} - \alpha_1^*} \qquad \text{if } \alpha_1 < \alpha_1^* \tag{6.15}$$

$$S = \frac{\alpha_1 - \alpha_1^*}{\alpha_{1_{+s}} - \alpha_1^*} \qquad \text{if } \alpha_1 \geq \alpha_1^* \tag{6.16}$$

6.1.4. DAVIS AND MILLAR'S MODEL

(a) Compute (θ/c) as per modified Monsarrat model and thus $\overline{\omega}_p^*$. Multiply $\overline{\omega}_p^*$ by a Reynolds number correction factor.

(b) If $M > M_{1C}$, add a correction to the minimum loss parameter, $\overline{\omega}_{cor}$, as per Moffatt and Jensen. If the blade operates away from design, then

(c) Compute the off-design loss parameter, $\overline{\omega}_p$, as per Swan.

(d) If the flow is supersonic, compute the shock loss parameter, $\overline{\omega}_{SH}$, by the standard NACA procedure.

(e) compute the actual loss parameter by

$$\overline{\omega}_p = \overline{\omega}_p^* f_{Re} + \overline{\omega}_{SH} + \overline{\omega}_{cor}$$

6.1.5. THE PRESENT MODEL

This model is basically that defined by Davis and Millar above.

(a) Calculate the minimum loss parameter, $\overline{\omega}_p^*$, either by Swan's or by Monsarrat's modified correlations.

(b) Calculate a correction to $\overline{\omega}_p^*$, when the blade is operating above critical Mach number, as per Moffatt.

(c) If the flow is supersonic, compute the shock losses, $\overline{\omega}_{SH}$, by the standard NACA procedure.

(d) Compute the secondary loss parameter, $\overline{\omega}_{sec}$, either by Howell [21] or by Griepentrog [22] (See section 6.3).

(e) Calculate the Reynolds number influence, f_{Re}, on frictional losses, in a similar way to Raw [23] (See Section 6.5).

(f) Compute the off-design loss parameter using Swan's modified correlations

(g) Compute the total loss parameter by

$$\overline{\omega}_T = \overline{\omega}_p \times f_{Re} + \overline{\omega}_{sec} + \overline{\omega}_{SH} + \overline{\omega}_{cor} \qquad (6.17)$$

After the total pressure loss parameter has been

calculated, the total pressure leaving the blade is known for a given inlet flow condition.

The total pressure loss parameter is defined as

$$\overline{\omega}_T = \frac{P_{t_{1R}} - P_{t_{2R}}}{P_{t_{1R}} - P_{t_R}} \tag{6.18}$$

where R stands for relative conditions.

The relative total pressure ratio is defined by

$$\left(\frac{P_{t_{2R}}}{P_{t_{1R}}}\right)_{ideal} = \left\{1 + \frac{\gamma - 1}{2} M_T^2 \left[1 - \left(\frac{r_1}{r_2}\right)^2\right]\right\}^{\frac{\gamma}{\gamma-1}} \tag{6.19}$$

where

$$M_T^2 = \frac{U^2}{\gamma R T_{t_{1R}}}$$

and

$$T_{t_{1R}} = T_{t_1} - \frac{V_0^2 - V_1^2}{2c_p}$$

is the relative total temperature at blade inlet

The absolute total pressure ratio is defined by

$$\frac{P_{t_2}}{P_{t_1}} = \frac{\left(\frac{P_{t_{2R}}}{P_{t_{1R}}}\right)}{\left(\frac{P_{t_{2R}}}{P_{t_{1R}}}\right)_{ideal}} \left(\frac{T_{t_2}}{T_{t_1}}\right)^{\frac{\gamma}{\gamma-1}} \tag{6.20}$$

The absolute total temperature ratio can be calculated from the energy equation:

$$H_{t2} - H_{t1} = U_2V_{\omega 2} - U_1V_{\omega 1} \tag{6.21}$$

$$\bar{c}_p\left(T_{t_2} - T_{t_1}\right) = U_2V_{\omega_2} - U_1V_{\omega_1}$$

so that

$$\frac{T_{t_2}}{T_{t_1}} = 1 + \frac{U_2V_{\omega_2} - U_1V_{\omega_1}}{\bar{c}_pT_{t_1}} \tag{6.22}$$

Combining the above equation and bearing in mind that

$$\frac{P_{t_{1R}}}{P_{1R}} = \left(1 + \frac{\gamma - 1}{2}M_1^2\right)^{\frac{\gamma}{\gamma-1}} \tag{6.23}$$

$$\frac{P_{t_{2R}}}{P_{t_{1R}}} = \left(\frac{P_{t_{2R}}}{P_{t_{1R}}}\right)_{ideal} - \bar{\omega}_T\left(1 - \frac{P_{1R}}{P_{t_{1R}}}\right) \tag{6.24}$$

finally,

$$\frac{P_{t_2}}{P_{t_1}} = \left\{1 - \bar{\omega}_T \frac{1 - \left(\frac{P_{1R}}{P_{t_{1R}}}\right)}{\left(\frac{P_{t_{2R}}}{P_{t_{1R}}}\right)_{ideal}}\right\}\left(\frac{T_{t_2}}{T_{t_1}}\right)^{\frac{\gamma}{\gamma-1}} \tag{6.25}$$

6.2. SHOCK LOSSES

There are several models for the evaluation of shock losses, but the simplest that gives reasonable results is the well-known NACA Model [24].

The NACA Model approximates the actual three-dimensional shock by a two-dimensional normal shock which would originate at the blade leading edges, normal to the mean streamline midway between two consecutive blades, as indicated by Fig. 6.4.

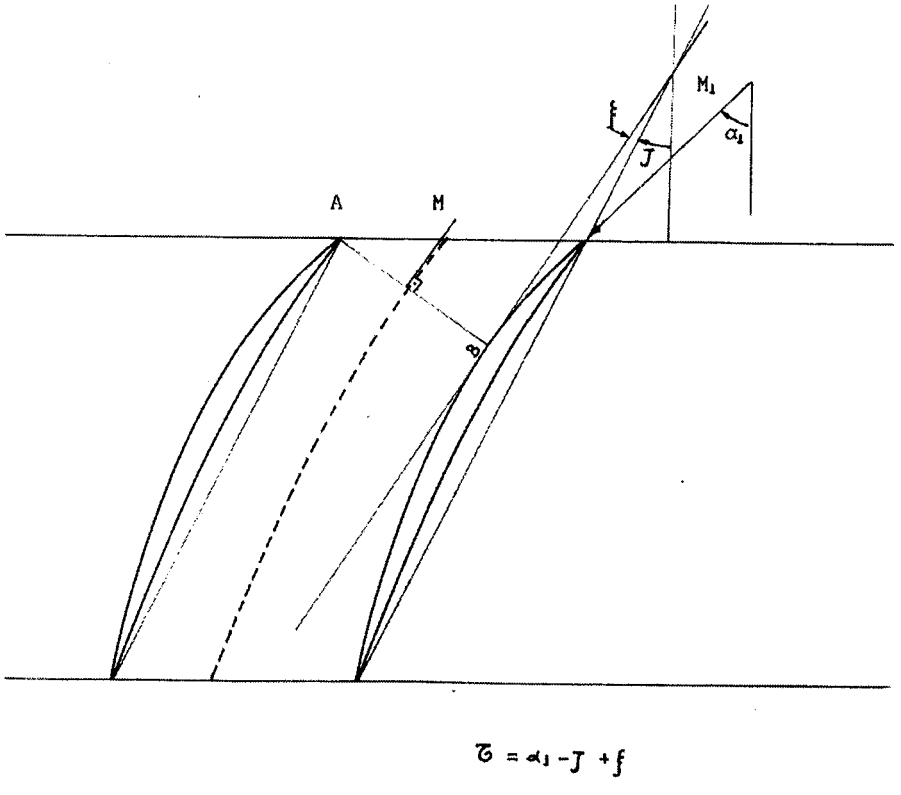

Figure 6-4 - Shock loss model

The Mach number just before the shock is computed by the arithmetic mean of the inlet Mach number M_1 and the resulting Mach number of a free Prandtl-Meyer expansion over the blade suction surface, from the inlet to the shock intersection point (point B on Fig. 6.4).

Let

M_1 be the relative inlet Mach number,

ξ be the angle between the chord and the tangent to the suction surface at B.

The amount of air turning, τ, from the leading edge to point B is, therefore,

$$\tau = \alpha_1 - \zeta + \xi \tag{6.26}$$

The Prandtl-Meyer expansion [15] can be estimated by

$$\Delta\theta = \theta_B - \theta_A \tag{6.27}$$

where

$$\theta_A = \theta_{ref} + \sqrt{\frac{\gamma+1}{\gamma-1}}\,tg^{-1}\left[\sqrt{\frac{\gamma+1}{\gamma-1}\left(M_A^2 - 1\right)}\right] - tg^{-1}\left[\sqrt{M_A^2 - 1}\right] \tag{6.28}$$

$$\theta_B = \theta_{ref} + \sqrt{\frac{\gamma+1}{\gamma-1}}\,tg^{-1}\left[\sqrt{\frac{\gamma+1}{\gamma-1}\left(M_B^2 - 1\right)}\right] - tg^{-1}\left[\sqrt{M_B^2 - 1}\right] \tag{6.29}$$

Then

$$\theta_B - \theta_A = \tau = \sqrt{\frac{\gamma+1}{\gamma-1}}\,tg^{-1}\left[\sqrt{\frac{\gamma+1}{\gamma-1}\left(M_B^2-1\right)}\right] - tg^{-1}\left[\sqrt{M_B^2-1}\right] + \\ - \sqrt{\frac{\gamma+1}{\gamma-1}}\,tg^{-1}\left[\sqrt{\frac{\gamma+1}{\gamma-1}\left(M_1^2-1\right)}\right] + tg^{-1}\left[\sqrt{M_1^2-1}\right] \tag{6.30}$$

Let

$$k_2 = \sqrt{\frac{\gamma+1}{\gamma-1}}\,tg^{-1}\left[\sqrt{\frac{\gamma+1}{\gamma-1}\left(M_1^2-1\right)}\right] + tg^{-1}\left[\sqrt{M_1^2-1}\right]$$

then

$$\tau = \sqrt{\frac{\gamma+1}{\gamma-1}}\,tg^{-1}\left[\sqrt{\frac{\gamma+1}{\gamma-1}\left(M_B^2-1\right)}\right] - tg^{-1}\left[\sqrt{M_B^2-1}\right] - k_2 \tag{6.31}$$

Therefore

$$M_B = \left\{1+\left[\sqrt{\frac{\gamma+1}{\gamma-1}}\,tg\left[\frac{\tau+k_2+tg^{-1}\left(M_B^2-1\right)^{\frac{1}{2}}}{\sqrt{\frac{\gamma+1}{\gamma-1}}}\right]\right]^2\right\}^{\frac{1}{2}} \tag{6.32}$$

Equation (6.32) is a recurrent formula to solve for M_B.

Once M_B is calculated, the shock loss $\overline{\omega}_{SH}$ is computed assuming a normal shock occurs and the flow is slowed down from $M = (M_1 + M_B)/2$, to the corresponding Mach number after the shock. Then:

$$\overline{\omega}_{SH} = \frac{P_{t_1} - P_{t_B}}{P_{t_1} - P_1} \tag{6.33}$$

From isentropic and normal shock relations,

$$\frac{P_{t_1}}{P_1} = \left(1 + \frac{\gamma - 1}{2} M_1^2\right)^{\frac{\gamma}{\gamma-1}} \tag{6.34}$$

$$\frac{P_{t_B}}{P_1} = \frac{\left(\frac{\gamma - 1}{2} M^2\right)^{\frac{\gamma}{\gamma-1}}}{\left(\frac{2\gamma M^2 - (\gamma - 1)}{\gamma + 1}\right)^{\frac{1}{\gamma-1}}} \tag{6.35}$$

If $M = (M_1 + M_B)/2$, equation (6.33) can be rewritten as

$$\overline{\omega}_{SH} = \frac{1 - \frac{P_{t_B}}{P_{t_1}}}{1 - \frac{1}{\frac{P_{t_1}}{P_1}}} \tag{6.36}$$

or

$$\overline{\omega}_{SH} = \frac{1 - \frac{\frac{P_{t_B}}{P_1}}{\frac{P_{t_1}}{P_1}}}{1 - \frac{1}{\frac{P_{t_1}}{P_1}}} \tag{6.37}$$

The Prandtl-Meyer angle, τ, can be computed [13] by:

$$\tau = \alpha_1 - \zeta + \xi \tag{6.38}$$

where

α_1 is the air angle

ζ is the stagger

$$\xi = \sin^{-1}\left\{\left(\frac{2x}{c'} - 1\right)\sin\left(\frac{\phi_S}{2}\right)\right\}$$

$c' = c - 2r_b$

$$\phi_S = 4tg^{-1}\left\{\frac{1-\cos\left(\frac{\theta}{2}\right)}{\sin\left(\frac{\theta}{2}\right)} + \frac{t_e - 2r_b}{c'}\right\}$$

$$\frac{2x}{c'} = 1 + \sin(2\Sigma)\cot g\left(\frac{\theta}{2}\right) - \cos(2\Sigma)$$

$$\Sigma = tg^{-1}\left\{\frac{\sin(\beta_1)\sin\left(\frac{\theta}{2}\right)}{\frac{c'}{s} + \cos(\beta_1)\sin\left(\frac{\theta}{2}\right)}\right\}$$

t_e = maximum thickness

c = chord

r_b = leading edge radius

θ = camber

6.3. SECONDARY LOSSES

Secondary flows in both cascades and turbomachines have been the subject of interest for several decades. So far, they are not yet completely understood.

Many theories have also been published on the subject,

a review of which can be found in [25]. As far as implementation into a computer programme is concerned, as part of an overall performance calculation, one must look for approaches that are simple when translated into equations but give accurate results.

Griepentrog [22] has stressed the importance of methods to evaluate secondary losses in axial compressors and compared some of the methods, from the simplest based only on the flow turning angle, to the more complex viscous models.

Obviously, simple models may not offer accuracy when highly loaded blades are analysed. The most sophisticated methods cannot be treated in the present context. Therefore, a compromise must be found and semi-empirical rules, like those the suggested in [22] adopted.

In this work, two options are available, one using the Howell method [21] and the other using Griepentrog's [22] semi-empirical rule.

6.3.1. HOWELL'S METHOD

Assumes the secondary loss is dependent only on the angle of turning of the air.

Defining $\alpha_m = \frac{1}{2}(\alpha_1 + \alpha_2)$

$$C_L = \frac{2\cos(\alpha_m)}{\sigma}\left[tg(\alpha_1) - tg(\alpha_2)\right] \tag{6.39}$$

$$C_{D_{is}} = 0.018 C_L^2 \tag{6.40}$$

$$\overline{\omega}_{sec} = \sigma\left(\frac{\cos(\alpha_1)}{\cos(\alpha_2)}\right)^2 C_{D_{is}} \tag{6.41}$$

Many researches have tried to improve equation (6.40), taking account of aspect ratio, solidity, etc. Vavra [26], for example, suggested equation (6.40) could be replaced by

$$C_{D_{is}} = \frac{0.04}{h/c} C_L^2 \tag{6.42}$$

Ehrich and Detra [27] combined aspect ratio and solidity and suggested equation (6.40) could be replaced by

$$C_{D_{is}} = 0.1178\ \theta^2 \frac{1}{\frac{h}{c}\frac{c}{s}\left(1 - \frac{2}{\frac{h}{c}\frac{c}{s}}\right)^3} \tag{6.43}$$

For blades of conventional h/c and s/c the results calculated by either of the above hypotheses (6.42 and 6.43) are similar.

6.3.2. GRIEPENTROG'S METHOD

An approximation is made to the flow in cascade blade passages and the induced drag due to trailing edge vortices is calculated by

$$C_{D_{is}} = 0.25\, C_L^2 \sigma \frac{1 - \frac{h'}{h}}{\left(1 - \left(1 - \frac{h'}{h}\right)^2\right)^{\frac{1}{2}}} \qquad (6.44)$$

where

$$\frac{h'}{h} = 1 - 0.75\,\frac{\delta}{H} \qquad (6.45)$$

where δ is the boundary layer thickness

$$\overline{\omega}_{sec} = \frac{\sigma C_{D_{is}}}{\cos(\alpha_m)} \qquad (6.46)$$

Different blades have been analysed [22] and good agreement between theoretical and measured values reached.

$\frac{\overline{\omega}_{sec}}{\overline{\omega}_{total}}$ is correlated against $\theta \frac{h}{c}$.

Let

$$f = \frac{\overline{\omega}_{sec}}{\overline{\omega}_{total}}$$

$$\overline{\omega}_{total} = \overline{\omega}_{P} + \overline{\omega}_{SH}$$

Then

$$\overline{\omega}_{sec} = \left(\overline{\omega}_{P} + \overline{\omega}_{SH}\right)\frac{f}{1+f} \qquad (6.47)$$

6.4. FRICTION LOSSES

Experience has shown that friction losses in the bladeless spaces are negligible when compared with other sources of loss. Nevertheless, when either long ducts are used or rows are far apart, friction losses must be taken into account. The computer program can calculate these, provided dummy blades are defined in those regions.

The losses are then calculated after a total pressure loss parameter has been specified and can be evenly distributed from hub to casing or lumped in the wall streamlines.

6.5. REYNOLDS NUMBER EFFECT

Since the loss correlations are derived for high Reynolds numbers, it is necessary to take account of the additional losses associated with low Reynolds numbers. In such cases, profile losses are higher than those estimated. A typical way to correct profile losses is by penalising them with a factor given by:

$$\left(\frac{Re}{Re_0}\right)^{0.2} \qquad \text{for } Re < Re_0 = 2.5\text{x}10^5. \tag{6.48}$$

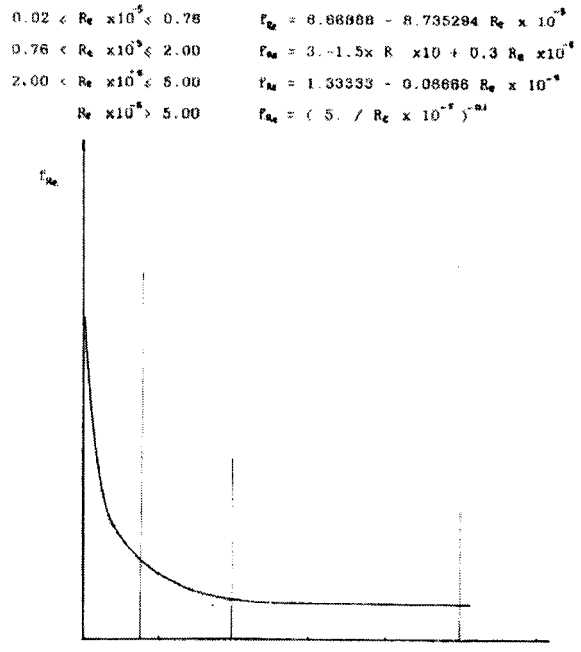

Figure 6-5 - Reynolds number effect on profile loss

The model adopted in this programme takes account of the fact that the losses are further increased due to the onset of laminar boundary-layer separation which occurs

below a certain limiting value of Reynolds number. This is a similar method to that shown in NASA SP 36 (figure 6.5) and by Raw [23].

The chord Reynolds Number is defined by

$$Re = \frac{V_1 c \rho_1}{\mu_1} \tag{6.49}$$

where

V_1 is the relative inlet velocity

c is the blade chord in the streamline direction

ρ_1 is the density

μ_1 is the absolute viscosity, calculated by Sutherland's relation below:

$$\mu = \frac{145.8187 \times 10^{-8} T_1^{1.5}}{110.35 + T_1} \tag{6.50}$$

Blade profile losses are corrected by multiplying the values obtained from the Swan correlation with the correction factor shown on Fig. 6.5:

$$\overline{\overline{\omega}}_p = \overline{\omega}_p \times f_{Re} \tag{6.51}$$

7. - ALGORITHMS

7.1. THE EXTERNAL ALGORITHM

The formulation of the flow model leads to a set of equations derived from consideration of momentum, energy, continuity and the equation of state. These must be solved in the domain defined by the compressor geometry (air passages) and depend on the initial conditions (mass flow and compressor speed).

The equations are

Momentum:

$$\frac{dV_m^2}{ds} = A + BV_m^2 \tag{7.1}$$

where

$$A = 2\cos^2(\alpha)\left[\frac{\partial I}{\partial s} - T\frac{\partial S}{\partial s}\right]$$

$$B = \cos^2(\alpha)\left[\begin{array}{l}\dfrac{\cos(\varepsilon+\gamma)}{R_c} - \dfrac{tg(\alpha)}{\cos^2(\alpha)}\dfrac{\partial\alpha}{\partial s} + \dfrac{2U}{V_m}tg(\alpha)\dfrac{\cos(\gamma)}{r} + \\ -tg^2(\alpha)\dfrac{\cos(\gamma)}{r} + \dfrac{\sin(\varepsilon+\gamma)}{V_m}\dfrac{\partial V_m}{\partial m}\end{array}\right]$$

Energy:

$$H_{t1} - H_{t2} = c_P(T_{t1} - T_{t2}) = U_1 V_{w1} - U_2 V_{w2} \qquad (7.2)$$

State:

$$P = \rho RT \qquad (7.3)$$

Second law:

$$\rho = \left(\frac{H_t}{c_P}\right)^{\frac{1}{\gamma-1}} e^{\left(-\frac{S-S_0}{R}\right)} \qquad (7.4)$$

The above equations show that an analytical solution cannot be obtained and therefore, to arrive at a solution is not a straightforward matter.

Accordingly, a numerical method must be adopted to find the solution.

The geometry of the flow is part of the momentum equation and is not known in advance. Therefore, it is necessary to use an iterative process initiated by a guess of the position of the streamlines.

There are many possible algorithms that can be adopted in this iterative process. All of these lead to solutions to the problem in a different time scale.

Since the global algorithm is complex, it is convenient to define types of algorithms that perform very specific tasks. The external algorithm is the one that

gives guidance for the solution of the problem and controls other local algorithms. In the context of this work, as a rule, a local algorithm is associated with its own subroutine and the external algorithm with the main programme.

The external algorithm tasks are, therefore:

1. Interface the input data, inputting the data from files and/or from the screen, in an interactive mode.
2. Convert the input data to a suitable form compatible with the numerical method adopted.
3. Define an initial mesh in the compressor meridional plane and evaluate the geometrical properties associated with that mesh at its nodes.
4. Establish the inlet conditions at each blade row from the compressor inlet to its outlet, satisfying equations (7.1) through (7.4) above.
5. Calculate the flow properties at each blade trailing edge satisfying equations (7.1) through (7.4) above
6. Store/retrieve data for the restart capability.
7. Reassess the streamline geometry once the flow properties are known throughout the compressor, and then adopt a new configuration, if needed.
8. Accept interventions in order to modify input data,

at the user's convenience.

9. Decide when the final solution is achieved.

10. Produce a graphical output for visual assessment.

A simplified flow chart for the external algorithm is shown in Fig 7.1.

External Algorithm

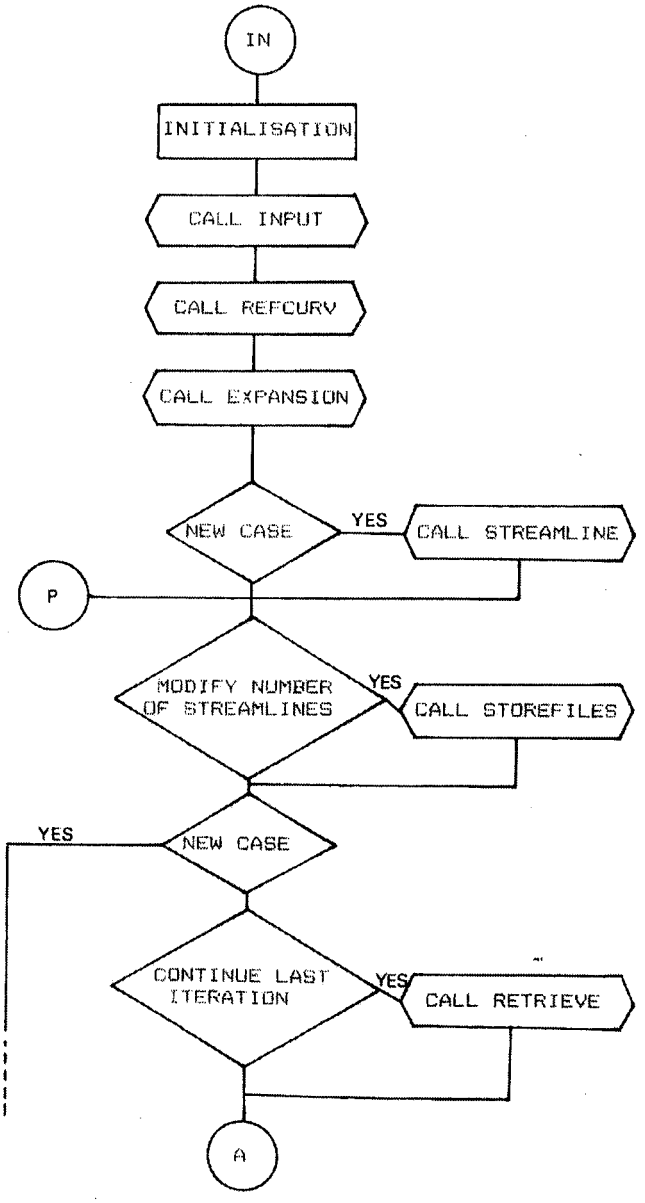

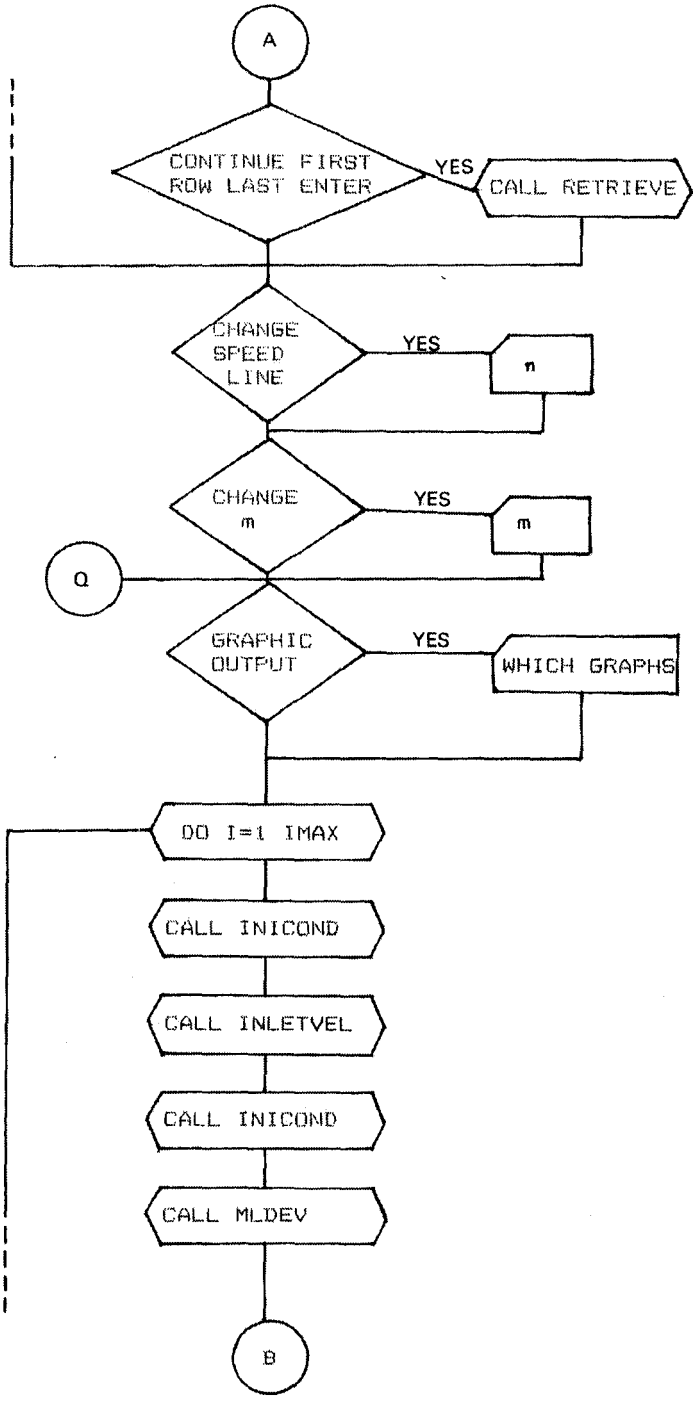
A
CONTINUE FIRST ROW LAST ENTER
YES
CALL RETRIEVE
CHANGE SPEED LINE
YES
n
CHANGE m
YES
m
Q
GRAPHIC OUTPUT
YES
WHICH GRAPHS
DO I=1 IMAX
CALL INICOND
CALL INLETVEL
CALL INICOND
CALL MLDEV
B

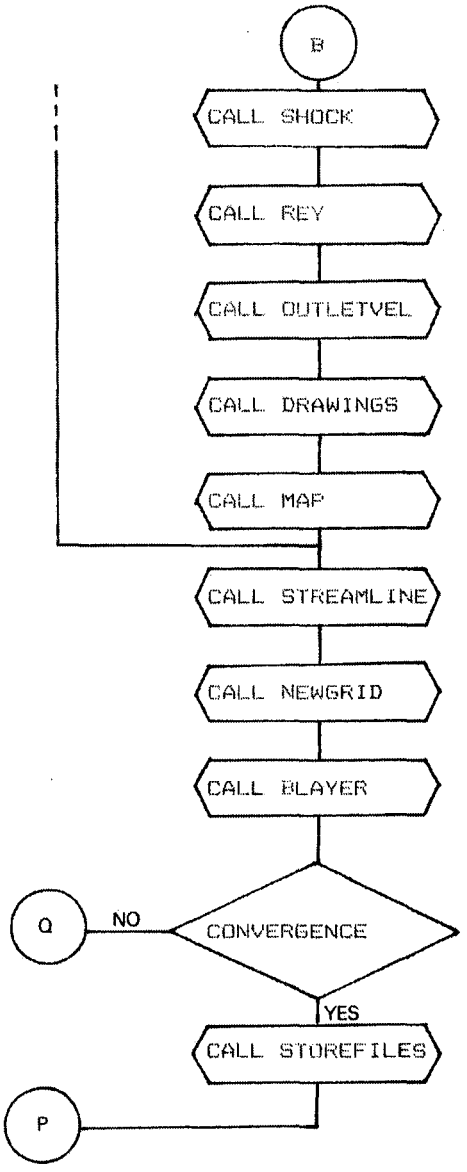

Figure 7-1 - External algorithm

7.2. THE LOCAL ALGORITHMS

Local Algorithms perform local specific tasks. Among these, only a few are worth specific attention because they

refer to special procedures chosen for the solution of the differential problem.

7.2.1. FILE MANAGEMENT ALGORITHM

During the execution of the program, several independent files are created in order to ease data handling. When fully explored, the capacity of the programme allows up to 50 different files to be utilised, some for temporary use, others for receiving the information during the analysis of a particular compressor.

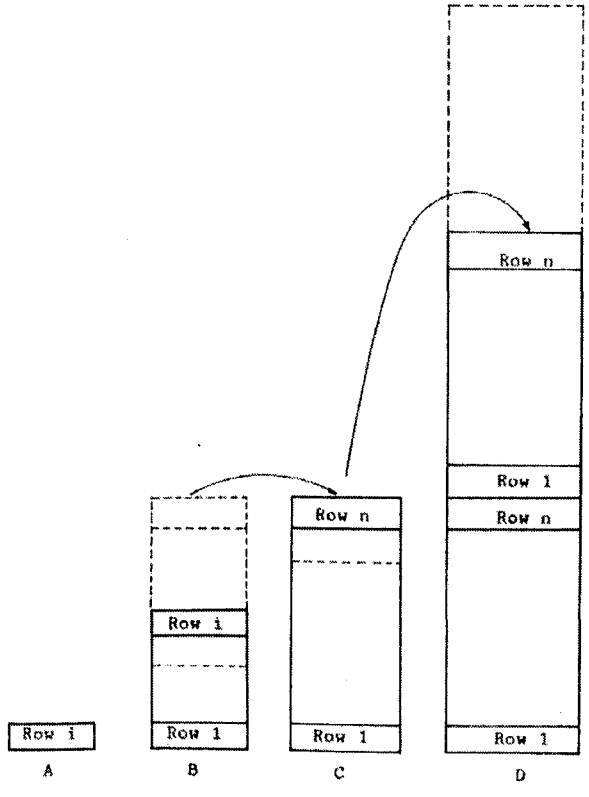

Figure 7-2 - Files Management

As a rule, there are always three files associated with the same sort of data, as indicated by Fig. 7.2:

A contains the results of the last iteration at the blade trailing edge

B contains the results of the calculations up to the actual row where the calculations are being carried out.

C contains a copy of B, after the last row is calculated and the convergence for mass flow is obtained.

D contains a copy of all C's.

File type A is used in order to recover the results of the last iteration, such that the programme can restart from the where it stopped.

File type B is used to recover results from calculations of previous rows.

File type C is used to recover results from the last iteration, when a convergence in mass flow has been achieved.

File type D is a copy of all C's such that the process can be restarted, if wished, at any point in previous iterations.

The user can decide whether to create extra files to

store data after a convergence for mass flow is achieved.

File type A is filled each time the calculations end at the blade trailing edges.

File type B is filled each time the calculations finish at the last station, at the compressor outlet.

File type C is filled each time the convergence is attained for a given mass flow and speed (in other words, when a point in the compressor map is calculated).

For the flow properties there are files type A ,B, C, and D.

For the streamlines there are files B, C and D.

For graphical output there are files B, C, and D.

Table 7-1 gives the files and their contents.

Table 7-1 - Files Management

Logical Unit	File Code	Type	Contents	Class
08	NR04	C	flow properties @ DP	P
10	NR01	C	flow properties	R
11	NR02	B	flow properties	R
12	NR03	D	flow properties	(P) Permanent
14	NG11	A	graph - streamlines	R
15	NG12	B	graph - streamlines	R
16	NG13	C	graph - streamlines	P
17	NG21	A	graph - velocities	R
18	NG22	B	graph - velocities	R
19	NG23	C	graph - velocities	P
20	NG31	A	graph - angles	R
21	NG32	B	graph - angles	R
22	NG33	C	graph - angles	P
23	NG41	A	graph - losses	R
24	NG42	B	graph - losses	R
25	NG43	C	graph - looses	P
26	NG51	A	graph - deviation	R
27	NG52	B	graph - deviation	R

28	NG53	C	graph - deviation	P
29	NG61	A	graph - Mach number	R
30	NG62	B	graph - Mach number	R
31	NG63	C	graph - Mach number	P
32	NG71	A	graph - Velocity triangles	R
33	NG72	B	graph - Velocity triangles	R
34	NG73	C	graph - Velocity triangles	P
35	NR05	B	streamlines properties	R
36	NR06	C	streamlines properties	R
37	NR07	D	streamlines properties	P
38	NR08	C	streamlines prop. @ DP	P
40	N001	B	flow properties	(R) Renewable
41	NR09	-	spare	
42	NR10	-	spare	
43	NR11	A	present row calculations	R
44	NR14	C	converged sol. flow prop.	P
45	NR15	C	converged sol. stream. prop	P
46	NR16	-	spare	
47	NR17	-	spare	
48	NR18	-	spare	
49	NR19	-	spare	
50	NR12	-	spare	

7.2.2. THE STREAMLINE ALGORITHM

The streamlines are defined in the meridional plane from hub to casing and from the compressor inlet to outlet. It is always convenient to define an annular duct both at the front and at the back of the compressor, in order to facilitate the calculation of geometric properties of the streamlines at these stations. The shape of the annular ducts must follow closely the actual compressor installation. The results that can be expected from the programme depend on the curvature of the streamlines that, in turn, are defined by the hub and casing walls.

The algorithm that is set up to evaluate those properties has the following tasks:

- Define the hub and casing walls as the inner and the outer streamlines.
- Locate the mesh points on those streamlines, corresponding to the blade leading and trailing edges.
- Locate the dummy blades in the inlet and outlet ducts.
- Divide the annulus into a given number of streamlines, with provision for varying the amount of mass flow in the streamtubes.
- Determine the remaining mesh points inside the annulus.
- Fit a smooth curve through the corresponding points at each blade to represent a streamline.
- Compute the derivatives, radii of curvature, slopes and meridional entropy gradient at each node.
- Reposition the streamlines when needed.
- Interpolate geometric data for the new positioning.

7.2.3. THE BLOCKAGE FACTOR ALGORITHM

The blockage factor accounts for the influence of boundary-layer growth on the compressor hub and casing. It is estimated by way of the meridional velocity variation at the walls, from inlet to outlet.

The algorithm for evaluating blockage factor has the following tasks:

1. Define the nodes, meridional distances and velocities at hub and casing corresponding to the blades at leading and trailing edges.
2. Interpolate those values at a larger number of points in the walls.
3. Calculate the blade wake momentum thickness at the nodes.
4. Calculate the shape factor at the nodes.
5. Calculate the boundary layer displacement thickness at the nodes.
6. Calculate the blockage at the walls.
7. Calculate the blockage factors at the blade leading and trailing edges.
8. Allow iterative intervention to change the blockage factors as well as adjustment of the coefficient to calculate the wake momentum thickness.

7.2.4. EXPANSION OF DATA ALGORITHM

The compressor geometry input data are sometimes known at points that do not coincide with the mesh nodes, either because they are measured or calculated at points outside the streamlines or because the number of streamlines differs from those given as input. It is, therefore, necessary to expand the known values to the actual calculating nodes.

The streamlines can be packed near the hub and near the casing if the mass flow distribution in each streamtube is decreased near the walls.

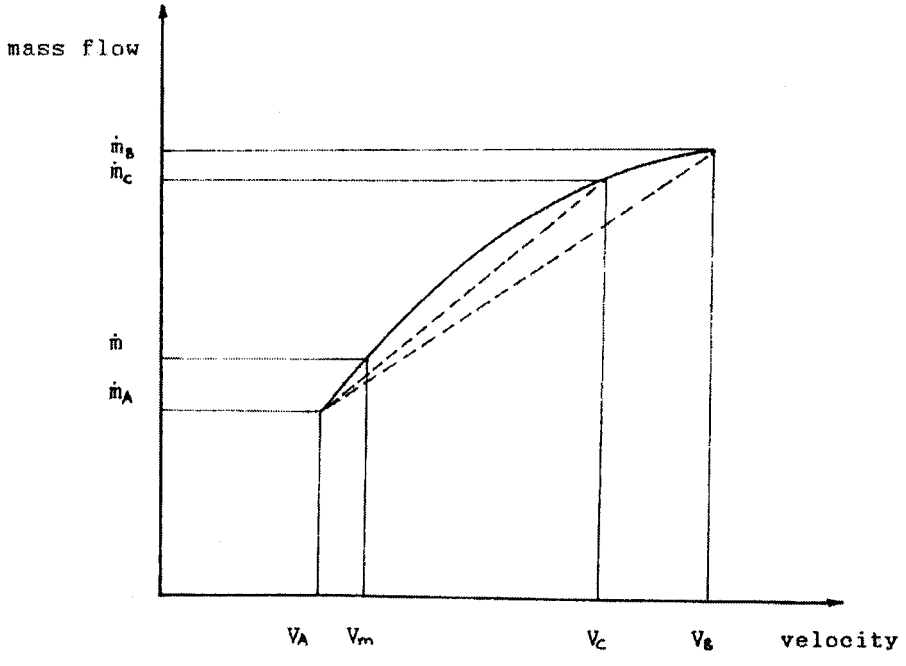

Figure 7-3 - Meridional Velocity Guesses

Fig. 7.3 indicates how to distribute the mass flow in each streamtube in order to vary the spacing between two streamlines.

According to Fig. 7.3, streamlines 1 to J2 define sections of area/mass flow A, streamlines J2 to J3 of area/mass flow kA and J3 to JMAX of A. J2 and J3 are set as a proportion of JMAX, the total number of streamlines, according to the user's convenience.

The total area is therefore

$$\{[(J2-1) + (JMAX-J3)] + k(J3-J2)\} \qquad (7.5)$$

and, consequently, each section has the fraction

$$\{(J2-1+JMAX-J3) + k(J3-J2)\} \qquad (7.6)$$

of the total area or mass flow.

The streamlines are first positioned, as a guess, according to an area distribution chosen at the beginning of the calculation. They are then repositioned as a function of mass flow, with the same distribution given by equations (7.5) and (7.6).

After the radial positions have been determined, the remaining geometrical properties are obtained by interpolation:

z_1, z_2 axial distances

c	blade chord
β_1, β_2	blade angles
ζ	stagger
s	spacing
t	maximum blade thickness
c	axial chord
s/c	space-chord ratio
t/c	thickness-chord ratio
$\sigma = c/s$	
$\theta = \beta_1 - \beta_2$	camber
γ_1, γ_2	blade radial angles
$\varepsilon_1, \varepsilon_2$	streamline slopes
λ_1, λ_2	blade skew angles
$\alpha_0, V_{\omega 0}$	inlet flow condition
T_{t1}	inlet total temperature
P_{t1}	inlet total pressure
c_p, γ	gas properties

7.2.5. INLET VELOCITY ALGORITHM

The inlet velocity algorithm is set up such that the velocity profile is calculated from hub to tip. In contrast, the outlet velocity algorithm allows for the

velocity profile being calculated from the mid-streamline.

The tasks are:

- Guess an initial position for the streamlines and calculate the geometrical properties.
- Guess a particular value for the meridional velocity at the hub.
- Calculate the average values of a selection of flow properties at a station situated half way between two consecutive streamlines.
- Calculate the meridional velocity at the next streamline, integrating the equation of radial equilibrium.
- Repeat the steps until the casing streamline is reached.
- Calculate the air mass flow, integrating the continuity equation at the blade leading edge from hub to tip.
- If the mass flow differs from the specified value, a new guess is made for the hub meridional velocity and the previous four steps repeated until the mass flow calculated matches the specified value, within a given tolerance.
- Compare the mass flow distribution with that specified, for each streamline.

- If different, interpolate for the specified mass flow, the actual positions of the streamlines.
- Reposition all the steps from the beginning, until reasonable agreement is achieved, if the interpolated values are not in agreement with those specified.

Choking is detected when an increase in the hub meridional velocity corresponds to a decrease in the mass flow.

It is left to the user to specify the process of integration of the radial equilibrium equation. The choice is between an iterative under-relaxed process and a fourth order Runge-Kutta method.

Experience shows that the Runge-Kutta method is faster for the early loops, where the guesses are far away from the final solution. The iterative under relaxed process is, however, faster for later loops.

7.2.6. OUTLET VELOCITY ALGORITHM

Experience has shown that it is not always possible to get convergence when the meridional velocity profile calculation starts at the hub. This is because, in some

cases, the large variation in loss occurring with a small change in the meridional velocity makes the process unstable. A second alternative is to start the calculations somewhere near the blade mid height where losses are lower and less susceptible to large variations with small changes in the meridional velocity.

The algorithm set up to calculate the outlet velocity profile differs from that for the inlet velocity because the streamline positioning is not yet known, while it is previously determined at the blade inlet. The constraints for the outlet are the annulus height and the fraction of the total mass flow each streamtube carries, determined by the positions of the streamlines at the blade inlet.

For calculations beginning at the hub the tasks are:

- Guess an initial value for the meridional velocity at the hub.
- Calculate the losses and outlet flow properties if the actual velocity is the initial guess.

For the remaining streamlines:

- Guess a position for the streamline at the blade trailing edge.
- Guess the meridional velocity at the outlet.
- Compute the losses and outlet flow properties if

that was the actual velocity.

- Calculate the corrected meridional velocity, integrating the radial equilibrium equation.
- If this calculated value is not in agreement with the guessed value, a new guess must be made until a reasonable agreement is achieved.
- Compute the mass flow carried by the streamtube, integrating the continuity equation.
- If the mass flow is different from the mass flow passing through the corresponding section at the blade inlet, a new guess for the position of the streamline must be made and the preceding five steps repeated until the mass flow agrees, within a specified tolerance.
- Go to the next streamline, repeating the whole cycle, until the last streamline is finished.

At this point, it is possible that the outer radius, corresponding to the last streamline, differs from the actual position of the casing. This disagreement results because the first guess for the hub meridional velocity was not good. Therefore, a new guess must be made for the hub meridional velocity, the outer loop repeated again, until agreement between the radial position at the casing and the

calculated outer radius is achieved within a specified tolerance.

After the outer loop has converged, the streamlines are already positioned throughout the trailing blade span and the calculations finished.

For the calculations beginning at the mid height, a different procedure is adopted because now the hub and casing positions are known.

The tasks are:

- Guess the positions of the streamlines from the hub to tip.
- Guess an initial meridional velocity for the position chosen (usually the mean streamline).
- Calculate the losses and flow properties assuming the velocity is correct.

Repeat for the next streamline, up to the casing and down to the hub:

- Guess an initial meridional velocity.
- Compute the losses and outlet flow properties

Assuming that the velocity is correct:

- Calculate the corrected meridional velocity integrating the radial equilibrium equation.

- If this calculated value is not in agreement with the guessed value, a new guess must be made until reasonable agreement is achieved.

At this moment, the velocity distribution from hub to casing is known at specified positions at the blade trailing edge. Then:

- Calculate the air mass flow corresponding to this velocity profile.
- If the mass flow differs from the specified value, a new guess must be made for the meridional velocity initially chosen.

All the previous steps are then repeated until the calculated mass flow agrees with the specified value, within a given tolerance.

At this point, the velocity distribution satisfying radial equilibrium and the other equations is known but the position of the streamlines is not. Therefore,

- Calculate the mass flow carried by each streamtube at the blade trailing edge.
- Interpolate, for the actual mass flow distribution known from the inlet calculations

and the actual positions of the streamlines.

- If the interpolated values are not in agreement with the initial guessed positions for the streamlines, a new guess must be made and the steps from the first repeated, until reasonable agreement is achieved.

Choking is detected when an increase in the mid height meridional velocity gives rise to a decrease in mass flow.

As in the inlet velocity algorithm, it is possible to choose between an under-relaxed iterative process and a fourth order Runge-Kutta method for the integration of the differential equation.

7.2.7. THE MERIDIONAL VELOCITIES ALGORITHM

When the calculation is carried out for the first time, there are no reference values to use as useful guesses.

The first inlet velocity profile calculation is based on a guess of uniform axial velocity entering the calculating plane. The calculations of the outlet velocity profile start with a guess of meridional velocity equal to this inlet velocity.

For the remaining rows, the inlet velocities are guessed as the leaving velocities from the previous rows and the outlet velocities from the inlet calculations.

After the calculations are carried out up to the last row, the resulting meridional profile is used as a new guess. This is stored and can be recovered any time later.

The guesses are updated during the execution of the internal loops, so that the closest guess to the actual solution becomes available at the beginning of each iteration.

Two distinct techniques are employed for the determination of the meridional velocity profile, namely at blade inlet and outlet. At blade inlet the integration is carried out from hub to tip because guesses closer to the solution are possible using information from the previous row. The instability introduced by steep loss characteristics is then avoided. At the blade outlet it is possible to choose the same technique or to guess the velocity at any other streamline, usually at the mid height. Hence, different algorithms are needed.

7.2.7.1. **BLADE INLET**

With the first guess of the meridional velocity made at the hub and the whole profile determined, the

integration of the equation of continuity will generally give a mass flow that is not the specified value(Fig.7.4).

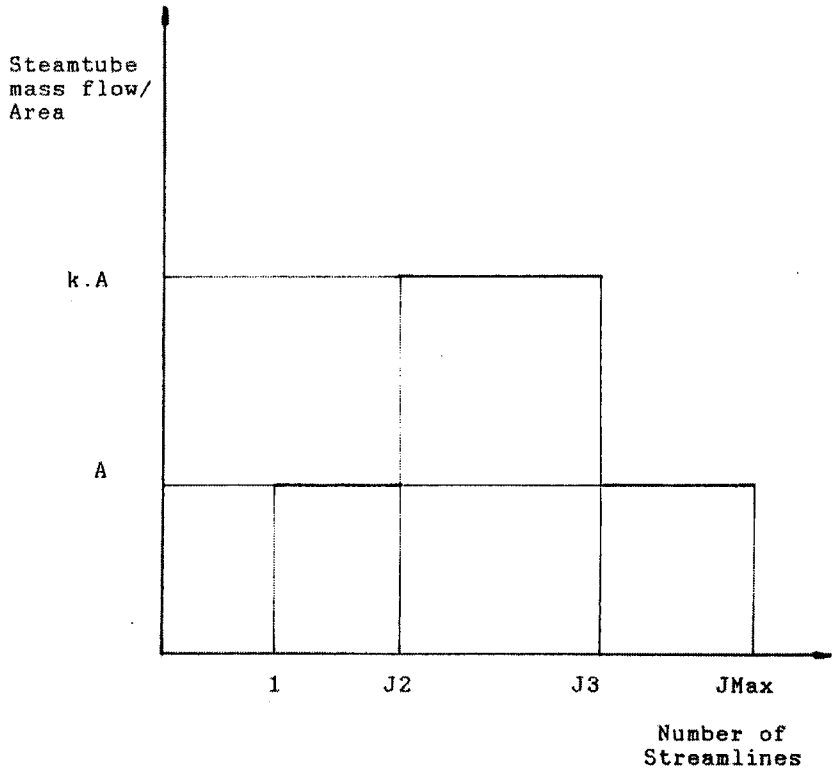

Figure 7-4 - Mass Flow and Area Distribution per Streamtube

If a new guess is needed then a linear approximation is adopted, that is, if

V_A = previous guess

V_B = present guess

$D_{V0} = V_B - V_A$

$\dot{m}_A$ = mass flow resulting from the previous guess

$\dot{m}_B$ = present mass flow calculation

$\dot{m}$ = specified mass flow, then

$$(V_{m1})_{n+1} = (V_{m1})_n + DV_1$$

$$DV_1 = DV_0 \frac{\dot{m} - \dot{m}_B}{\dot{m}_B - \dot{m}_A}$$

For the first guess $DV_0 = 10.$ and $\dot{m}_A = 0.$

7.2.7.2. **BLADE OUTLET**

If the calculation is started at the hub streamline, the procedure is similar to that for the blade inlet. After the velocity profile has been determined and the continuity equation integrated, the mass flow generally is again different from the specified value. The new guess for the hub meridional velocity is determined by a linear interpolation or extrapolation of the two previous guesses.

Let

R_A be the tip radius resulting from the previous guess V_A

R_B that resulting from the present guess V_B

R_2 the actual tip radius.

Then, the next guess will be

$$V_m = V_B + \frac{R_2 - R_B}{R_B - R_A}(V_B - V_A)$$

If the calculation started from the mid streamline and

once the meridional velocity profile has been determined, a new guess is obtained from a linear or parabolic interpolation or extrapolation (Fig. 7.4).

Let

V_A and V_B be two subsequent guesses

$\dot{m}_A$ and $\dot{m}_B$ the corresponding mass flows

$D_{V0} = V_B - V_A$, then

$V_m = V_B + DV_1$,

where

$$DV_1 = DV_0 \frac{\dot{m} - \dot{m}_B}{\dot{m}_B - \dot{m}_A}$$

If more than four guesses are needed, a parabolic interpolation/extrapolation replaces the linear one. This is because the rate of change of mass flow with meridional velocity is high.

7.2.8. THE DUMMY BLADE ALGORITHM

In order to standardise the calculations throughout the compressor, the ducts at inlet and outlet are imagined to be filled with rows of dummy blades. A dummy blade is a source that enables the calculations to be carried out in ducts and bladeless spaces. It does not impose any kind of

restriction on the flow other than that due to total pressure losses (see below).

The tasks performed by this algorithm are

- Evaluate the tangential velocity at the blade edge using the conservation of momentum equation.
- Guess a meridional velocity at the trailing edge.
- Calculate the entropy change from inlet to outlet.
- Calculate the flow properties at outlet.

The pressure losses are those due to wall friction only and are lumped in the wall streamlines. A provision is made to spread the losses through all the streamlines.

8. - RESULTS AND DISCUSSION

8.1. SUMMARY

This Section contains detailed discussion and conclusions relating to the scope of the prediction programme and to the extent to which the objectives have been achieved.

8.2. INTRODUCTION

The objectives of this work have been set out in detail in the INTRODUCTION to this report. To summarise, three major goals were established, namely:

- To produce an axial flow compressor overall characteristic prediction programme. Only the design mass flow, pressure ratio and speed together with geometrical details of blading and annulus were to be required as input data.
- To provide within the main programme the facility for it to be used as a design/development tool.
- To structure the programme in such a way that it

could be easily, quickly and effectively used as a teaching tool.

The original premise was not that the various applications above should be accessible, to the complete novice, nor that only specialists could use it.

In fact it was assumed from the outset that the user would have some background, perhaps through a supporting lecture course in turbomachinery, or some in-company experience. In other words, the user would be expected to have at least a familiarity with turbomachinery principles and terminology.

In its role as a teaching tool particularly, the provision of a comprehensive "Users-guide" was considered as absolute priority.

The following sections are structured so that each of the objectives of the work are dealt with sequentially.

8.3. THE PERFORMANCE PREDICTION PROGRAMME

8.3.1. THE THREE STAGE TRANSONIC COMPRESSOR

In order to demonstrate the ability of the programme to predict the overall performance,

an existing three-stage transonic axial flow compressor is

chosen.

The compressor has inlet guide vanes and develops a total pressure ratio of 4.6:1 at a design point mass flow of 16.375 kg/s when the rotational speed is 21,892 rpm. The average pressure ratio is 1.663 per stage.

This particular compressor was selected because it is both transonic and reasonable information about its geometry and flow field were available.

The required input data for the compressor was supplied by a proprietary source.

Accordingly, it is not possible to publish all the geometrical details. However, the fact is that this was, at the time, the only comprehensively documented compressor against which the prediction programme could be realistically tested.

In addition to the presence of transonic flows, the compressor is a very good test case for the programme, since it is of low hub-tip ratio. However, this in turn, together with the high stage pressure ratio, could be expected to introduce convergence problems due to the resulting large radial variations in streamline curvature. In addition, the blade sections close to the annulus walls operate at high levels of diffusion factor and therefore, in a regime of high rate of change of loss. The latter, together with high local velocity gradients generally makes

the iterative process unstable. In spite of these difficulties, instability was overcome through careful choice of relaxation factors in the iterative sub-processes. The relaxation factors to use are suggested in the input file of the user's guide (Vol. 2).

8.3.2. PREDICTION RESULTS - DESIGN SPEED

The overall measured performance of the three-stage compressor is shown in Fig. 8.1 and to a larger scale on Fig. 8.1a. The corresponding tabulated values are shown on Table 8-1 below. Superimposed on the characteristics are the Programme predictions over full range of mass flow at design speed, and three values of mass flow at 90% and 80% of design speed.

It should be noted that the physical scale of the actual characteristic of Fig. 9.1, is very small. In addition, the actual test values for the compressor against which the characteristic was originally plotted, were not made available to the author.

Inevitably, however, comparisons between actual and predicted values of mass flow, pressure ratio and

efficiency had to be made.

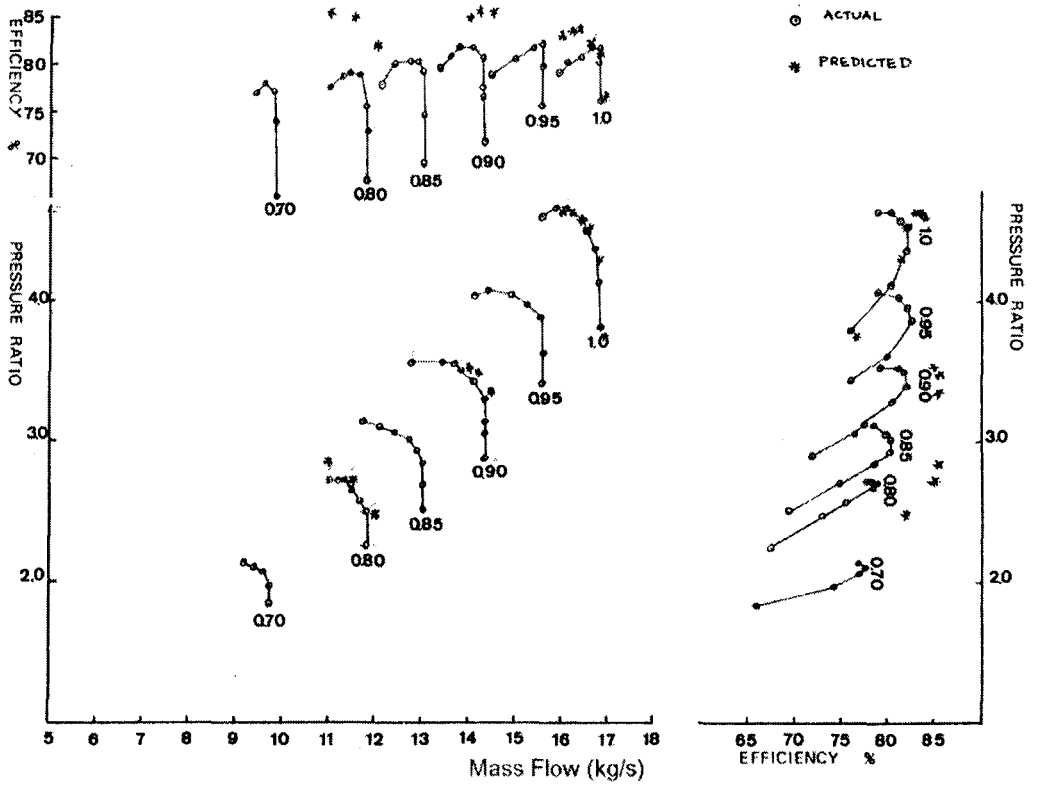

Figure 8-1- Overall Performance Data

Table 8-1 - Comparison of manufacturer's and predicted

% speed	mass flow	pressure ratio		efficiency	
		manuf.	predic.	manuf.	predic.
100	16.000	4.67	4.626	0.800	0.832
	16.200	4.63	4.625	0.805	0.837
	16.375 (DP)	4.60	4.60	0.810	0.838
	16.600	4.46	4.53	0.820	0.824
	16.780	4.38	-	0.820	-
	16.800	4.12	4.28	0.805	0.813
	16.800	3.82	-	0.763	-
	16.900	-	3.74	-	0.769
	17.000	3.82	CHOKED	-	-
90	14.000	3.45	3.52	0.820	0.850
	14.200	3.40	3.48	0.820	0.857
	14.500	-	3.35	-	0.856

	15.000	- CHOKED	-	-	-
80	11.000	2.70	2.85	0.775	0.855
	11.500	2.65	2.71	0.790	0.850
	12.000	-	2.46	-	0.820
	12.500	-	CHOKED	-	-

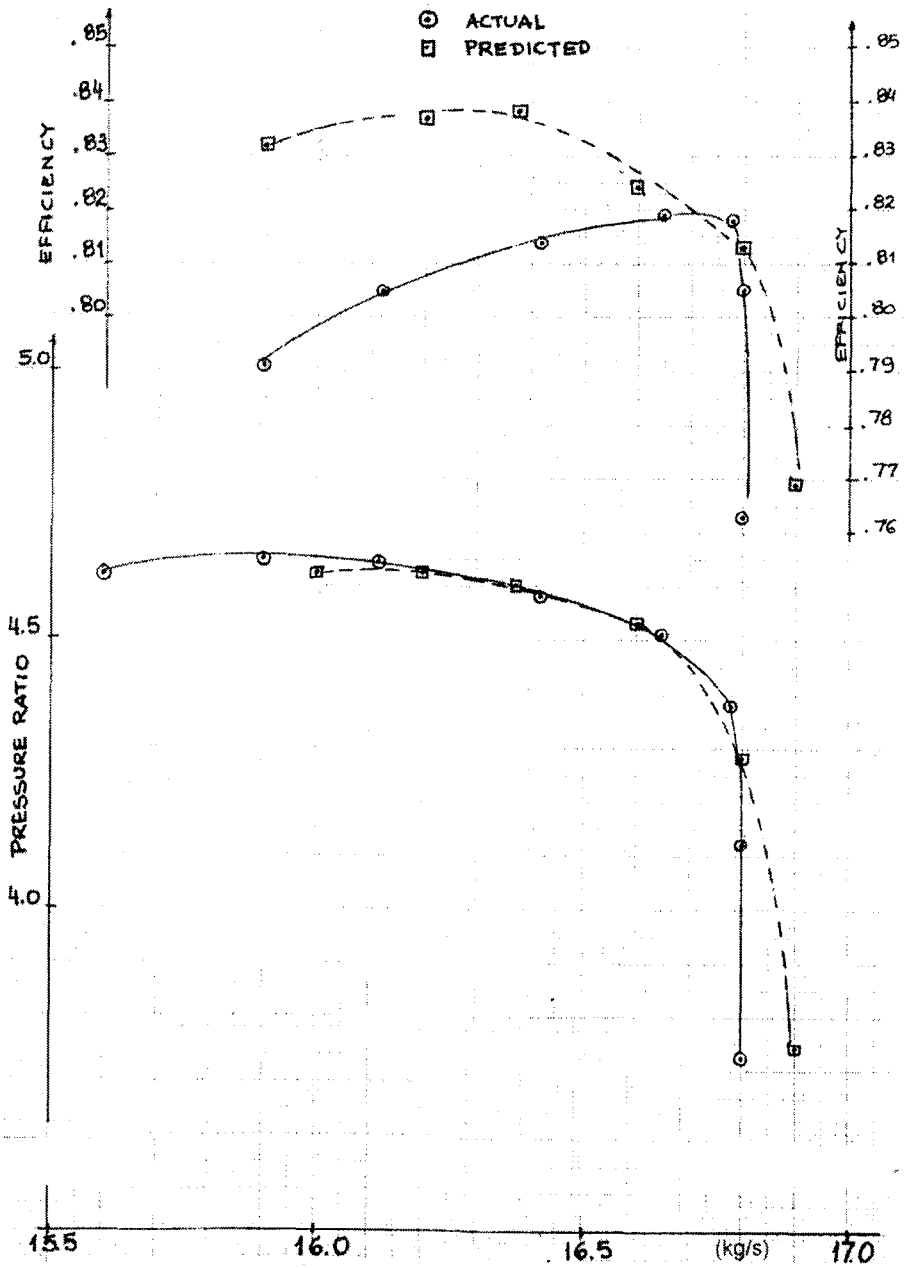

Figure 8.1a - Design Speed Characteristic

Figure 8.1a - Design Speed Characteristic

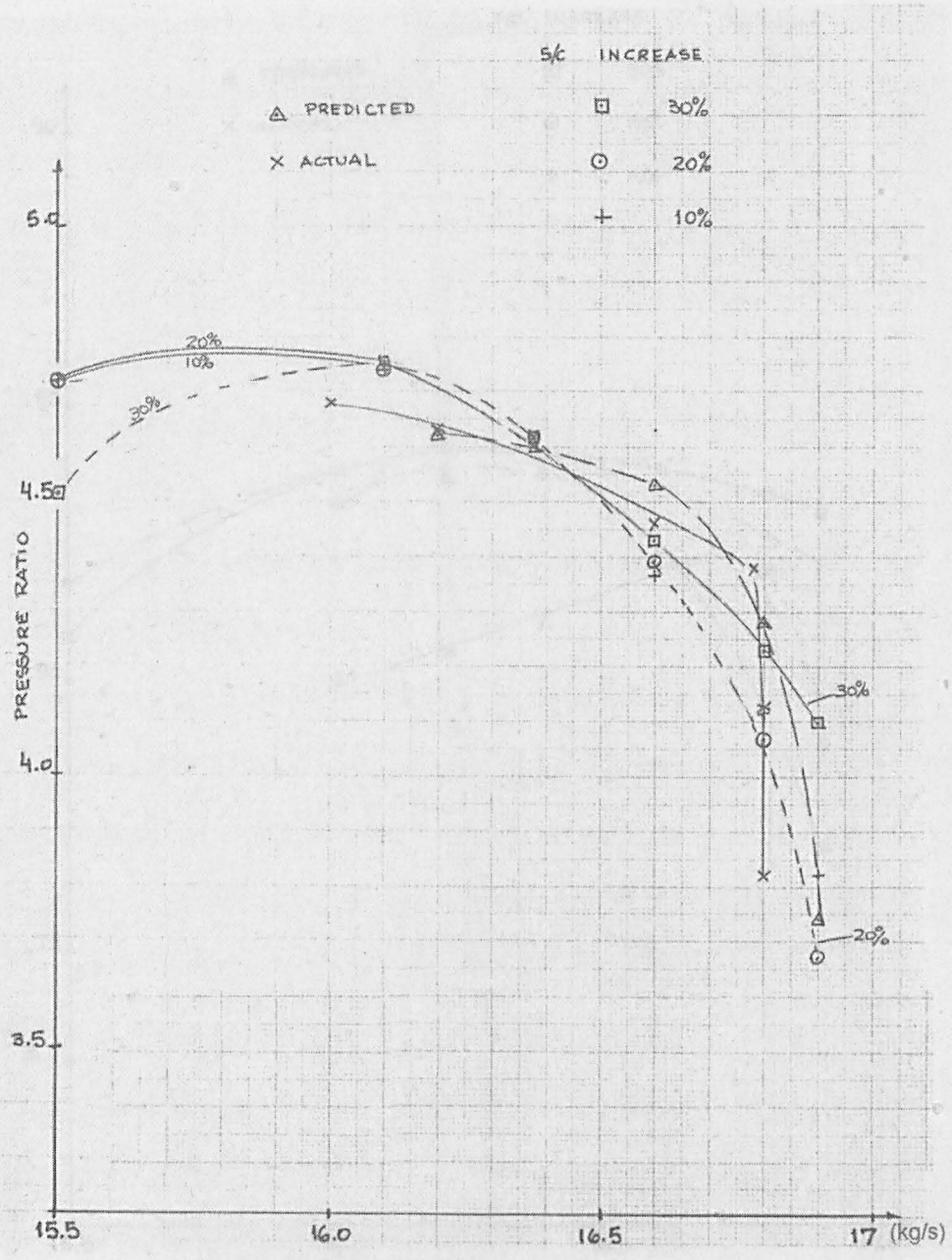

Figure 8.1b - Design Speed Characteristic
Effect of Stator Space-chord Ratio

Figure 8.1b - Design Speed Characteristic - Effect of Stator Space-chord Ratio on pressure ratio

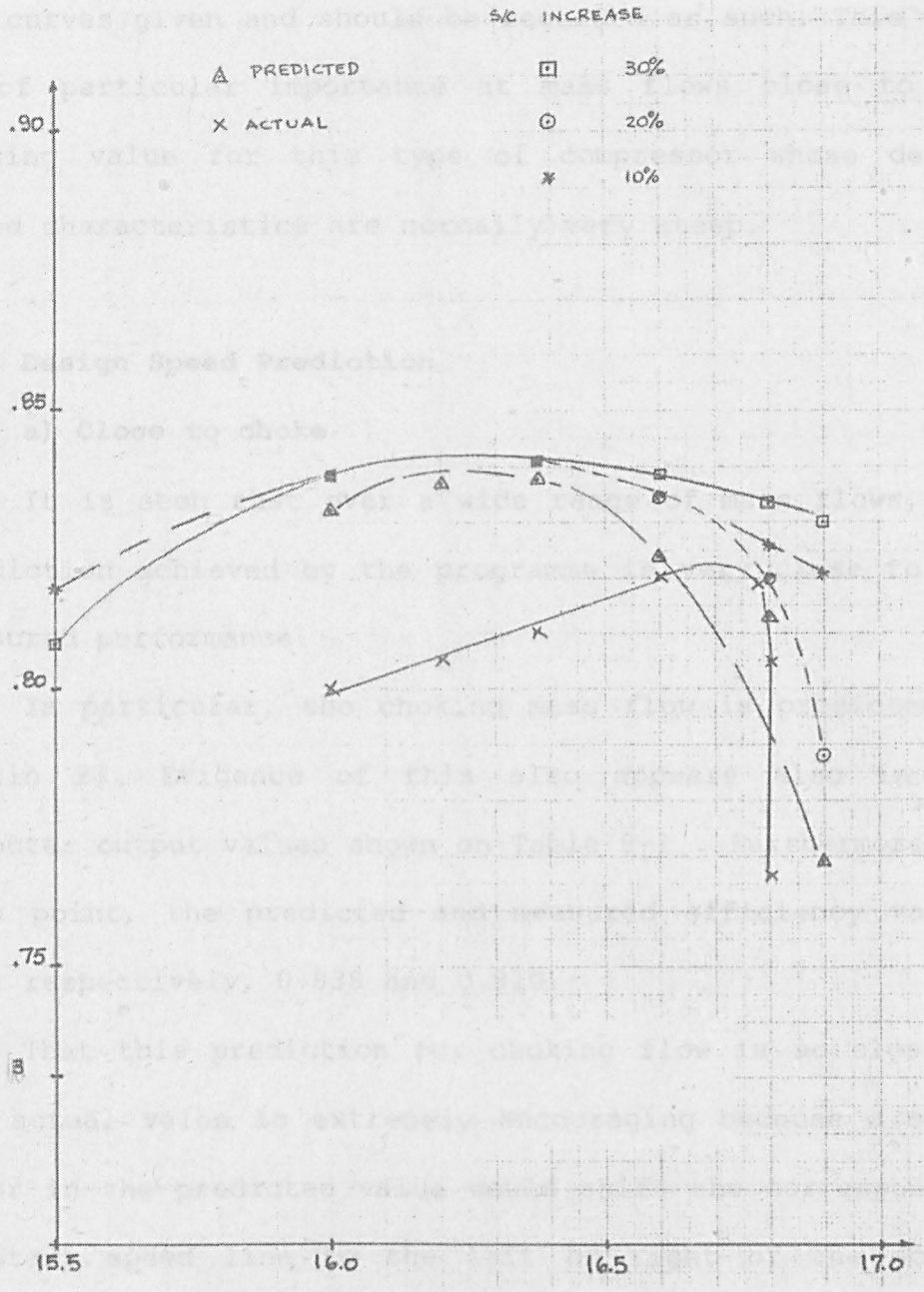

Figure 8.1c - Design Speed Characteristic
Effect of Stator Space-chord Ratio

Figure 8.1c - Design Speed Characteristic - Effect of Stator Space-chord Ratio on efficiency

The actual values quoted have been interpolated from

the curves given and should be regarded as such. This fact is of particular importance at mass flows close to the choking value for this type of compressor whose design speed characteristics are normally very steep.

Design Speed Prediction

a) Close to choke

It is seen that over a wide range of mass flows, the prediction achieved by the programme is very close to the measured performance.

In particular, the choking mass flow is predicted to within 2%. Evidence of this also appears also in the computer output values shown on Table 8-1 . Furthermore, at this point, the predicted and measured efficiency values are, respectively, 0.838 and 0.810.

That this prediction for choking flow is so close to the actual value is extremely encouraging because a small error in the predicted value would shift the corresponding constant speed line to the left or right of the actual curve. This, coupled with the local steepness of the characteristics of this transonic compressor, would give rise to significant errors in the corresponding values of both pressure ratio and to a lesser extent, efficiency.

In fact, in this regime of operation, only a very small change in compressor mass flow results in a large

velocity change incident on the blade rows. This in turn, gives rise to correspondingly large changes in pressure loss and, therefore, efficiency.

In general, this serves to underline the importance, for any analytical method, of being able to accurately predicting the choking mass flow. Furthermore, an appropriate loss model must adequately represent the sensitivity of loss to velocity in this regime. In so doing, the model must allow for the higher tip losses due to higher incident velocities. In these circumstances, Monsaratt's model as modified by the author has proved most useful since it distributes the losses unfavourably to the tip region and clearly gives the desired results.

It is interesting to note that early on in the development phases of the programme, alternative models were used (For example Swan [19]). It became clear, however, that these could underestimate losses at the root and, thereby, not realistically represent the real compressor situation where losses are high at both root and tip. This may not be the case for all compressors. For example, the influence of blade thickness is not explicitly accounted for in every loss correlation. In such cases, the data for them is gathered from numerous tests representing a non-specified range of thickness-chord ratios. A better estimate for future development of this programme would be

to use actual losses measured in the traditional way, namely (i - i*) versus ,the loss parameter for the particular base profile in use and appropriate to the specific level of Mach number. The latter was rejected for the current work for two reasons. Firstly because the data for high Mach number cases are very sparse in the open literature. Secondly, the additional computational time required for execution of this model using an interpolation (rather than analytical) technique was excessive. This was, of course, counterproductive to a major prerequisite of the final package, namely, that it should give, in its teaching role, fast results. In spite of this, it is important to note that it is possible to use proprietary or otherwise loss model. The user, who will need to compromise the contradictory requirements of a short running time and more precise representation of loss, appropriate to his own blades, can change it at will.

Design Speed Prediction

(b) Close to stall

Accurate loss prediction in this regime of operation is vital to a successful model where rates of change with mass flow of, for example, pressure ratio are expected to be very high. It should be noted that the actual compressor characteristic had not been revealed at the time when

alternative loss correlations were being considered. However, the fact that the expected characteristics were steep, led to careful consideration concerning losses. In particular, rotor tip sections operate supersonically whilst the roots are entirely subsonic. Consequently, any model chosen has to adequately accounting for shock loss near the tip.

The first model considered, namely, that due to Swan, suffered an under-prediction of rotor losses both in the opinion the author and the published experiences of others. As an alternative, Monsarrat's method was examined but in this case clearly exaggerated rotor tip losses. The latter were predicted as excessively high, to which shock loss had also to be added. This was due to implied very high values of wake momentum thickness, which were considered very unrealistic. In particular, the rate of change of loss with radial position increased considerably towards the tip. In some cases as much as 40% pressure loss was being predicted at the tip. Even though the actual compressor losses were, at this time, unknown, the author felt these unrealistic for any compressor operating free of stall. As a result, and sub-sequentially, extensive discussions were held with the expert originator of the actual compressor data. The conclusion led to the adoption of the modified form of Monsarrat's model.

In particular, the model chosen for the present work maintains an approximately constant rate of change of loss with radial position. The result of this modification is that the basic losses are now obtained by moving Monsarrat's loss loop shown on Fig. 6.3 radially by approximately 10%. The value of the rotor root loss, however, remains unchanged. This is shown on Figs. 6.3c and 6.3d.

The final estimate of pressure loss used in the programme includes an appropriate allowance for shocks. The latter is calculated using the well-known NACA shock loss model.

Design Speed Prediction

(c) At surge

This is undoubtedly, for any computer model, the most difficult point to predict. Within the literature, only limited reference to surge recognition is made. Lieblein and Swan, for example, suggested that local stalling of blade sections, recognised by a limiting value of diffusion factor is the point below which further reduction of mass flow can create overall instabilities. However, no attempt is made to quantify surge precisely.

In the interests of simplicity, the present model assumes that for a specific (low) mass flow, if a

convergent solution is achieved and the corresponding diffusion factor is greater than 2.2, the local section is stalled.

Comparison between the predicted and actual characteristics on Fig. 8.1 and 8.1a bare a remarkably good correlation. Over the full range of mass flows, at the design speed, this fact is also evident particularly in the difficult areas close to both surge and choke.

(d) Other General Results

Figures 8.2 through 8.37 are the design point results plotted by the programme.

The dots and stars over some of the graphs are the result of calculations undertaken by the manufacturer, at design point.

There is generally very good agreement between both predictions.

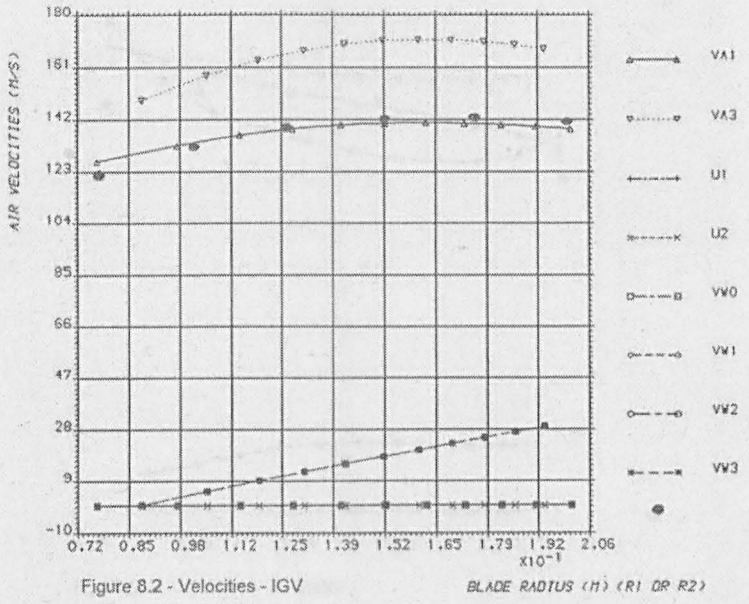

Figure 8.2 - Velocities - IGV

Figure 8-2- Velocities - IGV

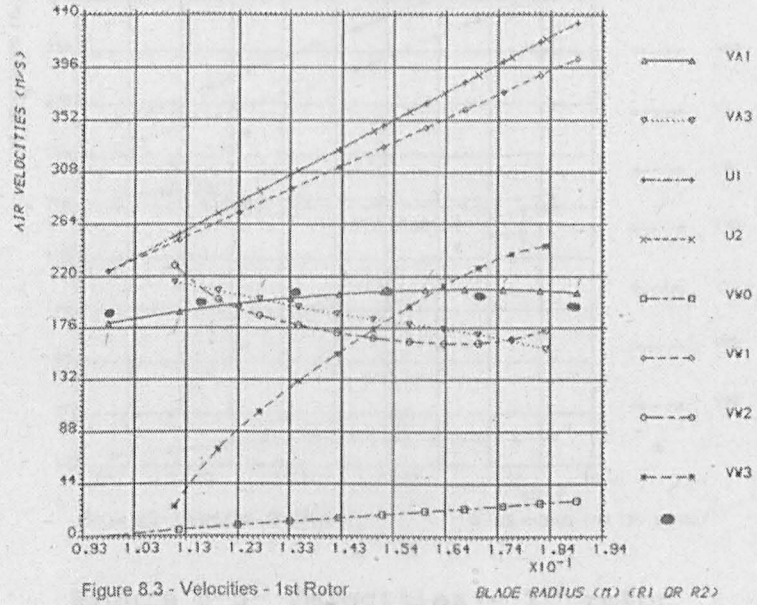

Figure 8.3 - Velocities - 1st Rotor

Figure 8-3- Velocities - 1st rotor

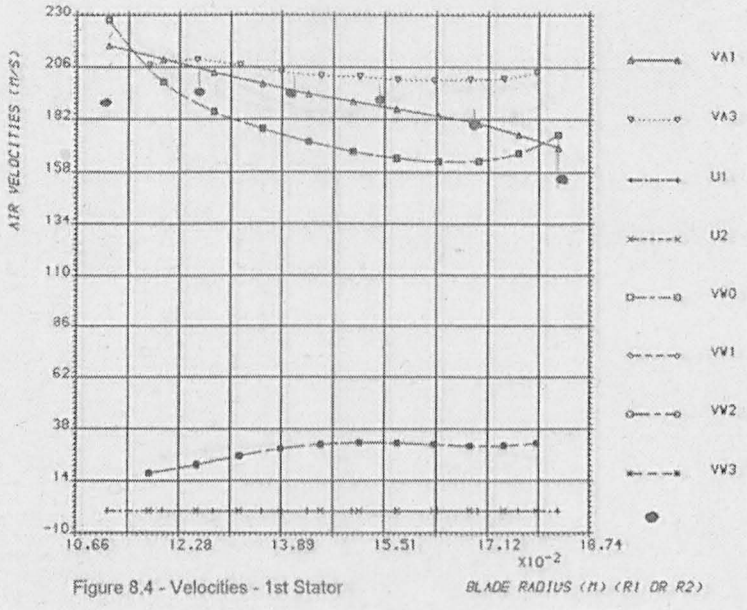

Figure 8-4- Velocities – 1st stator

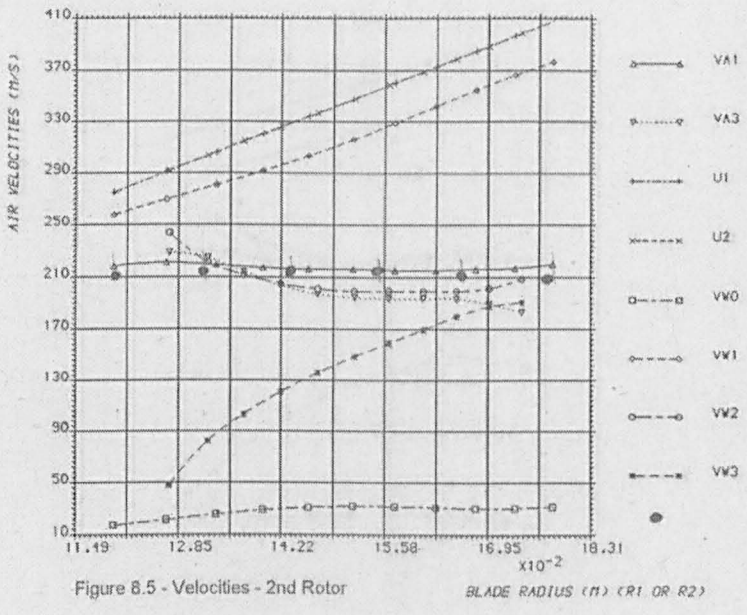

Figure 8-5- Velocities – 2nd rotor

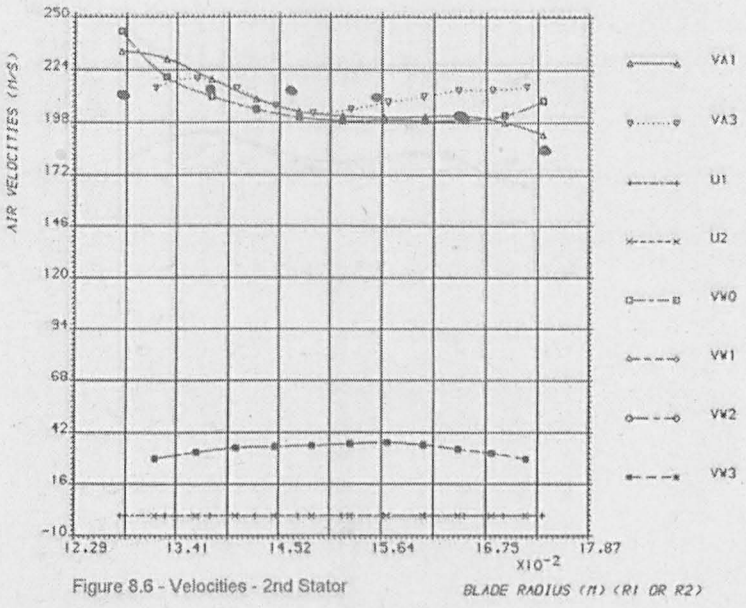

Figure 8.6 - Velocities - 2nd Stator

Figure 8-6- Velocities – 2nd stator

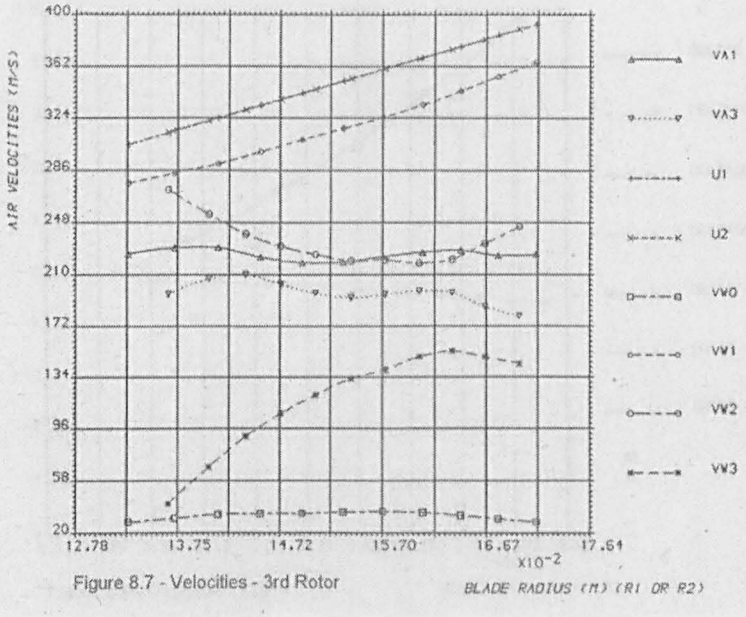

Figure 8.7 - Velocities - 3rd Rotor

Figure 8-7- Velocities – 3rd rotor

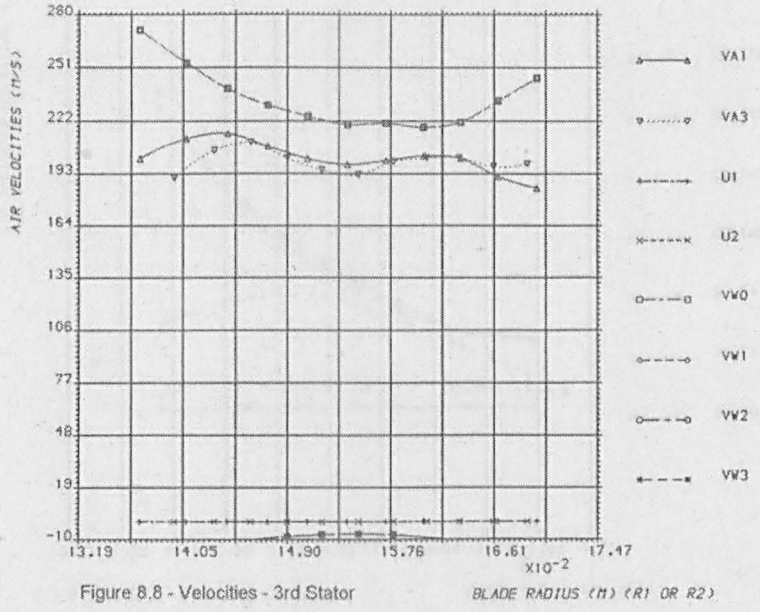

Figure 8-8- Velocities – 3rd stator

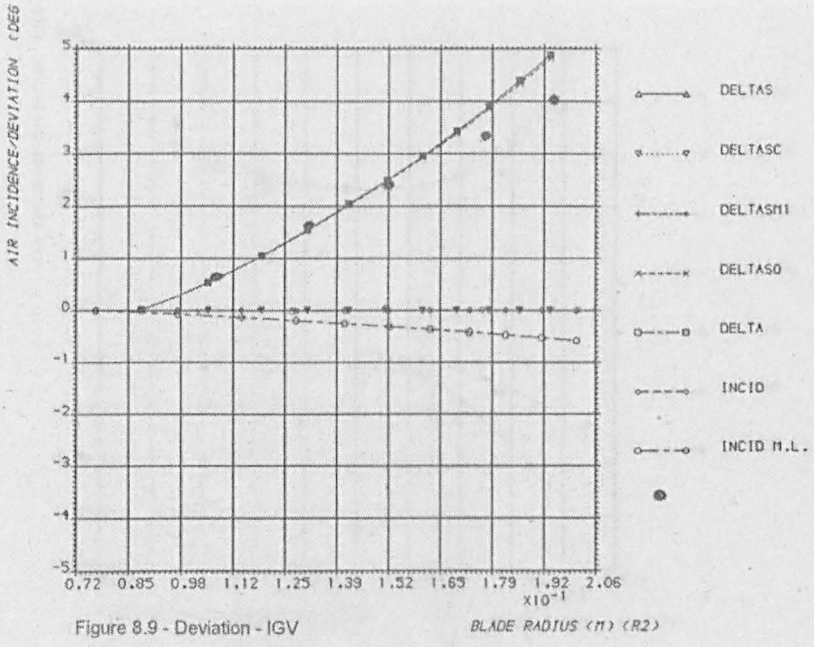

Figure 8-9- Deviation – IGV

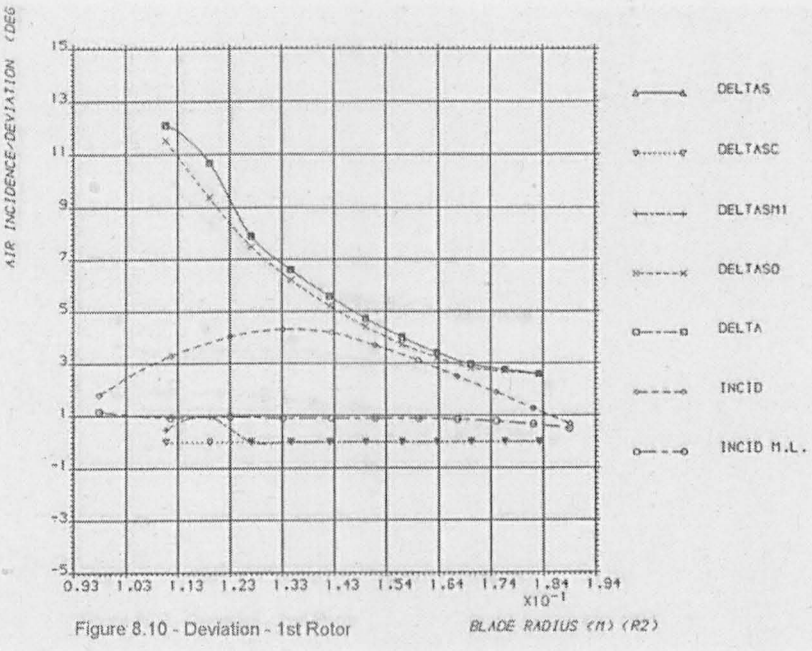

Figure 8-10- Deviation – 1st rotor

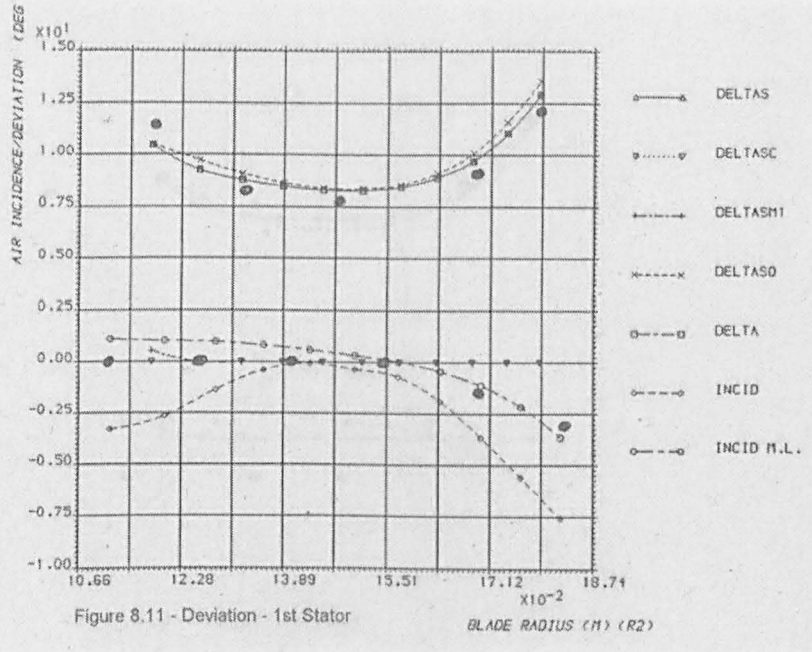

Figure 8-11- Deviation – 1st stator

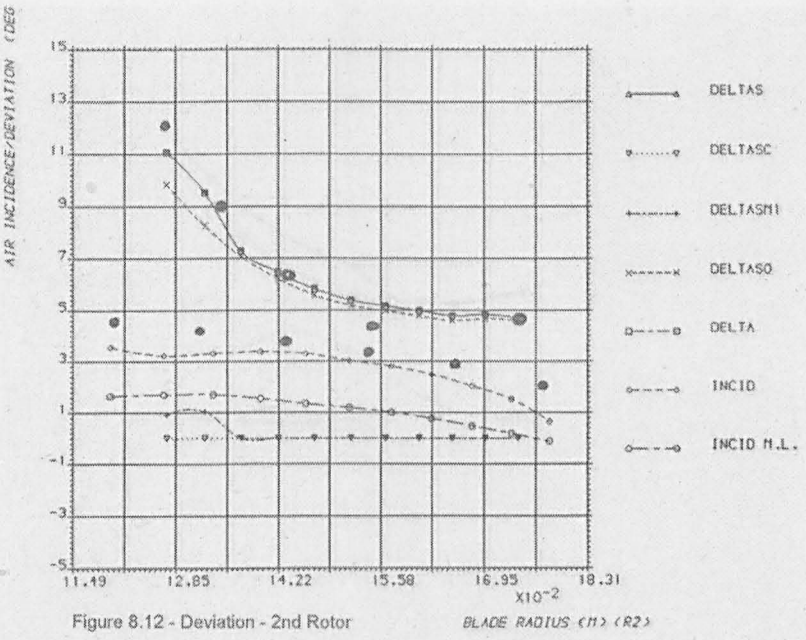

Figure 8.12 - Deviation - 2nd Rotor

Figure 8-12- Deviation – 2nd rotor

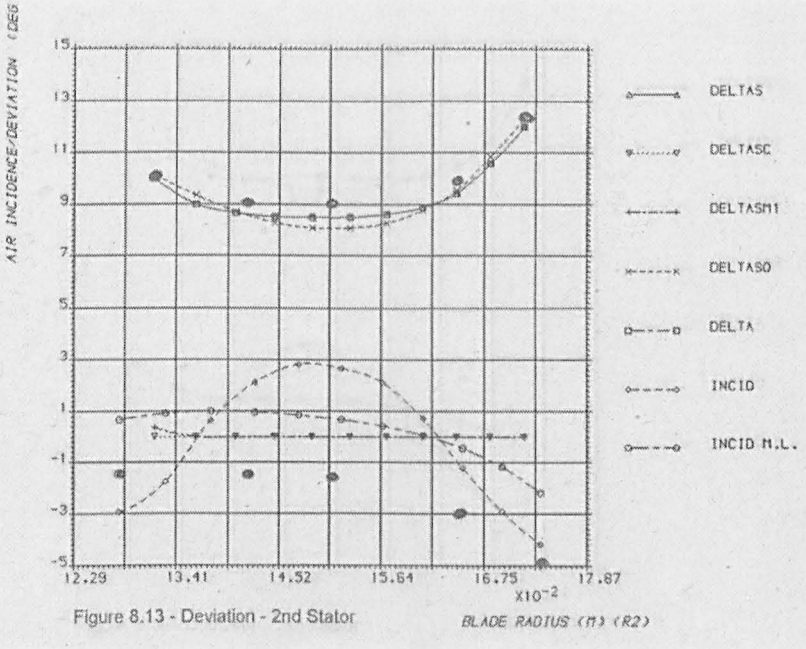

Figure 8.13 - Deviation - 2nd Stator

Figure 8-13- Deviation – 2nd stator

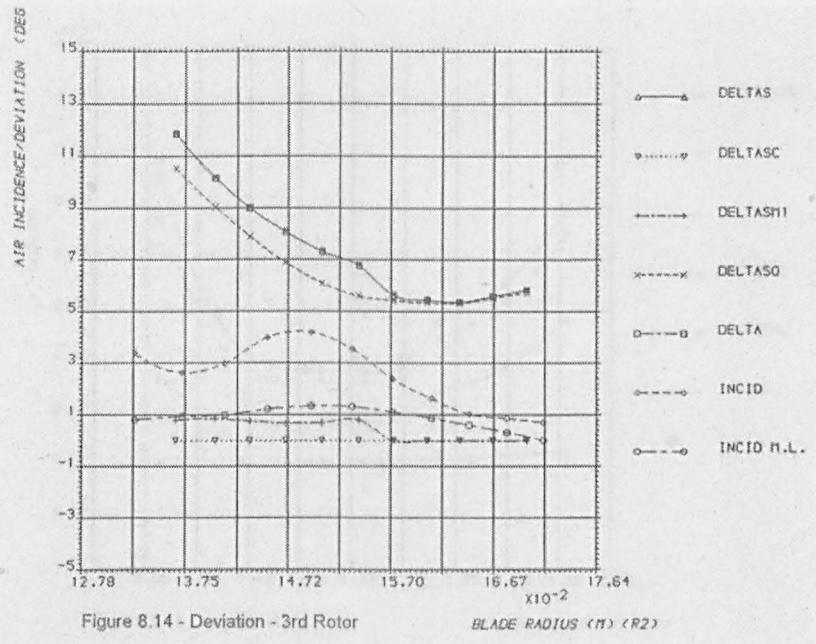

Figure 8.14 - Deviation - 3rd Rotor

Figure 8-14- Deviation – 3rd rotor

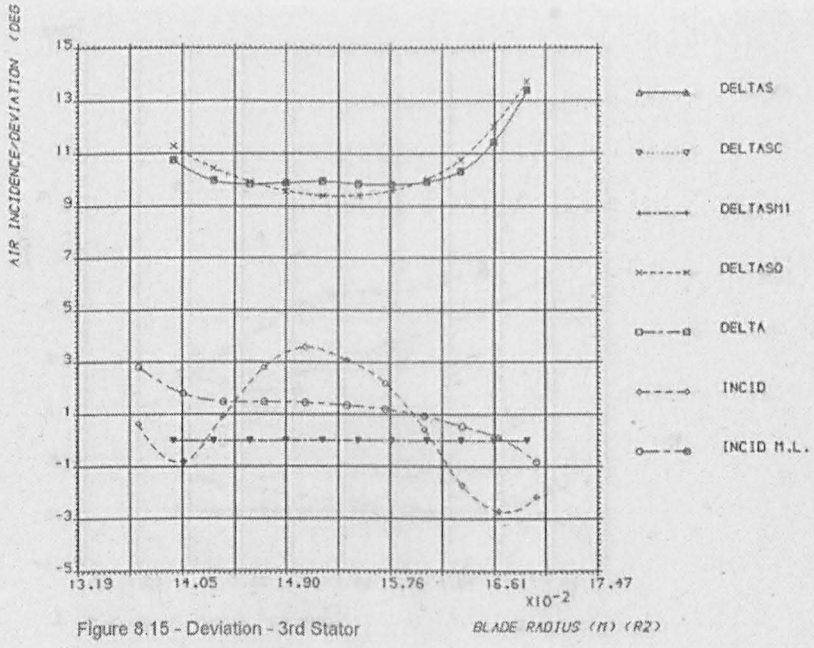

Figure 8.15 - Deviation - 3rd Stator

Figure 8-15- Deviation – 3rd stator

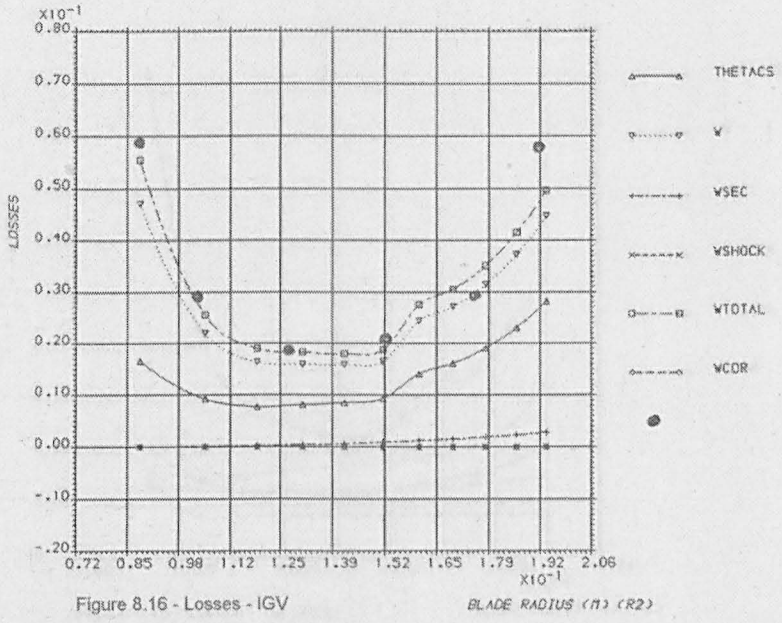

Figure 8-16- Losses – IGV

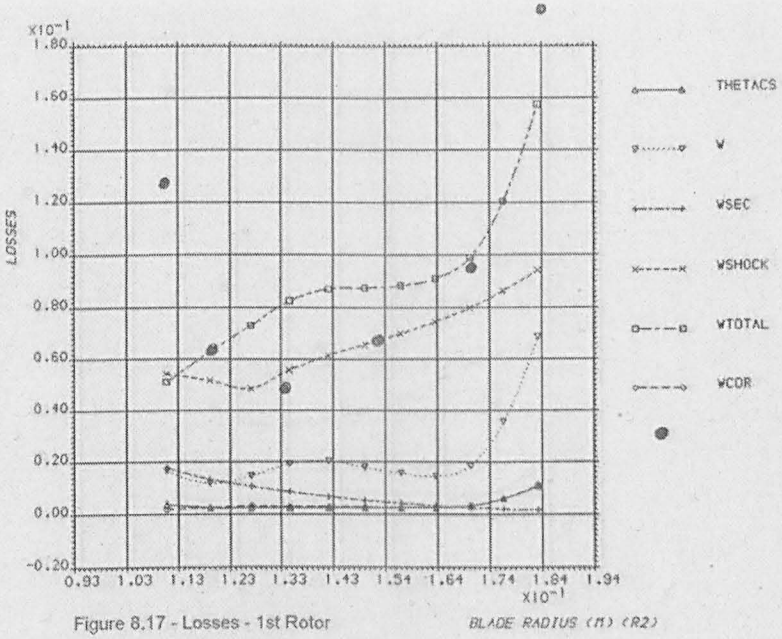

Figure 8-17- Losses – 1st rotor

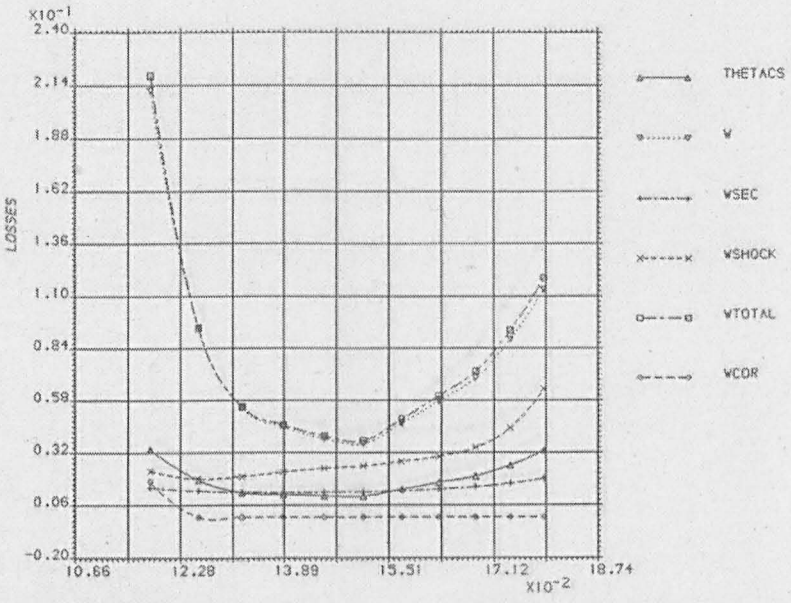

Figure 8.18 - Losses - 1st Stator

Figure 8-18- Losses – 1st stator

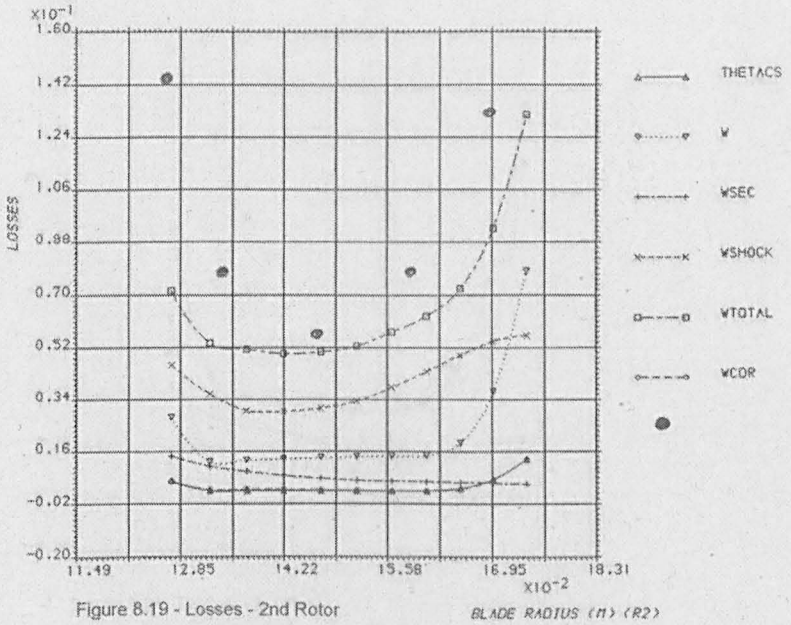

Figure 8.19 - Losses - 2nd Rotor

Figure 8-19- Losses – 2nd rotor

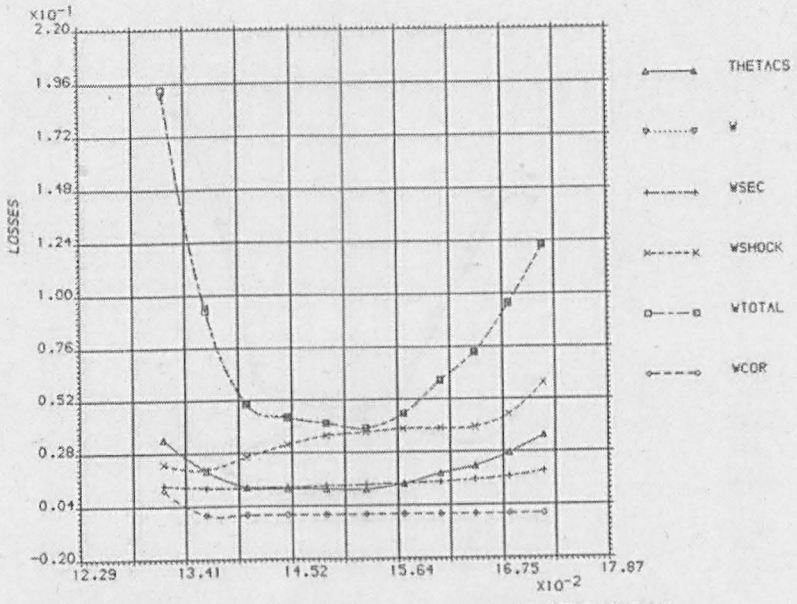

Figure 8.20 - Losses - 2nd Stator

Figure 8-20- Losses – 2nd stator

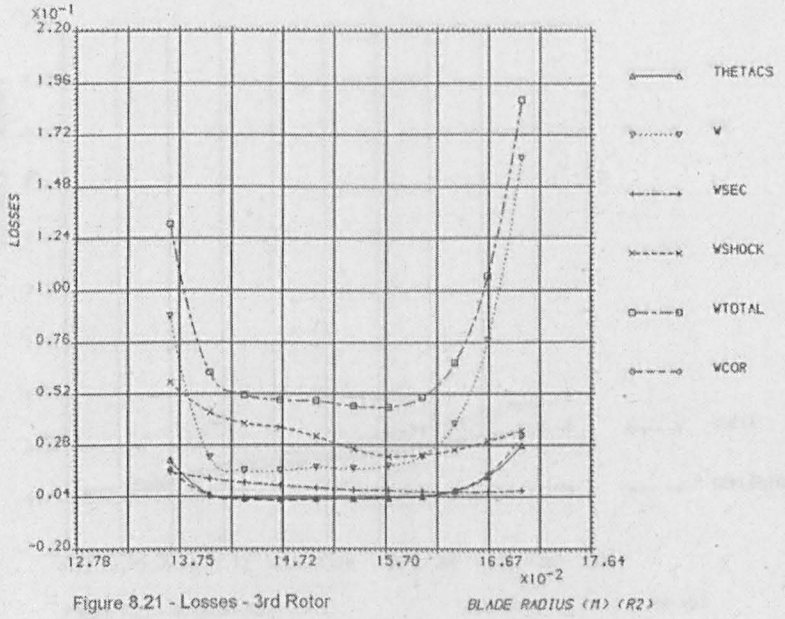

Figure 8.21 - Losses - 3rd Rotor

Figure 8-21- Losses – 3rd rotor

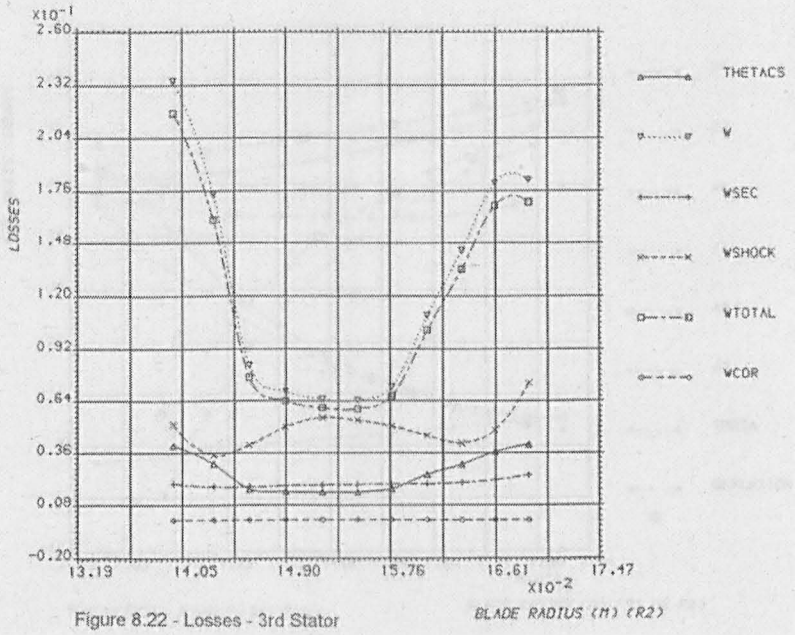

Figure 8-22- Losses – 3rd stator

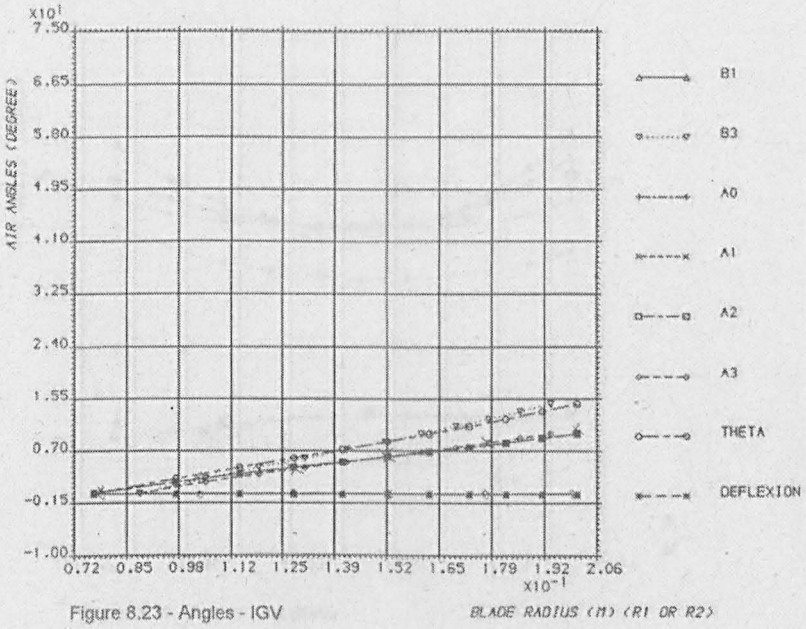

Figure 8-23- Angles – IGV

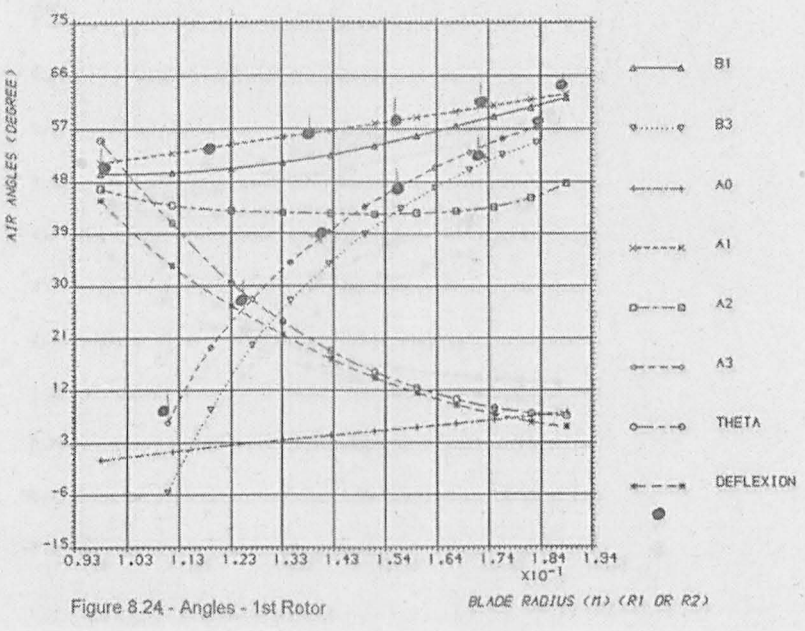

Figure 8.24 - Angles - 1st Rotor

Figure 8-24- Angles – 1st rotor

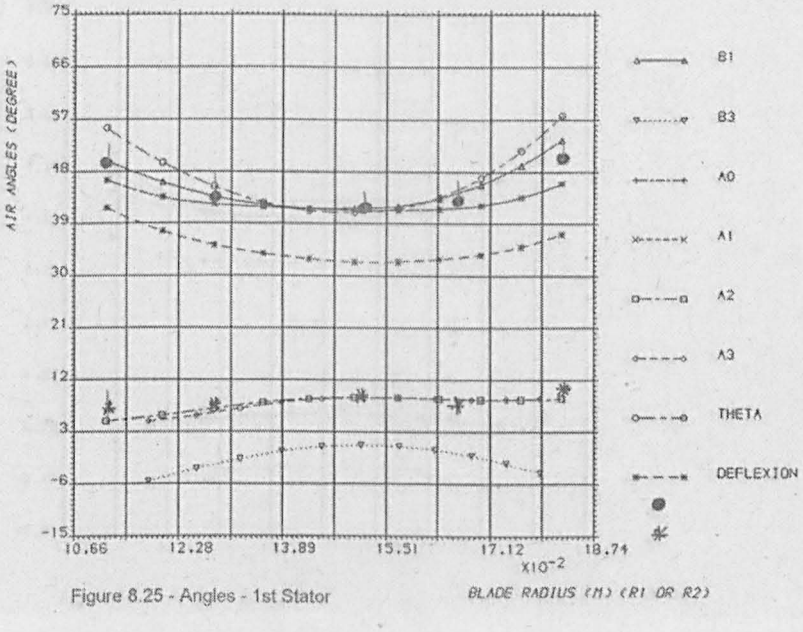

Figure 8.25 - Angles - 1st Stator

Figure 8-25- Angles – 1st stator

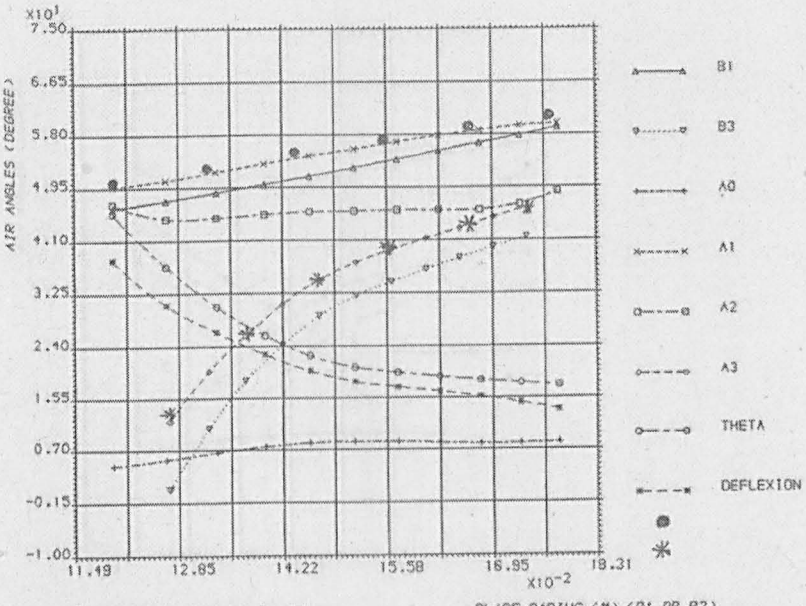

Figure 8.26 - Angles - 2nd Rotor

Figure 8-26- Angles – 2nd rotor

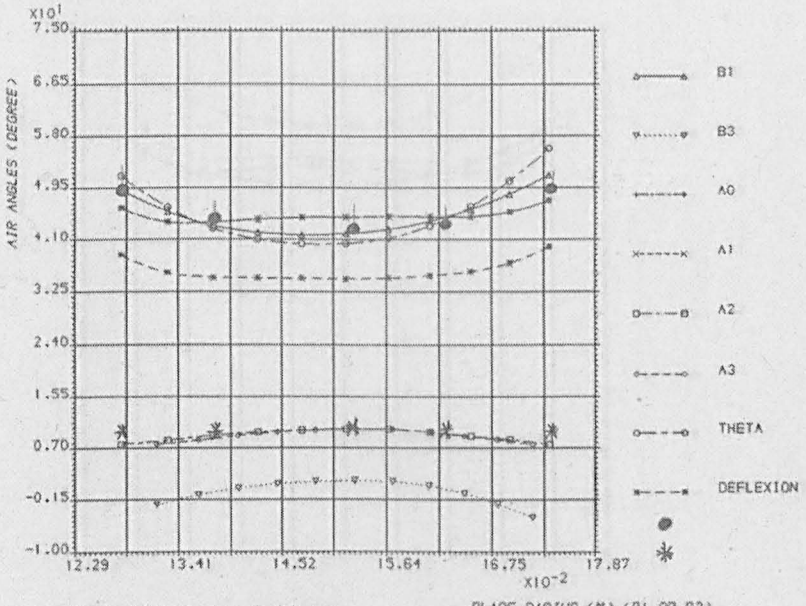

Figure 8.27 - Angles - 2nd Stator

Figure 8-27- Angles – 2nd stator

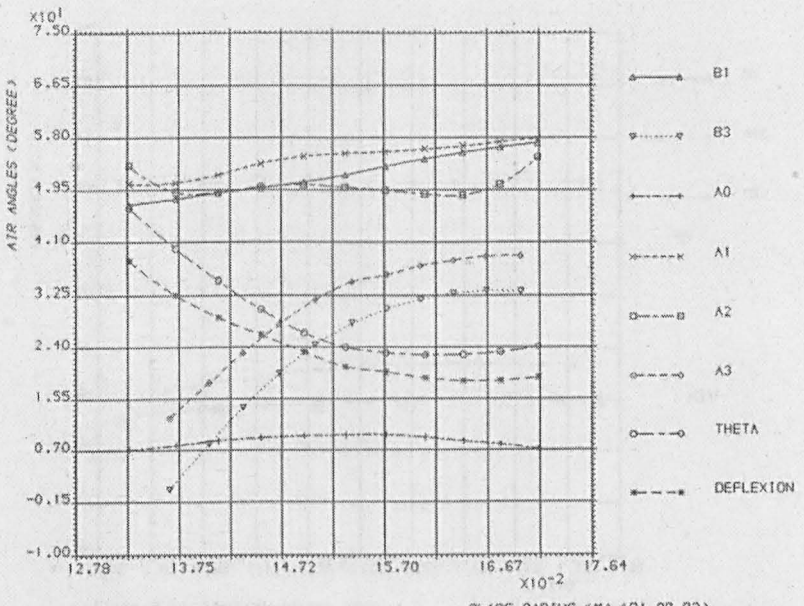

Figure 8.28 - Angles - 3rd Rotor

Figure 8-28- Angles – 3rd rotor

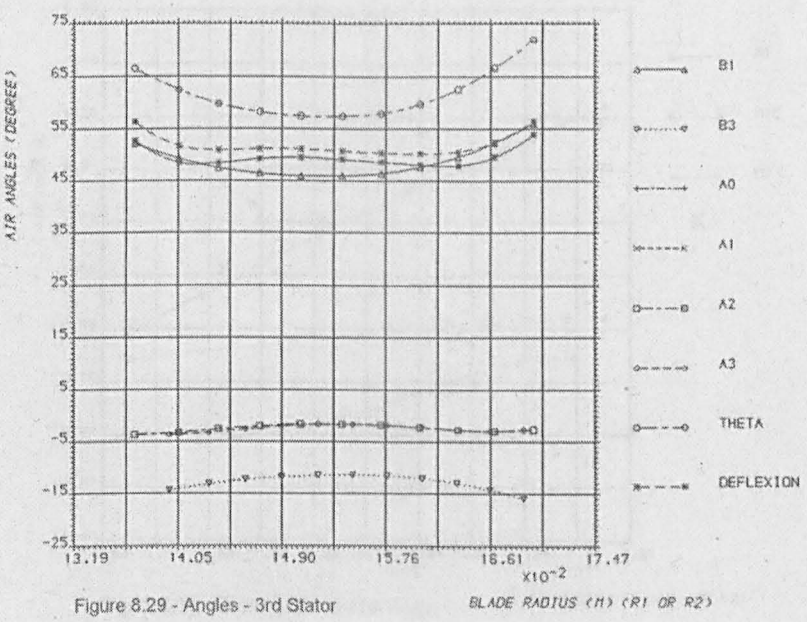

Figure 8.29 - Angles - 3rd Stator

Figure 8-29- Angles – 3rd stator

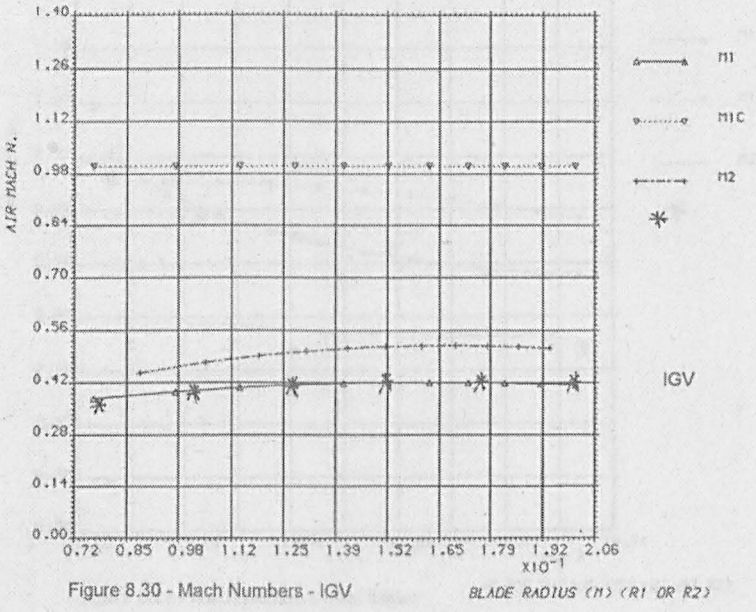

Figure 8-30- Mach Numbers – IGV

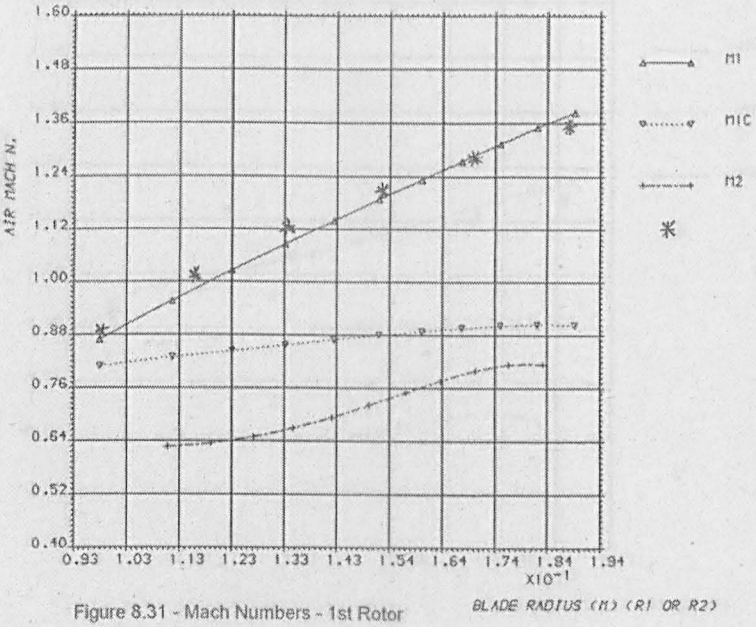

Figure 8-31- Mach Numbers – 1st rotor

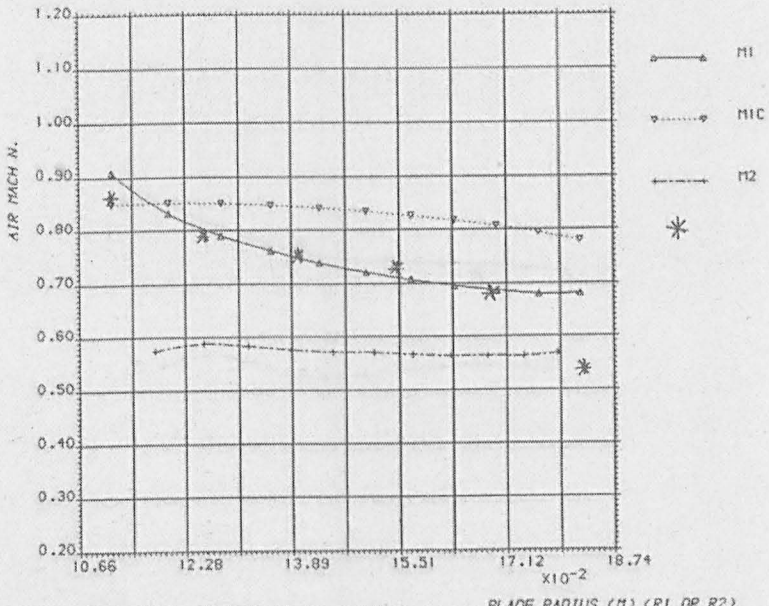

Figure 8.32 - Mach Numbers - 1st Stator

Figure 8-32- Mach Numbers – 1st stator

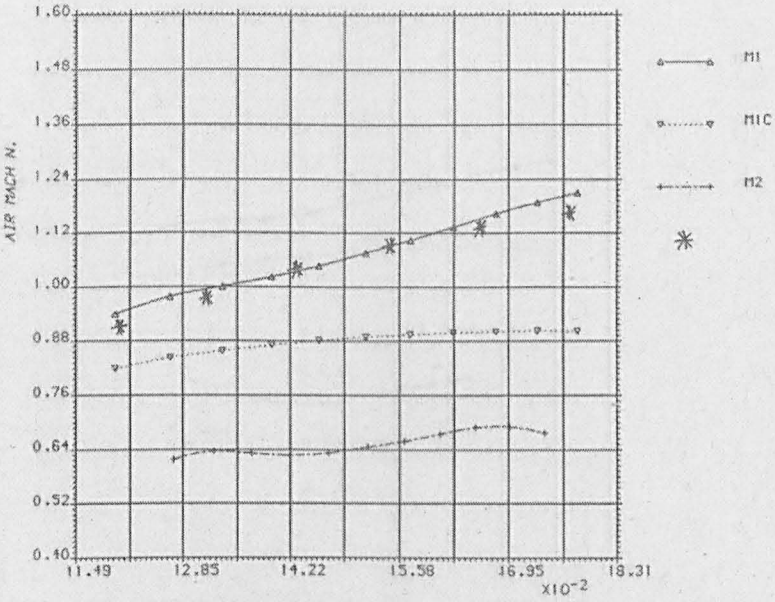

Figure 8.33 - Mach Numbers - 2nd Rotor

Figure 8-33- Mach Numbers – 2nd rotor

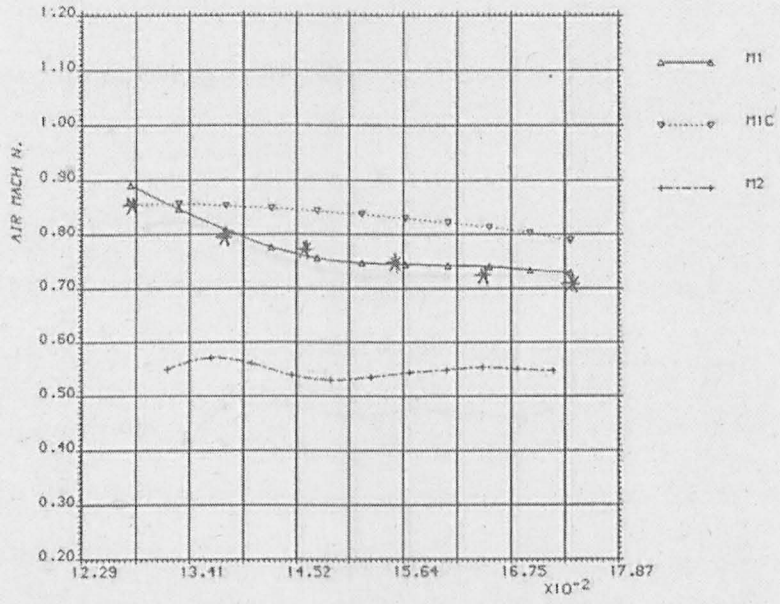

Figure 8.34 - Mach Numbers - 2nd Stator

Figure 8-34- Mach Numbers – 2nd stator

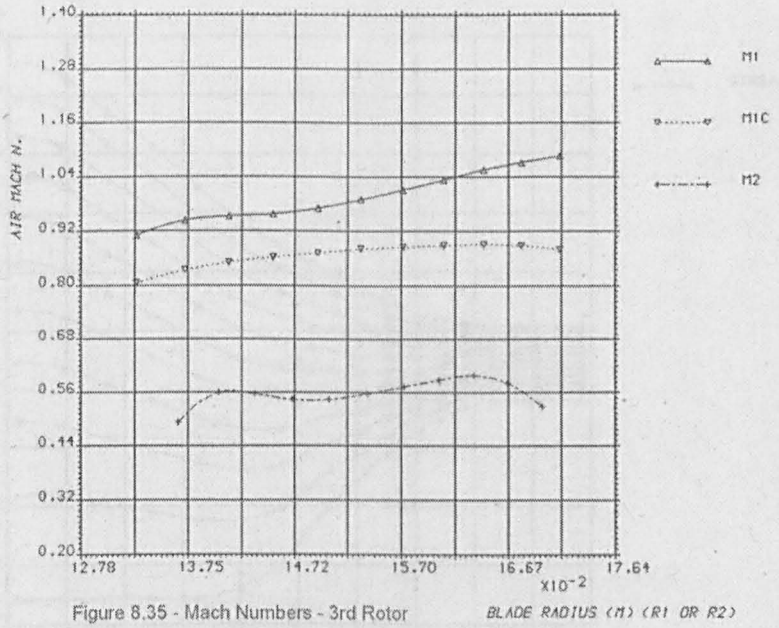

Figure 8.35 - Mach Numbers - 3rd Rotor

Figure 8-35- Mach Numbers – 3rd rotor

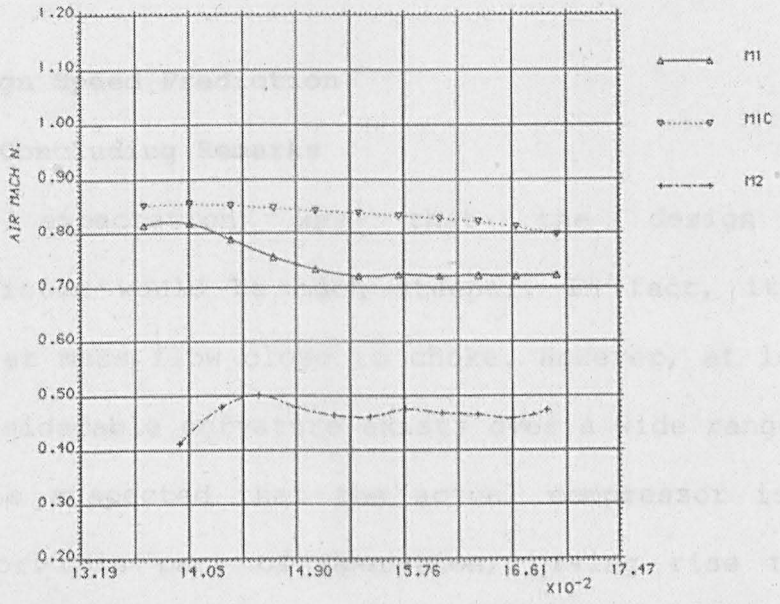

Figure 8-36- Mach Numbers – 3rd stator

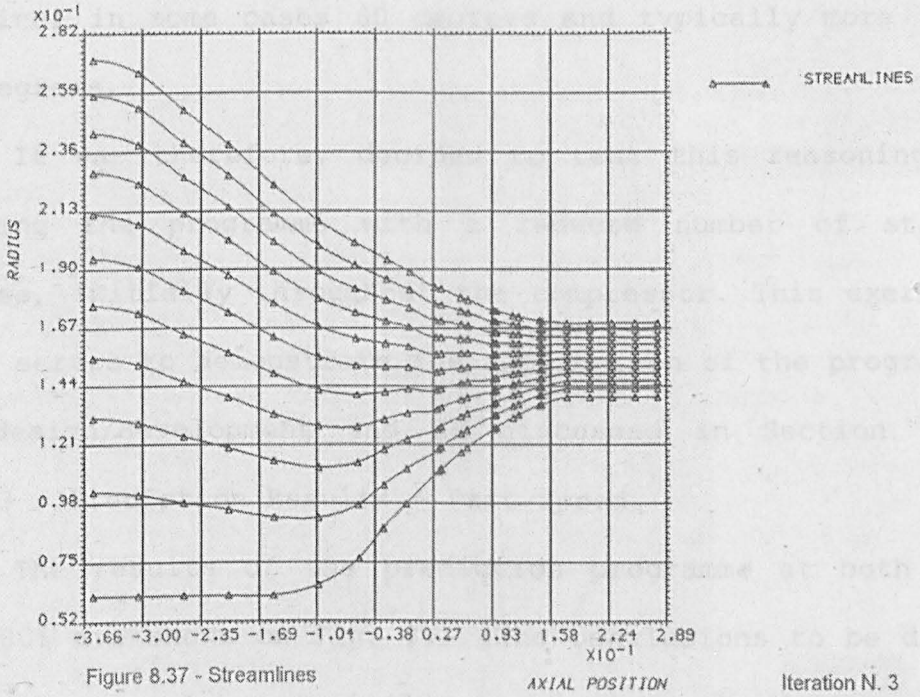

Figure 8-37- Streamlines

Design Speed Prediction

(e) Concluding Remarks

The expectation was that the design speed characteristic would be much steeper. In fact, it is as expected at mass flow close to choke. However, at low mass flow, considerable curvature exists over a wide range.

It is suspected that the actual compressor is over-bladed for this part of operation, giving rise to high losses which, in turn, cause low efficiency and low pressure ratio. The stator blades in particular are suspected, since they are large in number and very high in turning, in some cases 60 degrees and typically more than 40 degrees.

It was therefore, decided to test this reasoning by running the programme with a reduced number of stator blades, initially throughout the compressor. This exercise also serves to demonstrate the application of the programme to design/development and is discussed in Section 8.4.

8.3.3 - Prediction Results - Part Speed

The results of the prediction programme at both 90% and 80% are shown on Fig. 8.1. The conclusions to be drawn are, in general, very similar to those at the design speed already discussed.

In particular at the present state of development of

the programme, the prediction for pressure ratio is, in general, quite good. It must be said, however, that efficiency is consistently predicted higher than measured values. There is clearly a need for further development of the loss/deviation models if agreement is to be eventually achieved. Furthermore, no attempt has been made to estimate the choking mass flow precisely. In addition, near to surge values of mass flow problems with convergence of the iterative process was experienced.

8.4. THE PERFORMANCE PREDICTION PROGRAMME AS A DESIGN / DEVELOPMENT TOOL

One of the objectives of this work was to produce a design/development tool.

The fact that the actual characteristic curves for this compressor were flatter than expected gives an ideal opportunity to test the programme for this purpose.

It is, however, worthwhile initially to explain the author's reasons for suggesting that the compressor was over-bladed.

In particular, at low mass flows, at all speeds the actual pressure ratio is low. This is because corresponding pressure losses are high. It should be remembered that

losses arise mainly due to friction and of course, large blade numbers will give rise to high loss. As mass flow is reduced below the design value the turning in blade rows increases, eventually giving stall. Simultaneously and in general profile losses increase and efficiency falls. Profile losses can clearly be reduced by reducing blade numbers, i.e. increasing space-chord ratio. If the latter is increased too much, however, effective turning in the blade rows is not achieved because of reduced blade overlap. In consequence, deviation increases, and both turning and pressure rise decrease.

There is, therefore, an optimum space to chord ratio, which is normally chosen appropriate to the design point conditions.

It is suspected that the actual compressor geometry does not correspond to this optimum, especially the stators, since their numbers are very high.

However, the effect of blade removal on the overall compressor performance must first be taken into account, considering two off-design situations, namely at the design speed with reduced mass flow and at part speed.

Reduced mass flow at design speed.

If the mass flow, i.e. ρV_a, is reduced at the design speed the compressor pressure rise increases. However, the

front stage of the compressor is operating at a pressure and, therefore, density, fairly close to the design value. The reduction in mass flow is, therefore, manifested mainly as a reduction in axial velocity, V_a.

Conversely, the rear stage pressure (and density) is much higher than the design value so that the reduced ρV_a is accompanied by an even higher reduction in V_a. As a result, higher positive incidence increases occur and the rear stage moves closer to stall than does the front stage.

If the compressor is over-bladed at the design speed, it is then logical to remove blades from the front rather than the back since the latter would become even more susceptible to stall. That is, the corresponding increase of s/c would reduce channelling (overlap) and promote flow separation.

At part speed.

At part speed operation, it is the early stages of compressor that approach stall whilst rear stages approach choke. In this case, therefore, removal of rear stage blades is indicated to relieve the choke problem. In turn, this would clearly impair design speed performance.

In conclusion, in order to generally testing the design/development aspects of the programme, it was decided to remove blading from all three stages. Only stationary

blades were removed for this test for the reason explained earlier.

For the present, the following tests using the prediction programme were undertaken at design speed only.

- Remove 10%, 20% and 30% of all stationary blades throughout the compressor:

The result of this exercise is shown on Fig. 8.1b for pressure ratio and Fig. 8.1c for efficiency and the actual data tabulated below (Table 8-2).

As predicted, stator blade removal has a marked effect on pressure ratio at reduced flows. There is, furthermore clear evidence of an optimum increase of s/c in that the pressure ratio achieved is higher and peaks when approximately 20% of the stationary rows are removed.

For efficiency similarly, the predicted values are higher with reduced stationary blade numbers but no clear trend in terms of an optimum is established.

Table 8-2- Effect of increase in s/c on performance at design speed

% Blades removed	mass flow (kg/s)	pressure ratio	efficiency %
10	15.5	4.725	0.818
	16.1	4.742	0.839
	16.375 (DP)	4.605	0.840
	16.6	4.385	0.835
	16.8	4.092	0.821
	16.9	3.709	0.793
	17.0	choked	-
20	15.5	4.724	0.818
	16.1	4.749	0.839
	16.375 (DP)	4.616	0.841
	16.6	4.399	0.835
	16.8	4.069	0.820
	16.9	3.672	0.789
	17.0	chocked	-
30	15.5	4.514	0.808
	16.1	4.764	0.839
	16.375 (DP)	4.621	0.841
	16.6	4.429	0.839
	16.8	4.231	0.834
	16.9	4.100	0.830

It is unlikely that uniform reduction in blade numbers throughout the compressor would give the best result for reasons discussed earlier.

Clearly then, further detailed study involving selected, stage by stage reduction in stationary blades is needed for this particular compressor.

This exercise does, however, demonstrate that the programme as structured facilitates easy investigation of the effects; for example, of space to chord ratio and the results support the opinion that the actual compressor is over-bladed.

8.5. THE PERFORMANCE PREDICTION PROGRAMME AS A TEACHING TOOL

The development of the streamline curvature model has been extensively discussed in this work. The equations are developed in detail so that the student can easily pick up the concepts involved in the model. Loss models are presented side by side and comparison between them can easily be made.

The important algorithms adopted in the programme are also presented in detail.

In addition, a comprehensive User's Guide (Volume II of this work) has been written, containing detailed description of each subroutine in the programme, with special emphasis on the following entries:

- Introduction: a brief introduction to explain the context in which the subroutine is utilised.
- Purpose: description of tasks performed by the subroutine.
- Form: its CALL statement, indicating the arguments.
- Arguments: description of each argument.
- Output: list of variables modified within the subroutine.

- Limitation: possible limitation to its use.

The uniformity of presentation of the subroutine descriptions, repetitive in some cases, is intentionally adopted in order to give the user the information he needs locally in each individual subroutine named.

Since there are up to five levels of CALL's, that is, there are CALL statements inside subroutines, and to avoid excessive repetition, the outputs of called subroutines are not included in the output list. In this case, the user is asked to refer to the called subroutine.

To give extra flexibility to the Programme, variable names are unchanged throughout and the most important kept in COMMON.

This allows instant access to their values at any point in the programme.

Variable names are mnemonically chosen so that their identification is eased.

Reference data given by curves or families of curves, are treated as table functions. Only a few reference curves are defined by their analytical expressions. An input file is used to store the information on the curves so that any modifications to their values can be made externally to the programme simply by changing the input reference file.

The programme accepts user defined subroutines to define loss, deviation, blade profile, and different forms

of compressor data input as well as data printout. That is, in addition to the external modification to loss correlations already included in the programme, the user can define a completely new model.

The user can also write his own output subroutine to suit his needs and, therefore, avoid additional work of collecting data produced by the programme.

A graphical facility is incorporated and a selection of the most important parameters can be displayed both on the screen and on hard copy, according to the user's choice, namely streamlines, velocity triangles, velocities, angles, incidence and deviation, losses and Mach numbers.

If the programme is stopped for any reason, it has a restart capability.

This means that the calculations already done can be recovered and the programme can continue from a point near to that of the interruption.

The programme is fully modular in the sense that one type of calculation is done by one specific subroutine. This means that any changes required that do not violate the algorithms defined can be straightforwardly carried out by simple replacement of the spotted subroutine.

In conclusion, the programme is both interactive and user friendly, and the user's guide is comprehensive.

9. - RECOMMENDATIONS FOR FURTHER IMPROVEMENT TO THE PROGRAMME

9.1. BLADE PROFILE SELECTION:

This package has been designed having transonic axial flow compressors with circular arc camber lines in mind and implemented for the most common DCA blades, although 65- and C-series have been included. Future improvements could make provision for other types of blade profiles.

9.2. DESIGN MODE:

The package is ready for the analysis of a compressor defined by its geometry, although it can be utilised for design improvements when the ability to change the input data during the programme run is explored. Therefore, an improvement can be foreseen in the direction of it utilised as a design tool. Currently a previous rough design is needed to start the programme, if its design is to be improved during the programme run.

9.3. ANNULAR DUCTS:

The intake and exhaust ducts, as well as the bladeless spaces, can be analysed by the programme, based on a known total pressure loss through these ducts. Therefore, improvements could be made in the direction of estimating the duct pressure losses within the programme, based on an appropriate loss model.

9.4. AXIAL FLOW TURBOMACHINERY:

Although the programme has been developed for the specific purpose of analysing compressors, the basic structure makes no distinction whether the work is being added or extracted at each blade row. Therefore, the streamline curvature model could be applied to a turbine as well. The programme can accept the analysis of a turbine provided the deviation and loss models are modified accordingly. Therefore, it is foreseen that an improvement in this direction could be realised in future work, although it is not expected to be a straightforward job.

9.5. IMPROVEMENT IN THE NUMERICAL TECHNIQUES:

The interpolation technique used throughout the programme, mainly at the points where a fixed set of curves is used, can be faster if the spline and equations coefficients are calculated every time an interpolation is performed.

9.6. HELP SUBROUTINES:

In order to give hints to the user during the programme execution, Help Subroutines, containing information and suggestion about how to run the programme, could be added to the package, making its use easier and friendly. The help subroutines are complimentary to the instructions from the user's guide.

10. - REFERENCES

1. WU, C.H. - A general theory of 3-d flow in subsonic and supersonic turbomachines of axial, radial and mixed flow types. NACA TN 2604, 1952.
2. HOWELL, A.R. and CALVERT, W.J. - A new stage stacking technique for axial flow compressor performance prediction. Trans. ASME, Vol. 100, Oct 1978.
3. SEROVY, G.K. - System development - lessons from 30 years of history. In: AGARD LS-83, 1976.
4. DAVIS, W.R. and MILLAR, D.A.J. - Through flow calculations based on matrix inversion: loss prediction. AGARD CP 195.
5. DAVIS, W.R. and MILLAR, D.A.J. - A comparison of the matrix and streamline curvature methods of axial flow turbomachinery analysis from the user's point of view. ASME Paper 74-WA/GT-4, 1974.
6. AGARD LECTURE SERIES LS 83 - Modern prediction methods for turbomachine performance, 1976.
7. JANSEN, W. and MOFFATT, W.C. - The off-design analysis of axial-flow compressors. J. Eng. Power, Oct. 1967.
8. DRANSFIELD, D.C. and CALVERT, W.J. - Detailed flow measurements in a four stage axial compressor. ASME paper 76-GT-46, 1976.

9. STRATFORD, B.S. - The use of boundary-layer techniques to calculate the blockage from the annulus boundary-layers in a compressor. ASME paper 67-WA/GT-7, 1967.

10. JANSEN, W. - The application of end-wall boundary-layer effects in the performance analysis of axial compressors. ASME paper 67-WA/GT-11, 1967.

11. SCHILICHTING, H. - Boundary-layer theory. Mc-Graw-Hill Book Co., Inc., N.Y., 1960.

12. LIEBLEIN, S. - Analysis of experimental low speed loss and stall characteristics of 2-D compressor blade cascades. NACA RM E57A28, 1957.

13. OLDHAN, R.K. - Some design data for double circular arc compressor blading. NGTE NOTE NT 589, 1985.

14. SMITH, L.H. Jr and YEH, H. - Sweep and dihedral effects in axial flow turbomachinery. ASME paper no. 62-WA-102, 1963.

15. ROBBINS, W.H., JACKSON, R.J. and LIEBLEIN, S. -NASA SP 36.

16. LEVINE, P. - The two-dimensional inflow conditions for a supersonic compressor with curved blades. WADC TR 55-387, 1956.

17. LICHTFUSS, H.J. and STARKEN, H. - Supersonic cascade flow. Progress in Aerospace Science, Vol. 15, Pergamon Press, 1974.

18. CARTER, A.D.S. and HUGHES, H.P. - A theoretical

investigation into the effect of profile shape on the performance of aerofoils in cascade. Power Jets Report no. R192, 1946.

19. SWAN, W.C. - A practical method of prediction transonic compressor performance. J. Eng. Power, Jul. 1961.

20. MONSARRAT, N.T., KEENAN, M.J. and TRAMM, P.C. - Design Report - Single stage evaluation of highly loaded high Mach number compressor stages. NASA CR 72562, 1969.

21. HOWELL, A.R. - Development of the British Gas Turbine Unit. In: Fluid Dynamics of Axial Compressors, ASME reprint, 1947.

22. GRIEPENTROG, H.R. - Secondary Flow losses in axial compressors. AGARD LS 39.

23. RAW, J.A. and WEIR, C.G. - The prediction of off-design characteristics of axial-centrifugal compressors. SAE paper no. 800628, Turbine power for executive aircraft meeting, Arizona, 1980.24.

24. SCHWENK, LEWIS and HARTMANN - A preliminary analysis of the magnitude of shock losses in transonic compressors. NACA RM E57E30, 1957.

25. HORLOCK, J.H. and LAKSHMINARAYANA, B. - Secondary flows. Annual review of fluid mechanics, no. 5, 1973.

26. VAVRA, M.H. - Aerothermodynamics and flow in turbomachines. Wiley, 1960.

27. EHRICH, F.W. and DETRA, R.W. - Transport of the Boundary Layer in Secondary Flow. J.A.S., 1954.

28. WALSH, F.M., AHLBERG, J.H. and NILSON, E.N. - Best approximation properties of the spline fit. J. of Math. Mech., vol. 11, n.2, 1962.

11. - APPENDICES

11.1. INTERPOLATION

There are two options of interpolation that can be chosen through one of the subroutine parameters: cubic spline and parabolic.

The cubic spline curve fit technique is based on [28] with the condition of the radii of curvature at the end points equal half the radii of curvature at adjacent points.

The parabolic curve fit technique is based in the assumption that a parabola fitted to three adjacent points represents well the function to be interpolated. Let $y = ax^2 + bx + c$ be the approximation function that will be used for interpolation and let

$$(x_{k-1}, y_{k-1}),\ (y_k, y_k) \text{ and } (x_{k+1}, y_{k+1})$$

be the points of a given curve.

It is required that $y = y(x)$ passes through these points so that

$$\begin{bmatrix} y_{k-1} \\ y_k \\ y_{k+1} \end{bmatrix} = \begin{bmatrix} x_{k-1}^2 & x_{k-1} & 1 \\ x_x^2 & x_k & 1 \\ x_{k+1}^2 & x_{k+1} & 1 \end{bmatrix} \cdot \begin{bmatrix} a \\ b \\ c \end{bmatrix}$$

Writing system (11.1) as $Y = XA$, then A can be calculated by $A = X^{-1} Y$, where

$$X^{-1} = \frac{1}{\det(X)} (\text{Cof } X)^t$$

$$\det(X) = x_{k-1}^2(x_k - x_{k+1}) + x_k^2(x_{k+1} - x_{k-1}) + x_{k+1}^2(x_{k-1} - x_k)$$

$$(\text{cof } X)^t = \begin{bmatrix} x_k - x_{k-1} & x_{k+1} - x_{k-1} & x_{k-1} - x_k \\ x_{k+1}^2 - x_k^2 & x_{k-1}^2 - x_{k+1}^2 & x_k^2 - x_{k-1}^2 \\ x_k^2 x_{k+1} - x_k^2 x_{k+1} & x_{k+1}^2 x_{k-1} - x_{k-1}^2 x_k & x_{k-1}^2 x_k - x_k^2 x_{k-1} \end{bmatrix}$$

$A_1 = x_k - x_{k+1}$

$A_2 = x_{k+1} - x_{k-1}$

$A_3 = x_{k-1} - x_k$

$C_1 = x_{k-1}^2$

$C_2 = x_k^2$

$C_3 = x_{k+1}^2$

$D_1 = C_1 - C_3$

$D_2 = C_3 - C_2$

$D_3 = C_2 - C_1$

$$E_1 = C_2x_{k+1} - C_3x_k$$

$$E_2 = C_3x_{k-1} - C_1x_{k+1}$$

$$E_3 = C_1x_k - C_2x_{k-1}$$

then

$$\det(X) = A_1C_1 + A_2C_2 + A_3C_3$$

$$a = \frac{A_1y_{k-1} + A_2y_k + A_3y_{k+1}}{\det(X)}$$

$$b = \frac{D_1y_{k-1} + D_2y_k + D_3y_{k+1}}{\det(X)}$$

$$c = \frac{E_1y_{k-1} + E_2y_k + E_3y_{k+1}}{\det(X)}$$

If any interpolating point lies outside the interval $[x_1, x_N]$, the approximating function is that defined over the nearer interval.

After **a**, **b** and **c** have been calculated, the interpolated value is

$$y_1(x_1) = ax_1^2 + bx_1 + c$$

11.2. INTERPOLATION OF FUNCTIONS OF TWO VARIABLES

Most correlations are represented by curves, in a two-dimensional plane, dependent on parameters. Mathematically speaking, those curves are representation of functions of two variables. The use of curves depending on parameters is

due to the fact that it is easier to handle functions of one variable, and their graphs. More complex correlations are represented by the summation or the product of simpler one- or two-variable functions. Even more difficult is to find the equations that represent a fitted curve. Most experimental curves must be, therefore, handled by numerical techniques. When a function of 2 variables is used to represent a set of experimental curves, such as the Total Pressure Loss Parameter as a function of the Equivalent Diffusion Factor, for varying Percentage of Blade Height, three procedures can be adopted:

- Curve-fit the experimental points such that only one equation, involving the parameter, is discovered.
- Curve-fit the experimental points and use one equation for each of the curves.
- Interpolate among the experimental points.

In terms of computation time, the first procedure is ideal, because one calculation gives the result. In terms of allowance for adjustments, however, it is the worst. Since the equation is discovered, there is little or no possibility of trimming. The second procedure is also favoured as far as computing time is concerned but, for the same reasons, there is little or no possibility of

trimming. The pure numerical interpolation, despite the extra time of computation, allows for any kind of adjustment. This is the technique adopted throughout this work because the kind of experimental curves that are dealt with are statistical curve fits and as such, allow for adjustments.

An additional advantage of adopting this technique is that virtually all the functions to be interpolated can be treated the same way and there is no need for curve-fitting every time an adjustment is required.

The interpolation utilizes linear, quadratic and spline techniques, depending on the curve's behaviour.

The technique for double interpolation is as follows:

let $F = F(x,K)$ be a function that represents a certain correlation graph, x and K being the two independent variables. Let (X_o,K_o) be the point at which it is wanted to know the value F_o of F (Fig. 11.1), that is

$$F_o = F(X_o,K_o)$$

For $x = X_o$ held constant, auxiliary interpolated values F_1, F_2, F_3, ..., F_n are calculated such that

$$F_1 = F(X_o,K_1),\ F_2 = F(X_o,K_2),\ \ldots,\ F_n = F(X_o,K_n)$$

Hence a new curve is defined, for the particular value of X_o, that is

$$G(K) = F(X_o,K)\ ,\ \text{such that}$$

$$G(K_1) = F_1,\ G(K_2) = F_2,\ \ldots,\ G(K_n)=F_n.$$

Interpolating for K_o from this auxiliary curve will result

$G(K_o) = F(X_o, K_o) = F_o$, the final interpolated value.

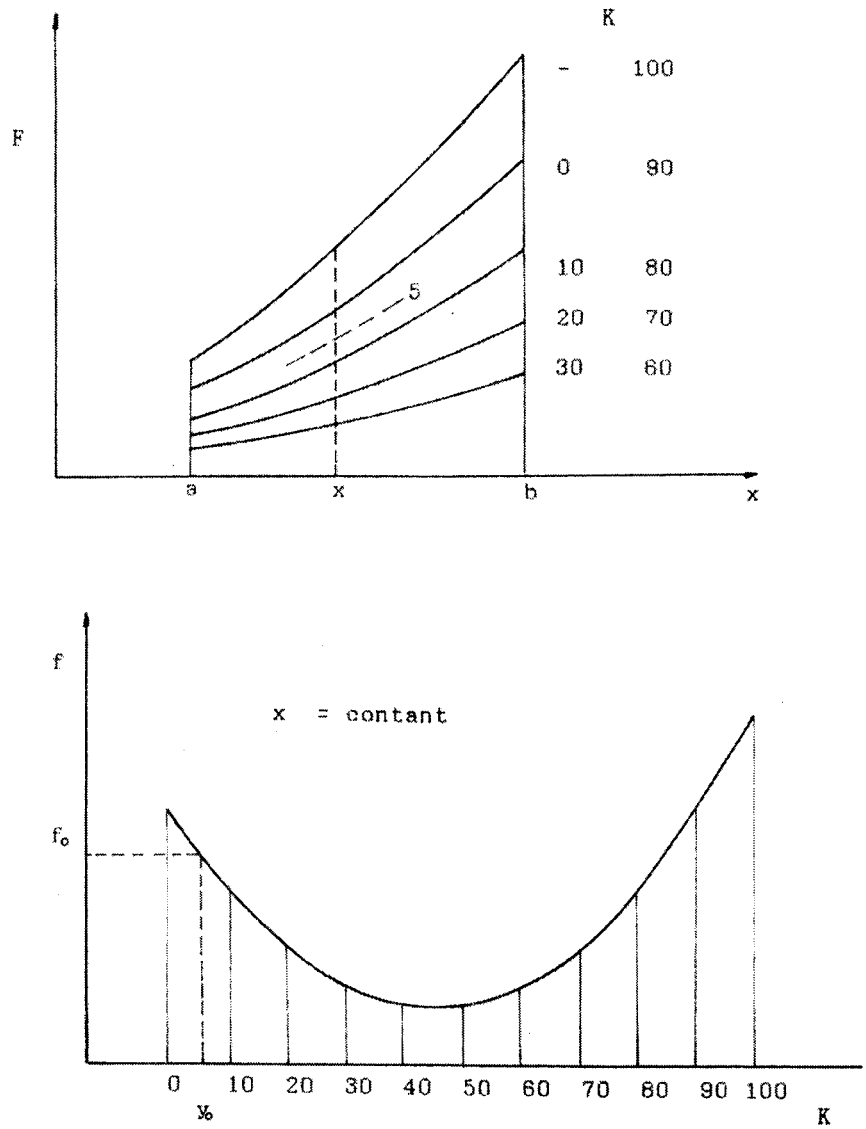

Figure 11.1 - Double Interpolation

Figure 11-1- Interpolation of function of 2 variables

11.3. DERIVATION

The method adopted for the calculation of the first and second derivatives, for the calculation of the radii of curvature of the streamlines, plays an important part in the success of the solution of the equations by the streamline curvature method. Several authors have already discussed this problem and it has been noticed in the present work. It has been the author's experience during the use of the streamline curvature model that the utilisation of the spline technique for the determination of second derivatives and radii of curvature gives instability to the process. The spline technique calculates first the second derivatives and then the first. The inability to calculate precisely the second derivative is the cause of instabilities in the method. To avoid this problem, the second derivative is recalculated from the derivation of the first derivative. The user can chose the technique he wants among the spline, parabolic or linear approximation. The spline technique follows a paper by Walsh [28] et al., with the conditions of the second derivatives, at the end points, being half the values at the neighbouring points. The parabolic technique derives a

parabolic curve fit to 3 adjacent points.

If $y = ax^2 + bx + c$, then $y'' = 2a$.

The coefficients **a**, **b** and **c** are calculated as indicated above.

The linear technique assumes that the function is a piecewise continuous linear function over the subinterval where the calculating point is located and that the first and second derivatives are piecewise continuous and linear over the interval. Then

$$y' = \frac{1}{2}\left\{\frac{y_{k+1} - y_k}{x_{k+1} - x_k} + \frac{y_k - y_{k-1}}{x_k - x_{k-1}}\right\}$$

$$y'' = 2\left\{\frac{\dfrac{y_{k+1} - y_k}{x_{k+1} - x_k} + \dfrac{y_k - y_{k-1}}{x_k - x_{k-1}}}{x_{k-1} - x_k}\right\}$$

11.4. INTEGRATION OF THE DIFFERENTIAL EQUATIONS

The full radial equilibrium equation given by equations (2.42), (2.43) and (2.44) cannot be solved analytically.

Two techniques are adopted for the numerical integration: the under-relaxed iterative technique and the fourth order Runge-Kutta.

Analysing the functions A and B given by equations

(2.43) and (2.44), it indicates that they vary little when calculated at two points not far apart. Then, for the nodes on a streamtube defined by two adjacent streamlines, the values of A and B can be approximated by the average of their values at the nodes. Therefore, A and B can be treated as constants over that streamtube.

Equation (2.42) can then be rewritten as

$$dV_m^2 = \bar{A} + \bar{B}V_m^2 \tag{11.1}$$

which is an ordinary differential equation with constant coefficients. Making the substitution

$$Y = V_m^2$$

equation (11.1) becomes

$$\frac{dY}{ds} = \bar{A} + \bar{B}Y \tag{11.2}$$

which is a first order ordinary linear differential equation with constant coefficients.

The general solution of the homogeneous equation associated to (11.2), is

$$Y_h = Ce^{\bar{B}s} \tag{11.3}$$

A particular solution of (11.2) is

$$Y_p = K \tag{11.4}$$

From (11.2) and (11.4), $0 = \bar{A} + \bar{B}K$ and $K = -\bar{A}/\bar{B}$

The general solution of (11.2) is

$$Y = C_1 e^{\bar{B}s} - \frac{\bar{A}}{\bar{B}} \tag{11.5}$$

Let Y_1 be the value of Y at one node. Then,

$$Y_1 = C_1 e^{\bar{B}s_1} - \frac{\bar{A}}{\bar{B}}$$

$$C_1 = \left(Y_1 + \frac{\bar{A}}{\bar{B}}\right) e^{-\bar{B}s_1}$$

$$Y = \left\{\left(Y_1 + \frac{\bar{A}}{\bar{B}}\right) C_1 e^{-\bar{B}s_1}\right\} e^{\bar{B}s} - \frac{\bar{A}}{\bar{B}}$$

Finally,

$$Y = Y_1 e^{\bar{B}(s-s_1)} - \frac{\bar{A}}{\bar{B}}\left\{1 - e^{\bar{B}(s-s_1)}\right\}$$

The solution of (11.2) is, then,

$$V^2_{m_{j+1}} = V^2_{m_j} e^{\bar{B}(s-s_1)} - \frac{\bar{A}}{\bar{B}}\left\{1 - e^{\bar{B}(s-s_1)}\right\} \tag{11.6}$$

It must be stressed that $\bar{A}$ and $\bar{B}$ are functions of the blade geometry, streamline geometry and of the solution velocity, V_{m_j}, what makes the integration of (11.2) a non-

straightforward process.

Due to the rough assumption that $\overline{A}$ and $\overline{B}$ can be made constants inside a streamtube, the distance between two streamlines must be kept small.

11.4.1. THE ITERATIVE TECHNIQUE

Let j and j+1 be two neighbouring streamlines such that the assumption of $\overline{A}$ and $\overline{B}$ constant holds. Let the flow and streamline properties be known at j. Let $V_{m_{j+1}}$ be the solution of (11.2) at j+1. If $V_{m_{j+1}}$ is the solution, then the calculation of the second term of (11.6) would give $V^2_{m_{j+1}}$.

An iterative procedure can be set up starting with an initial guess for the value of $V_{m_{j+1}}$. For this value of $V_{m_{j+1}}$, the value of the second member of (11.6) can be calculated and checked against the value of the first member. If they are not the same, the guess was not the correct and a new guess must be made. It naturally follows that the second guess would be the value obtained from the second member of (11.6). The process can be repeated until the identity is eventually achieved. In practice, the final solution is accepted if the first and second members of (11.6) differ

only by a little. If the values calculated by the second member of (11.6) are used as the next guess, sometimes the process diverges. To avoid divergence, a linear combination of the values of the guess and the calculated value is recommended. Then a new guess can be computed by

$$V_{m_{j+1}}^{(n+1)} = aV_{m_{j+1}}^{(n)} + (1 - a)V_{m_{j+1}}^{(n-1)} \qquad (11.7)$$

where a is the under-relaxation factor.

The choice of a can make the process either converge or diverge. It will dictate the speed with which the process converges. It can be optimised in order to make the process converge with the minimum number of iterations.

11.4.2. THE RUNGE-KUTTA METHOD

Let $y' = f(x, y)$ be a first order non-linear ordinary differential equation and $y(x_0) = y_0$ the initial condition. Equation (11.2) is a particular representation of this equation.

The Runge-Kutta procedure for determining a numerical solution of $y' = f(x, y)$ is summarised in the steps below.

Let $0 \neq h = x_1 - x_0$

Step 1 - first approximation y

$$y_{k_1} = y_0 + \frac{1}{2}(k_1 - 2q_0)$$

$$k_1 = hf(x_0, y_0)$$

$$q_0 = \begin{cases} 0 & \text{for } x_n = x_1 \\ q_4 & \text{for } x_n \neq x_1 \end{cases}$$

Step 2 - second approximation y_{k_2}

$$y_{k_2} = y_{k_1} + \left(1 - \frac{1}{\sqrt{2}}\right)(k_2 - q_1)$$

$$k_2 = hf\left(x_0 + \frac{h}{2}, y_{k_1}\right)$$

$$q_1 = q_0 + 3\frac{k_1 - 2q_0}{2} - \frac{k_1}{2}$$

Step 3 - third approximation y

$$y_{k_3} = y_{k_2} + \left(1 + \frac{1}{\sqrt{2}}\right)(k_3 - q_2)$$

$$k_3 = hf\left(x_0 + \frac{h}{2}, y_{k_2}\right)$$

$$q_2 = q_1 + 3\left(1 - \frac{1}{\sqrt{2}}\right)(k_2 - q_1) - \left(1 - \frac{1}{\sqrt{2}}\right)k_3$$

Step 4 - solution y

$$y_1 = y_{k_4} + (k_4 - 2q_3)$$

$$k_4 = hf\left(x_0 + \frac{h}{2}, y_{k_3}\right)$$

$$q_3 = q_2 + 3\left(1 + \frac{1}{\sqrt{2}}\right)(k_3 - q_2) - \left(1 + \frac{1}{\sqrt{2}}\right)k_3$$

$$q_4 = q_3 + 3\frac{k_4 - 2q_3}{6} - \frac{k_4}{2}$$

In order to obtaining generalised formulae for the calculation of the four steps, let

$$\Delta V = hf(x_i, y_i)$$

$$A_i = C_i(\Delta V_i - C_2 Q_{i-1})$$

$$Q_i = Q_{i-1} + 3A_i - C_3\Delta V_i, \text{ so that}$$

$$C_1 = \left[\left(\frac{1}{2}\right)\ \left(1 - \frac{1}{\sqrt{2}}\right)\ \left(1 + \frac{1}{\sqrt{2}}\right)\ \left(\frac{1}{6}\right)\right]$$

$$C_2 = \left[(2)\ (1)\ (1)\ (2)\right]$$

$$C_3 = \left[\left(\frac{1}{2}\right)\ \left(1 - \frac{1}{\sqrt{2}}\right)\ \left(1 + \frac{1}{\sqrt{2}}\right)\ \left(\frac{1}{2}\right)\right]$$

$$x = \left[(x_0)\ \left(x_0 + \frac{h}{2}\right)\ \left(x_0 + \frac{h}{2}\right)\ (x_0 + h)\ (1)\right]$$

$$y = \left[(y_0)\ (y_{k_1})\ (y_{k_2})\ (y_{k_3})\ (y_1)\right]$$